Nearshore morphological changes and their relation to wave-induced forcing at Isipingo embayment, KwaZulu-Natal.

By

Arissa Shanganlall (BSc. Hons)

Supervisor: Prof Andrew Green and Dr Carlos Loureiro

Submitted for the fulfilment of the academic requirements for the degree of
Master of Science in the Discipline of Geological Sciences
School of Agriculture, Earth and Environmental Sciences
University of KwaZulu-Natal
Westville
Durban

December 2017

Declaration

The research described in this thesis was undertaken in the School of Geological Sciences (Marine Geoscience Unit), University of KwaZulu-Natal, under the lead supervision of Prof. Andrew Green and co-supervision of Dr.Carlos Loureiro. The duration of the work performed spans January 2016 to December 2017. These studies represent original work by the author and have not been submitted in any form to another university. Where use was made of the work of others, it has been duly acknowledged in the text.

Signature..... Date.....

Author

Signature..... Date.....

Lead Supervisor

Abstract

The nearshore zone is one of the most active sedimentary environments on the continental shelf, frequently impacted by energetic wave conditions and storm–generated waves and flows. Despite its proximity to the beach and shoreline, the nearshore is a difficult domain to study and little is understood with regards to its response to storm waves and the agents responsible for the morphological evolution of the region. Previous research has provided insight into the nearshore, however high-resolution approaches to gain a three dimensional understanding of these environments are still lacking. This is especially true in geologically constrained environments as coastal embayments. Advances in the acquisition and analysis of high-resolution multibeam bathymetry of the nearshore, coupled with wave modelling techniques, can provide an improved understanding of coastal response to high energetic wave conditions and the subsequent morphological changes that result from the impact of storm events.

Detailed nearshore multibeam bathymetric surveying conducted at the Isipingo embayment before and after the 2017 winter season provided a framework to analyse the seasonal morphological changes that were driven by winter storms along the KwaZulu-Natal coastline. High-resolution bathymetric grids were implemented in the hydrodynamic model SWAN (Simulating Waves Nearshore) to simulate the nearshore wave field of Isipingo embayment for a variety of wave conditions. Morphological changes were evaluated in conjunction with wave-induced forcing to determine the potential for sediment mobilisation. Spectral wave modelling results of the wave field and bed shear stresses agree with the observed morphological changes. Significant erosion and deposition occurred in the shallower regions (5 m to 14 m) of the study area and along the northeast and southwest sections of the embayment.

Modelling results presented in this study indicate that the spatial variation and distribution of orbital bottom velocities and bed shear stresses are strongly dependent upon the bathymetric configuration of large-scale bedforms and the magnitude of the nearshore wave field. Consequently, the greater the energy of the wave conditions (i.e. as a result of major storm events) the greater the wave-induced forcing, which causes the change of the bedforms and the morphological evolution of the nearshore. Large-scale features such as shoreface-connected ridges, rippled scour depressions and large subaqueous dunes tend to increase the significant wave height and the bed shear stresses acting on the seabed. Thus, waves are focussed towards the NE headland resulting in an extensive zone of erosion in the embayment.

The main geological constraints at the embayed region of Isipingo are imposed by the NE and SW headlands and the shoreface-connected ridges. Such constraints drive the development of topographically controlled rips against the NE headland, set up by the prevalent south-north longshore current, and the shadowing effect of the SW headland also contributes to the observed erosional (NE region) and accretion (SW region) patterns on the nearshore. The hydrodynamic forcing of rippled scour depressions and shoreface connected ridges control the persistence of the non-stationary rip currents of the NE section of the embayment. As a consequence, the absence of rip activity at the centre of the embayment creates a relatively stable region. Additionally, the study reveals that the patterns of morphological change in the nearshore mimic those of the apparent rotation of the beach, explained by the breathing mode described from other embayments. Model simulations of extreme storm events depict that the morphological change is driven by an energetic wave field, and the wave induced orbital motions and bed shear stresses have a strong bathymetric imprint.

This study demonstrates the usefulness of high-resolution bathymetry in understanding nearshore morphological change. In providing a complete three dimensional image of changes at incredibly high-resolutions, and with high (2-3 month) temporal resolution, an increased level of understanding of the nearshore changes seaward of bars can be garnered. This includes rip-dynamics, erosion patterns, geological control on wave-forcing and seasonal accretion/erosion monitoring. These are areas which have not yet received attention in this level of detail and in which it is demonstrated that good results can be obtained.

Acknowledgements

This work is a contribution to EU H2020-MSCA NEARControl project, which received funding from the European Union's Horizon 2020 Research and Innovation programme under the Marie Sklodowska-Curie grant agreement No. 661342. The author was supported by an ETDP SETA Bursary No. 2016217010

My most heartfelt thanks go out to Prof. Andrew Green for his tireless direction, guidance and enthusiasm throughout the supervision of this thesis, as well as the endless bouts of inspiration he provided when times were tough. I also thank my co-supervisor Dr Carlos Loureiro for his continued direction and appraisal for the project, and continuously providing critical reviews of this dissertation. The encouragement, motivation and belief in this research from both my supervisors is gratefully acknowledge. Thanks goes out to Professor J.A.G. Cooper for providing an incredible wealth of knowledge and his willingness to assist me on various aspects of this topic is truly appreciated.

The author thanks Subtech for providing the multibeam bathymetry data and the CSIR for kindly providing the wave buoy data.

To Kreesan Palan, who I have had the great pleasure of sharing this journey with. He has brought, and continues to, bring an immense amount of happiness, joy and laughter in my life. I am eternally grateful for his support and strength through difficult times, both academically and personally. Here's to sharing more amazing memories and adventures together.

To my friends, Lauren Pretorius and Dr Errol Wiles, who I have spent many hours sharing jokes, stories, and pizza with. Their motivation and friendship has made this journey so much more enjoyable.

Thanks goes out to the technicians in the lab and the academic staff at the Discipline of Geological Sciences at the University of KwaZulu-Natal, for offering their help and knowledge.

To my parents who never failed to lift my spirits even through the most stressful times and always offered their support and love. I will remain forever grateful for the guidance and light they continue to bring into my life

Table of Contents

Abstract ..... **i**

Acknowledgements ..... **iii**

Table of Contents ..... **iv**

Chapter 1: Introduction **1**

Chapter 2: Literature Review **3**

2.1. Nearshore Zone 3

2.2. Nearshore Hydrodynamics 5

2.3. Nearshore Morphology 8

2.4. Nearshore Sediment 12

2.5. Nearshore Sediment Transport 13

2.6. Nearshore Surveying Systems 14

2.7. Numerical Wave Models 15

Chapter 3: Regional Setting **18**

3.1. Regional Environmental Setting 18

3.2. Regional and Local Geology 22

Chapter 4: Methods and Materials **29**

4.1. Geophysical Data Collection 29

4.2. Geophysical Data Processing 32

4.3. Wave Modelling 34

4.4. Morphological Changes 41

Chapter 5: Results **42**

5.1. Bathymetry 42

5.2. Wave Modelling 50

5.3. Nearshore Morphological Changes 60

Chapter 6: Discussion **67**

6.1. Bathymetric control on wave field 67

6.2. Geological Constraints and nearshore hydrodynamics 72

6.3. High-energy Morphodynamics 78

Chapter 7: Conclusion **80**

References **82**

Chapter 1: Introduction

The nearshore zone is the coastal region where the influence of wave processes during normal conditions and extreme events is more significant (Elko & Holman, 2014), The nearshore, seaward of bars, is poorly understood with regards to its response to storm waves and sediment dynamics and, unlike the adjacent and better studied beach environment, little is known regarding the agents responsible for changing seabed morphology and sediment mobility in these areas. With the rapid increase in coastal engineering schemes and marine activities in the past decade, there has been a growing need to understand the nearshore response to energetic wave conditions and recognition of the morphological changes associated with the impacts of storm events. The potential role of changing nearshore bathymetry is widely acknowledged and observed as a control on coastal behaviour (Munk & Traylor, 1974; U.S. Army Corps of Engineers, 1984) and the advances of non-hydrostatic models have led to an accurate and computationally affordable solution to modelling nearshore physical processes (Casulli & Stelling, 1998; Ma et al., 2012; Zijlema et al., 2011). Coupling the analysis of high resolution bathymetric data with wave modelling procedures further provides a comprehensive understanding of nearshore morphological responses that are driven by energetic wave conditions in geologically constrained environments.

This study examines the nearshore of an embayed coastal compartment, Isipingo Durban, KwaZulu-Natal from bathymetric and wave modelling perspective, so as to investigate the morphological changes of the seabed over a winter period. This work forms part of an Ulster University-UKZN collaborative research project NEARCONTROL, the aims of which are to quantify the role and impact of nearshore geological control in hydrodynamic and morphosedimentary processes along coastal areas exposed to energetic wave conditions.

This thesis makes use of detailed multibeam bathymetry that spans an austral winter period (June, July, August), in order to characterize the changing nearshore morphology as related to winter storm events. High-resolution bathymetric grids are then used to simulate the nearshore wave field and bed shear stresses of Isipingo embayment for a variety of wave conditions that range from fairweather conditions to extreme storms.

The specific objectives of this project include:

1. To collect and process ultra-high resolution multibeam bathymetry data from the nearshore zone of a rocky embayment at Isipingo Beach, offshore Durban.
2. To characterize the nearshore morphology of the Isipingo embayment and to analyse the morphological changes that occurred over a winter season.
3. To create high-resolution bathymetric grids for the implementation of the wave model SWAN (Simulating Waves Nearshore). This is to simulate the nearshore wave field of the embayment for a variety of wave conditions, as recorded in historical wave data from offshore Durban.
4. To evaluate the nearshore morphological changes in combination with wave-induced forcing and its potential for sediment mobilisation.
5. To evaluate changes and mobility of characteristic bedforms and their relation to wave induced forcing.

Chapter 2: Literature Review

2.1. Nearshore Zone

The nearshore zone is the coastal region where the influence of wave processes during normal conditions and extreme events is more significant (Elko & Holman, 2014), as such it extends from the limit of wave-induced swash action to the seaward limit of significant interaction between waves and seabed sediment. This definition has also been used to describe the boundaries of the shoreface as introduced by Aagaard et al. (2013), but has been favoured in this study to define the nearshore. This nearshore zone is one of the most dynamic marine systems and is significantly influenced by gravity waves (Holman & Haller, 2012). The offshore boundary of the zone is explained in relation to the time scale of interest and corresponds to the wave base, which is, as Komar (1976) redefined, the wave depth that is approximately ¼ of the wavelength. Svendsen (2006) defines this depth as approximately ½ the wavelength. This depth for the offshore limit takes into consideration the interaction between waves and the seabed and depends upon the wave motion itself (Cowell et al., 1999; Svendsen, 2006).

Based on the definitions of Cowell et al. (1999), Holman & Haller (2012) and Aagaard et al. (2013), the nearshore zone for this study is divided into 3 zones: 1) shoaling zone, 2) surf zone, 3) swash zone (Fig 2.1.). These zones are commonly referred to as morphodynamic zones and each is defined by characteristic sediment transport mechanisms and hydrodynamic processes. The boundaries between each of these zones is a function of the local relative wave height and the local wave steepness (Price & Ruessink, 2008).

1) The shoaling zone extends in an onshore direction to the wave base where the interaction between the seabed and waves become more intense and wave transformation processes become increasingly relevant. Three types of wave bottom interaction cause wave energy dissipation within this zone: bottom friction, percolation and bed fluctuation (Stutz et al., 1998). The rate of wave energy dissipation varies substantially between the different types of interactions but generally increases in shallow water. Waves in the shoaling zone become progressively skewed and asymmetric due to the limitations in water depth. As a result, sediment transport and morphological changes associated with this zone are ultimately driven by increased wave-orbital motions (Hsu et al., 2006).

2) The surf-zone extends towards the foreshore, varying with beach slope and wave conditions (Davidson-Arnott, 2010). Wave breaking is the main hydrodynamic mechanism in the surf-zone as wave energy is lost through breaking and the transferred momentum forces water in the direction of wave propagation (Castelle et al., 2016). Therefore, breaking waves generate changes in wave momentum flux, or radiation stresses (Longuet-Higgins & Stewart, 1964), forcing water onshore and causing a set-up in mean water level (Bowen et al., 1968). Wave energy dissipation in the surf zone occurs primarily due to turbulence generated during breaking (Stutz et al., 1998). Nearshore bars are characteristic features of the surf zone and are typically found at water depths of < 10 m; there is morphodynamic coupling between the surf-zone breaking and nearshore bars (Castelle et al., 2016).

3) The swash zone defines the region where waves run up and down the beach face, and dissipate or reflect their energy after travelling towards the shore (Larson et al., 2004). The energy dissipation of waves is dominated by the processes of bottom friction, percolation and turbulence (Stutz et al., 1998). Despite its narrow width, the swash zone plays a significant role in the exchange of sediment between land and sea, which has an effect on the subaerial and subaqueous evolution of the beach (Larson et al., 2004). Morphological processes are related to this sediment exchange, such as erosion during severe storm events, post-storm recovery, the evolution of rhythmic features and seasonal variation in the foreshore shape (Larson et al., 2004).

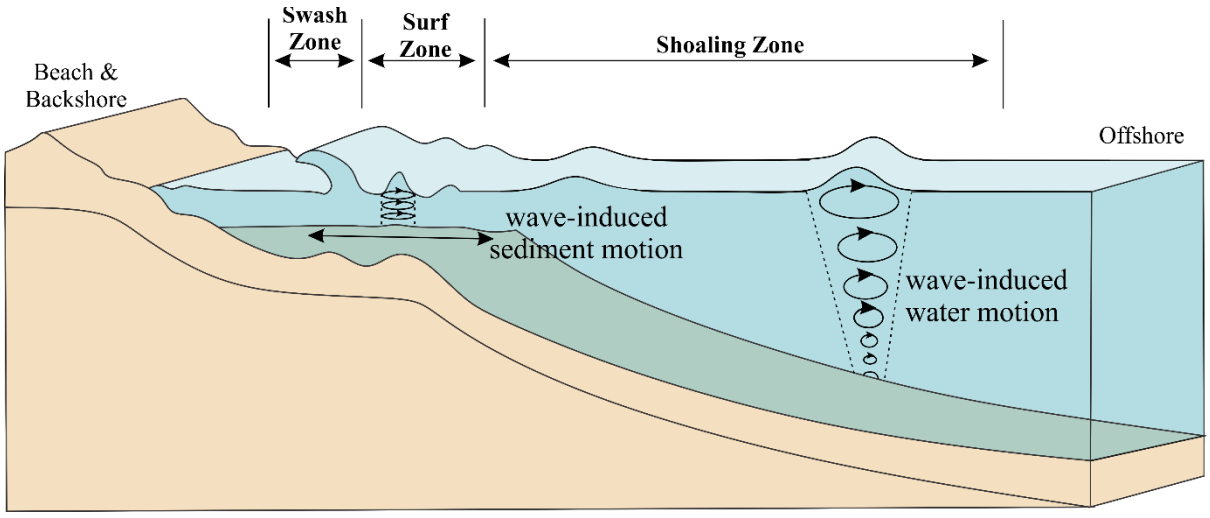

Figure 2.1: Profile of the nearshore zone, indicating the extent of the shoaling zone, surf zone and swash zone (modified from Cowell et al., 1999)

2.2. Nearshore Hydrodynamics

2.2.1. Wave Propagation and breaking

Waves, and the currents they generate, are the primary factors responsible for the transport and deposition of sediment in the nearshore zone. Wave-induced motions effectively move this material and consequently distribute the sediment and modify the bottom configuration (Davis, 1978).

In deep water, a wave propagating over a regular seabed topography with gentle slopes and no current will retain its frequency (Holthuijsen, 2007). The profile of such deep-water waves is low and long, approaching a sinusoidal form, and these are organized in wave trains or groups (a system of sinusoidal waves) with a dominant frequency, amplitude and vector wavenumber (Bretherton & Garrett, 1969). As the waves propagate from deep waters into shallower waters, their amplitude and direction become affected by the limited water depth in the coastal region (Holthuijsen, 2007). The wavelength and speed of the propagating waves decrease, and the waves steepen, resulting in an increase in wave height until the wave trains comprise peaked crests separated by flat troughs (Davis, 1978; Holthuijsen, 2007). This transformation is most pronounced for storm waves, which are characteristically steep and have longer periods (Holthuijsen, 2007).

The wave field of surface waves propagating from deep water into coastal waters is transformed as a consequence of shoaling and dissipation, refraction, and diffraction and breaking (Nwogu, 1993). Wave shoaling is the process that describes the shallow-water transformation of waves that commences when deep-water waves propagate into intermediate and shallow waters (depth is approximately ½ the deep-water wavelength) and the waveform starts to be influenced by the seabed (Davidson-Arnott, 2010). As a result, the wave height increases and wave celerity decreases until the water particle velocity at the crest exceeds the wave celerity (Ruessink & Ranasinghe, 2014).

In shallow water, propagating waves undergo significant energy dissipation as a result of bottom friction in the nearshore area (Guillou, 2013). The process occurs due to the interaction between the wave and the seabed, whereby energy and momentum is transferred from orbital motions of the water particles to the turbulent layer of the seabed (Holthuijsen, 2007). This type of dissipation mechanism is dominant on continental shelves with sandy bottoms (Holthuijsen, 2007; Guillou, 2013). Wave energy dissipation by bottom friction is likely to

lead to a substantial decrease of significant wave height in the order of 40-50% during extreme storm events (Guillou, 2013).

Upon entering intermediate to shallow water, wave crests tend to align themselves to underwater contours through the process of refraction (Davidson-Arnott, 2010). The process is a result of variable decrease in wave celerity as the wave shoals, causing the portion of the wave in deeper water to travel faster than the portion in shallow water, and resulting in the bending of the wave crests towards the bottom contours. Wave diffraction is the process that occurs as a consequence of energy being transferred in a lateral direction along the wave crest as a response to the rapid changes in the underwater topography, most notably around a headland, as well as spits or harbour jetties (Davidson-Arnott, 2010). Waves travel into the shadow of the headland in an almost circular pattern of crests with their amplitudes rapidly diminishing (Holthuijsen, 2007). The amount of shoaling, refraction, diffraction and dissipation is a function of the direction of wave propagation, wave period, configuration of the coastline, and the bathymetry of the seabed.

When a wave breaks, a significant part of its energy is dissipated and the characteristics of this dissipation are influenced by the underlying beach profile (Ruessink & Ranasinghe, 2014). In the case of a steep beach profile, the waves break directly at the shoreline as plungers and run up the beach immediately, however, if the beach slope is mild, then dissipation is gradual over a wide surf zone, characterized by spilling breakers. If the profile consists of bars and troughs, then the majority of the waves will break over the bars and little to no breaking will occur over deeper troughs (Ruessink & Ranasinghe, 2014).

2.2.2. Wave-generated nearshore currents

Wave-generated currents in the nearshore are generally separated into longshore currents, rip currents and bed return flows (Aagaard & Masselink, 1999). The onshore wave-action in the breaker zone, the lateral flow path inside the breaker zone by longshore currents, the seaward return of the flow through the surf zone by rip currents and the longshore movement of the expanding head by rip currents all constitute the nearshore circulation system (Fig. 2.2.). Nearshore circulation is fundamental in the study of the transport of nearshore littoral material (Ebersole & Dalrymple, 1980).

As waves propagate into shallower water at an oblique angle onto a straight coastline, they produced an energy vector parallel to the shore. This produces a longshore current, which flows inside the breaker zone and is dependent on the wave height and the angle at which the wave approaches the shore (Davis, 1978). As waves break onto a straight coastline at an oblique angle, a mean current setup occurs parallel to the coastline (Longuet-Higgins, 1970).

Rip currents are shore-normal, seaward-directed jets of water that originate within the surf zone and broaden out offshore in the breaker zone (MacMahan et al., 2006). Generally, rip currents are generated by the alongshore variations in wave heights and wave breaking to create spatial variations in radiation stress that result in regions of higher wave set-up (the higher the wave, the greater the intensity of wave breaking) and lower wave set-up (the lower the wave, the less the intensity of wave breaking). This imbalance between the breaking wave force and spatial pressure gradient result in rip currents (Castelle et al., 2016). The type of rip current that occurs is controlled by the dominant forcing mechanism in that area (Castelle et al., 2016). Rip currents are generally categorised into three broad groups: 1) hydrodynamic rips that are solely driven by hydrodynamic forcing mechanisms in the absence of any morphological control. These types are generally spatially and temporarily variable. 2) Bathymetric rips are strongly influenced by the variability in alongshore morphology in the surf zone and inner shelf. 3) Topographic or boundary rips are dominated by the effect of a rigid lateral boundaries that may be both natural and anthropogenic (Castelle et al., 2016).

The seaward return flow or ‘undertow’ is the term used to describe the seaward return flow of water to compensate the mass movement of water in the shoreward direction by the breaking waves in the surf zone, in a two-dimensional situation (Svendsen, 1984). It compensates the shoreward mass flux of water above the trough level, driven by the water momentum flux and set-up by water volume brought in towards the shoreline by the breakers (Stive & Wind, 1968; Svendsen, 1984). The strength of the return flow is approximately 10 % of the wave celerity and persistent enough to cause the net offshore transport of sediment during storm events (Dally, 2006).

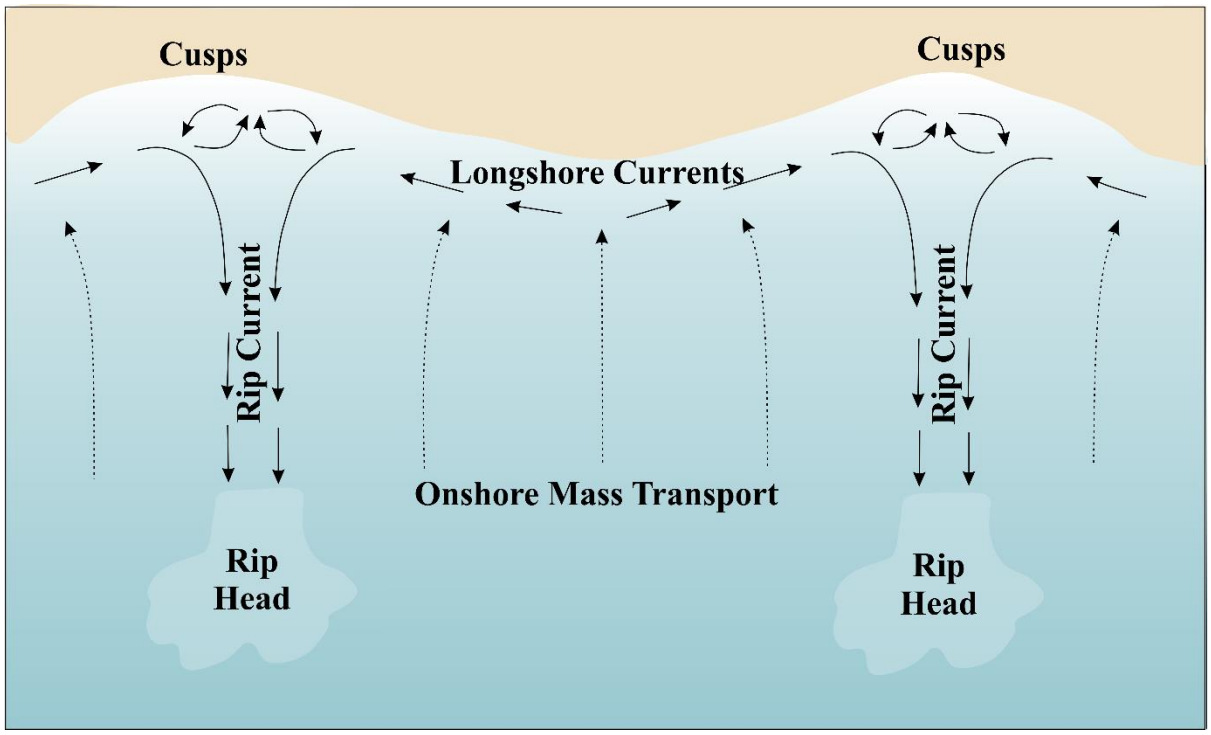

Figure 2.2: Rip current circulation regime, referred to as the exit flow, within the nearshore (modified from Castelle et al., 2016)

2.3. Nearshore Morphology

The nearshore zone is an area that undergoes active sediment transport that may be observed over periods that can range from seconds to decades or even centuries. However, most relevant morphological changes in the nearshore occur over seasonal to event time scales (Masselink & Gehrels, 2014). The interaction between sediment, ocean waves and currents over a range of spatial and temporal scales generate a variety of morphological features observed in the nearshore. These range from wave ripples (Wiberg & Harris, 1994; Gallagher et al., 1998; Traykovski et al., 1999; Clarke & Werner, 2004), crescentic, transverse and multiple sandbars in the surf zone (Ruessink & Kroon, 1994; Shand & Bailey, 1999; Konicki & Holman, 2000; van Enckevort et al., 2003) and large scale bedforms including shoreface-connected ridges (van de Meene & van Rijn, 2000), sorted bedforms (Murray & Thieler, 2004), sand banks and sand waves (Dyer & Huntley, 1999). Large-scale sand bars modify their position and form in response to storms, wave-induced ripples change in configuration in a matter of seconds to adjust their heights because of the passage of higher and lower waves in a wave group.

2.3.1. Wave-ripples

The surface of the nearshore seabed, seawards of the breaking and surf zone, is typically dominated by ripples (Davis, 1978). Wave-induced ripples found in the shoaling zone are the smallest scale patterns examined here, and generally have wavelengths in the range of 10 cm to 100 cm and height-over-length ratios of approximately 0.2 (Ruessink & Ranasinghe, 2014). Wave ripples contribute to the reduction of the energy of waves and currents and; therefore, they are referred to as roughness elements. They also influence the transport direction and rate of sedimentation. There are several classification schemes for the wave ripples, however the most commonly adopted scheme is that of Clifton (1976). The scheme consists of three main types: orbital ripples, anorbital ripples and suborbital ripples. During high-energy storm conditions, the nearshore zone undergoes significant changes; ripples are absent and plane beds and dunes predominate (Davis, 1978)

2.3.2 Subaqueous dunes

As waves shoal they generate oscillatory and unidirectional currents that may result in the formation of 2-dimensional and 3-dimensional bedforms with spacing's that range from 1m to 3 m (Ashley, 1990). 2D bedforms have straight crests, perpendicular to the flow, whereas the 3D varieties are defined by curved lee faces and scour pits (Ashley, 1990). The shape, symmetry and migration direction of the bedforms reflect the relative dominance of the onshore and offshore currents as well as, in some cases, modification by waves. As discussed by Ashley (1990), all large-scale, flow-transverse bedforms, irrespective of their origins in fluvial, coastal and shallow marine environments, share a similar formative process and may be assigned a single name. Therefore, the single term 'dune' is accepted, which the modifier subaqueous is attached to discriminate these bedforms from aeolian dunes and emphasize the difference between wave- and water-generated types (Ashley, 1990). The morphological-based classification scheme for subaqueous dunes is based on a series of descriptors (Table 2.1). This classification scheme categorises dunes based on 1) shape and size 2) superposition (simple or compound bedforms) and 3) details of bedform morphology.

Table 2.1: Classification scheme used to categorise subaqueous dunes (modified from Ashley, 1999)

Subaqueous Dunes					
First Order Descriptors		**Small**	**Medium**	**Large**	**Very large**
Size	Spacing (m)	0.6-5	5-10	10-100	> 100
	Height (m)	0.075-0.4	0.4-0.75	0.75-5	> 5
Shape	2-D				
	3-D				

2.3.3. Large scale bedforms

The nearshore zone is an active sedimentary environment that is often impacted by storm-waves and flows as a variety of wave-induced currents. Such an environment is conducive for forming some of the largest bedforms observed on the continental shelf (Goff et al., 2005). For example, oblique sand ridges or shoreface-connected ridges (SFCR's) have been studied over decades in the nearshore locations all over the world (Swift & Field, 1981; Parker et al., 1982; Dalrymple & Hoogendoorn, 1997; van de Meene & van Rijn, 2000; Park et al., 2003). These bedforms often form along the nearshore in regions where there is excess sediment supply and may reach lengths that span tens of kilometres long and heights of several meters. Additionally, other types of large bedforms have been recognised as ubiquitous in the nearshore where there is low sediment supply; these are referred to as rippled scour depressions: (RSD's) (Cacchione et al., 1984). RSD's are bathymetrically more subtle features (< 1 m of relief) in comparison to SFCR's and are orientated approximately shore-perpendicular. They are most clearly identified in backscatter imagery and are characterised as elongate deposits of coarser-grained sediment with long-wavelength bedforms depressed < 1 m below the surrounding finer-grained sediment (Reimnitz et al, 1976; Cacchione et al., 1984; Murray & Thieler, 2004; Ferrini & Flood, 2005; Garnaud et al., 2005; Holland & Elmore, 2008; Iacono & Guillen, 2008; Bellec et al., 2010). RSD's previously studied along the coasts of New Zealand and North America were classified based on their morphologies, depth and distance to the shore (Table 3.3.2) (Cacchione et al.,1984; Ferrini & Flood, 2005; Green et al., 2004). Based on the classification descriptions proposed by Green et al. (2004), Davis et al. (2013) provided a summarised scheme to categorise RSD's into five classes based on their depth, size and proximity to bedrock and/or reef (Table 2.2)

Table 2.2.: Summary of characteristics used to classify RSD's based on their distance from and orientation to the shore, proximity to bedrock, shape and size (after Davis et al., 2013)

Class	Description	References
Inshore	Centroid < 20 m	Cacchione et al., 1984 Davis et al., 2013
Offshore	Centroid > 20 m	
Inshore-rock associated	Centroid < 20 m, touching bedrock reef outcrop	
Offshore-rock associated	Centroid > 20 m, touching bedrock reef outcrop	
Mega	Total area > 10 km^2. Dominant sediment type along the portion of the coast	
Elongate	Length to width ratio greater than or equal to 3:1	Ferrini & Flood, 2005
Shore Parallel	Orientation to the shore: 0^0-30^0	
Shore normal	Orientation to the shore: 31^0-60^0	
Oblique	Orientation to the shore: 61^0-90^0	

2.3.4 Nearshore Sandbars

Sandbars are the largest bedforms in the nearshore and can be observed in the subtidal section on many sandy beaches (Davidson-Arnott, 2013). Sandbars are generally aligned roughly parallel to the shore and present an asymmetric profile; the seaward slope is relatively gentle, with rounded to flat crests, and the landward slope is often steeper with curved or rectilinear transition to the trough landward of the bars. The height of the bar, the water depth over the bar crest and the spacing between the bars are a function of the breaking wave height and their distance offshore. These bars exist under a wide variety of hydrodynamic systems, ranging from storm-dominated to swell-dominated wave environments and microtidal to macrotidal settings (Wijnberg & Kroon, 2002). There are a variety of mechanisms that may contribute to the formation of the bars through the influence sediment transport and water motion. Other mechanisms include those associated with the shoaling and breaking of waves, infragravity waves and rip cell circulation and undertow (Davidson-Arnott, 2010).

In general, the classification of nearshore bars is based on the locational and morphological characteristics relating to the influences of the wave climate, beach slope, tidal range and

proximity to the beach; as a result they may be distinguished into two wave-formed systems (Davidson-Arnott, 2010). The outer bar systems are formed and located seaward some distance from the shoreline and are distinctively uninfluenced by processes operating in the low-tide and foreshore terrace. On the other hand, the inner bar systems are present relatively close to the shoreline and are often found attached to the trough of transverse bars. This bar system is under the influence of developing beach cusps and rip cells.

Subtidal sandbars are generally limited to mesotidal conditions and are present in single- and multi-bar settings. These morphological features may assume wide range of configurations including longshore uniform bars, crescentic bars and obliquely positioned transverse bars (Ruessink & Ranasinghe, 2014). All the varieties are generally located at depth of less than 10 m and extend several kilometres along the shoreline. The morphological appearance of subtidal nearshore bars is highly variable. Therefore, as defined by Wijnberg & Kroon (2002), they may be classified into three morphological classes based on their plan view: two-dimensional longshore bar, three-dimensional longshore bar and shore-attached bars. The two-dimensional longshore bars are uniform and straight bars that are orientated parallel to the shoreline. The three-dimensional longshore bar systems are non-straight bars, with their onshore component protruding and unattached from the shore (Wijnberg & Kroon, 2002). Based on their longshore variability, they may range from regular crescentic patterns to irregular and complex patterns. As expressed by their name, shore-attached bars are those attached to the shore by one end and terminate at the other end by a rip channel. Their morphology is defined by well-developed rip and feeder channels (Wijnberg & Kroon, 2002).

2.4. Nearshore Sediments

Nearshore sediments are deposited on continental margins under a wide range of chemical and physical conditions (Chester, 2009). These sediments vary from gravel, sands, silts and mud, being composed of a mixture that includes terrigenous, authigenic and biogenic components. The properties of sediment such as the grain size and sediment fall velocity have been recognised as controlling factors in sediment transport processes and play a key role in coastal morphodynamics (Guillén & Hoekstra, 1997). As described by Wright & Short (1984), the grain size of the sediment is a discriminating factor in distinguishing between dissipative, intermediate and reflective beach and surf zone processes. In addition, the spatial distribution of grain sizes may be considered as a parameter to evaluate the various hydrodynamic

processes operating within the nearshore zone. The principal sources of sediment in the nearshore and beach include the large quantities of sand supplied by rivers, unconsolidated material released from sea cliffs due to erosion by waves, and material of biological origin such as skeletal remains (Inman & Jenkins, 2006).

A wave-dominated coast is one subjected to physical processes that are driven by wave-energy (Davis & Hayes, 1984). On these types of coasts, the sediment ranges from detrital sand to gravel-sized material that has undergone physical reworking and periods of burial before being deposited (Roy et al., 1994). The sediment on a wave-dominated coast mainly comprises gravel and sand that are well sorted and abraded and contain high proportions of resistant minerals and rock types (Roy et al., 1994). Cross-shore distribution of sediment in the nearshore mainly reflects the coarsest sediment located in the swash zone and wave breaker line, and finer sediment generally found landward of the breaker bar (Wang et al., 1998).

2. 5. Nearshore Sediment Transport

Sediment transport in the nearshore zone occurs as suspended load and bed load; and the hydrodynamic processes that mobilize and transport the sediment may be different for these two transport modes (Aagaard et al., 2013). Waves are responsible for the movement of sand as suspended-load, which occurs mainly in the surf zone because the turbulent flow of water and vertical mixing are most effective in causing the suspension of sediment (Inman, 2002). In addition, suspended load transport is computed as the cross product of sediment concentration and fluid velocity (Aagaard & Masselink, 1999). Wave-driven currents transport suspended sediment landward (and alongshore), as well as seaward (with alongshore components) (Manson et al., 2016)

The bed-load transport and morphodynamics of the nearshore zone are primarily controlled by the local wave and current environment (Niedoroda et al., 1984). Bed-load is defined as sediment grains moving in more or less constant contact with the bed by either rolling, jumping or sliding (Aagaard & Masselink, 1999). Bed-load transport is associated with the orbital motions of waves and is determined by the effective bed shear stresses on the grains (Aagaard & Masselink, 1999; Manson et al., 2016)

In the nearshore zone, longshore sediment transport occurs due to: 1) oblique wave action on the beach face due to swash motions. 2) Wave generated longshore currents in and just seaward

of the surf zone. 3) Some limited transport outside the breaker/surf zone by tidal and wind driven currents (Davidson-Arnott, 2010). Longshore currents are essential in the transport of sand and gravel to create beaches and dune systems, and large depositional features such as barrier islands and spits. They are also a key factor in defining littoral cells and determining local beach budgets, which are critical in the evaluation of many coastal engineering projects. Sediment movement by longshore transport mechanisms is often referred to as longshore drift. This refers to the movement of sediment in an alongshore direction that occurs in the nearshore zone and intertidal and supratidal beach (Cooper & Pilkey, 2004). A feedback mechanism exists between the processes that control longshore drift and the morphology that results from this type of transport (Calder & Mayer, 2003; Cooper & Pilkey, 2004).

Cross-shore sediment transport is the cumulative movement of beach and nearshore sediment perpendicular to the shore and driven by waves, wind and tidal action (Seymour, 2005). This results in the continuous movement of sand by suspension in the water column or in bed-load at the surface of the seafloor (Seymour, 2005). The physical processes responsible for cross-shore transport include incident and infragravity waves, near-bed seaward return flow and rip currents (Wright et al., 1991). The offshore and onshore sediment transport on various sandy beaches tends to be at equilibrium over periods of months to years; the offshore transports dominates during storm conditions while the onshore movement occurs during fairweather conditions (Wright et al., 1991).

2.6. Nearshore Surveying Systems

Nearshore research requires methods and instruments to observe the topographic surface as well as the variation in seabed composition in order to provide an overview analogous to aerial photography, resulting in the improved ability to interpret seafloor sedimentary processes (Hughes Clarke, 2012). Hydrographic surveys collect data that provides information about the geological process of the seafloor and the geomorphology in the coastal zone and continental shelf (Hughes Clarke et al., 1996). These surveying techniques have undergone fundamental changes in measurement technology and now include high-resolution systems like multibeam acoustics and airborne laser systems, which provide total coverage of the seafloor (International Hydrographic Organization, 1998). These technologies are capable of accurately measuring the bathymetry and compensate for wave induced motions and variable sound velocity in the water column (Dugan, et al., 2001).

Echo sounder surveying technology is an acoustic remote sensing technique that involves the transmission of a pulse of sound directed towards the seafloor (Makowski & Finkl, 2016). This surveying technology may be separated into single beam echo-sounders (SBES) and multibeam echo-sounders (MBES) systems, which are remote sensing acoustic instrumentation that play a fundamental role in determining the nature and shape of the seafloor (Goff & Kleinrock, 1991). Multibeam echo-sounder systems employ the use of various transmitting and receiving transducers that generate an array of narrow beams directly beneath the vessel, as well as laterally. These simultaneously measure the acoustic time-travel over a swath, which is dependent on the water depths surveyed and the specific settings of the instrumentation (Brown & Blondel, 2009; Preston, 2009). However, within the shallow sections of the nearshore, using multibeam is not always possible or feasible and single beam systems are typically employed instead to survey regions closer to the shore that are usually dominated by large breaking waves.

2.7. Numerical Wave Models

The estimation of wave height distribution, wave direction and wave periods have always been of importance in coastal processes research and engineering. There are several wave modelling systems that have been developed and used for solving coastal problems in a reliable, cost effective and time saving manner (Thomas & Dwarakish, 2015). Numerical models are used for wave hindcasting and forecasting in coastal and oceanic waters, which provides critical knowledge needed to effectively plan and manage activities in coastal and offshore locations. Third-generation wave models have been effectively used to model waves in the deep ocean (Booij et al., 1999). However, these wave models cannot be realistically applied to shallow water depths of 20-30 m due to: 1) the exclusion of the effects of depth-induced wave breaking in shallow waters and the triad wave-wave interaction. 2) the numerical techniques applied to small scale, shallow water regions are prohibitively more expensive (Booij et al., 1999).

As a result of the increase in coastal hazards in the past decades, there has been a growing need to extend the forecast of wave parameters into the nearshore region (van der Westhuysen, 2012). This requires high-resolution wave modelling systems that take into to consideration additional physical processes occurring in the nearshore, including: refraction, depth shoaling, nonlinear transfer of energy through wave-wave interaction, and wave energy dissipation as result of bottom friction, whitecapping and depth-induced breaking (Guillou, 2013).

2.7.1. Phase-Resolving vs. Phase-Averaged Wave Models

The propagation and dissipation of coastal and ocean waves can be simulated by two types of numerical models: phase-resolving wave transformation models or phased averaged spectral models (Thomas & Dwarakish, 2015). Phase-resolving models are commonly applied for solving wave diffraction and reflection that are caused by rapidly changing bottom topography and coastal structures, mainly in the vicinity of harbours (Chen et al., 2009). Beyond the surf zone, these types of models have been successfully applied in ocean engineering projects that require information concerning the shape and flow of waves (Roland & Ardhuin, 2014). Examples of phase-resolving models include CGWAVE (Demirbilek & Panchang, 1998) and BOUSS-2D (Nwogu & Demirbilek, 2001). The computational demand required for this class of wave models limits their domain to a relatively small scale, as the results present challenges for defining incident waves along open boundaries (Chen et al., 2009).

Spectral phase-averaged models are commonly used nowadays to solve problems of wave transformation conditions at varying scales from far field to near field (Rusu & Soares, 2013). Spectral wave models represent the random nature of the sea surface elevation in terms of its generalized Fourier spectrum, as it evolves in both space and time. Available models may also provide information about wave's asymmetry and skewness (Roland & Ardhuin, 2014).

2.7.2. Nearshore Wave Models

A study performed by Buckley & Lowe (2013) quantitatively reviewed and compared the results of three commonly used nearshore spectral wave models in a reef environment. Nearshore wave models have been primarily developed and calibrated on sandy beaches which have a mild slope; though Buckley & Lowe (2013) were able to test the suitability of these models to simulate various hydrodynamic processes (infragravity waves, wave setup and sea-swell) within a steep reef system. The three models were: SWAN (Booij et al., 1999), a phase-average spectral model, SWASH (Zijlema et al., 2011), phase-resolving nonlinear wave model, and XBeach (Roelvink et al., 2009), phase-average spectral model.

SWAN (Booij et al., 1999) was the first third-generation spectral wave model developed for nearshore applications. The model incorporates the nearshore physical processes of refraction, reflections, shoaling, wave-induced setup, triad wave-wave interaction, depth-induced breaking and bottom friction. In addition, the processes specific to deeper water such as white capping, quadruplet wave-wave integration and transfer of energy from wind are also included in this model (Rusu & Soares, 2013).

SWASH (Simulating WAves till Shore) is an open-source deterministic non-hydrostatic model that was developed by Stelling & Zijlema (2003) to predict the transformations of surface waves and varying shallow water flows in coastal waters. The wave model solves nonlinear shallow water equations that account for non-hydrostatic pressure and provide a description for the complexity of rapidly flowing water that are usually found in coastal flooding due to tsunamis and dyke breaks, wave transformation in the swash and surf zones, wave and current interaction, wave breaking, and wave run-up onto the shore (Zijlema et al., 2011).

XBeach is an open source nearshore morphodynamic model developed to simulate the hydrodynamic and morphologic evolution processes that impact sandy coasts, with time scales that are in the domain of storms and spatial scales up of hundreds of meters to kilometres (Roelvink et al. 2009). The hydrodynamic processes that the model simulates include short wave transformation (refraction, shoaling, and breaking), long wave transformation (generation, propagation and breaking), unsteady currents, wave-induced setup, and overwash and inundation. The model includes morphodynamic processes of bed load and suspended load sediment transport, bed update and breaching, dune face avalanching and the effects of vegetation and hard structures (Roelvink et al. 2009). The wave action equations solved by XBeach are similar to that of SWAN, however XBeach implements the wave equation for a single frequency, whereby the mean flows and infragravity wave motions are modelled in the deterministic mode, using a finite difference scheme to solve nonlinear shallow water equations (Buckley & Lowe, 2013).

As the demand to forecast waves in the nearshore area grows, other wave modelling techniques incorporate high-resolution nearshore nested implementations in their systems (van der Westhuysen, 2012). The first development in this regard was the global operational multigrid WAVEWATCH III model (Tolman, 2008). Subsequently, other examples of such system include the NOAA/National Weather Service's Nearshore Wave Prediction System (NWPS, Van der Westhuysen et al., 2013), which provides high-resolution nearshore wave simulations by applying SWAN and WW3 as underlying wave models (Gibbs et al, 2013). These systems operate on a global domain and resolve small-scale problems in the nearshore by nesting at various resolutions as required. In addition, unstructured grid spectral models provide further capabilities to solve the vast spatial scales with variable resolution, including the nearshore region (van der Westhuysen, 2012)

Chapter 3: Regional Setting

The study area for this study is located between Isipingo and Reunion Rocks, on the inner continental shelf, spanning depths of 2 m to 32 m bellow mean sea level. It covers an area of approximately 2.5 km^2. Reunion Rocks is located ~15 km south of Durban, on the KwaZulu-Natal coastline (Fig 3.1), and directly opposite the Isipingo fluvial/estuarine system.

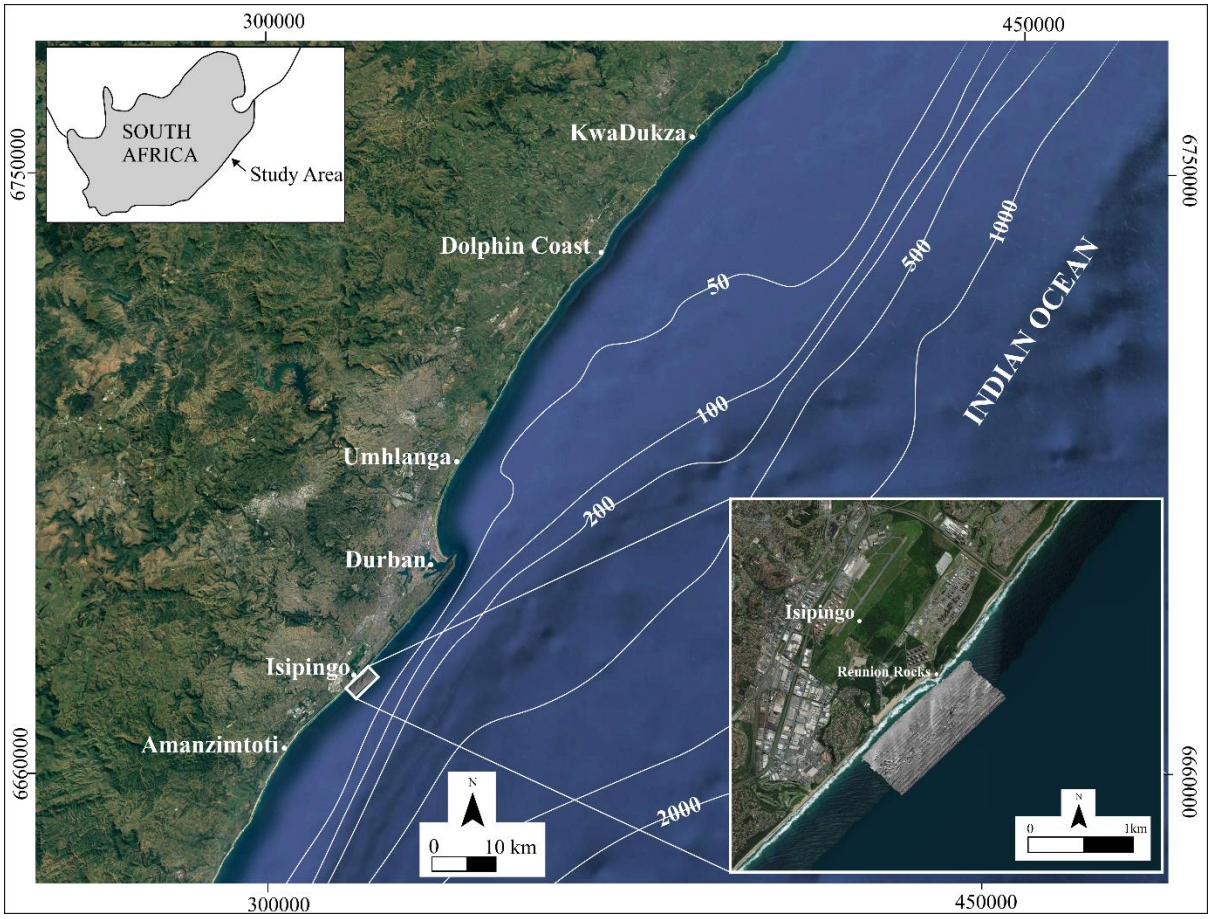

Figure 3.1: Locality map of the study area, detailing South Africa, the KwaZulu-Natal coastline and the location of the study area. Isobaths represented by white lines, detail the continental shelf morphology.

3.1. Regional Environmental Setting

3.1.1. Climate

The climate along the KwaZulu-Natal coastline is dominated by a subtropical high-pressure belt, characterized by elevated air humidity and mean annual rainfall of 845 mm (Palmer et al., 2011). Due to a steep hinterland gradient, there is orographic forcing of rain, with an annual average rainfall of approximately 1000 mm/ year in the region of Durban (Jury & Melice,

2000). The average monthly temperatures in Durban reach a maximum of 32.6^{o} C and a minimum of 5.8^{o} C. The moderating influence of the adjacent warm Indian Ocean characterises the temperatures by relatively low seasonal changes (Preston-Whyte & Tyson, 1988)

Dominant winds are almost equally distributed blowing alongshore from the northeast and southwest, and have an average wind speed of 40 km/hr (Cooper, 1991a). The northeast winds blow alongshore to onshore, transporting and depositing sediment on dunes and back beaches, whereas the southwest winds are generally alongshore to offshore depositing sediment below the high-watermark (Swart, 1987)

3.1.2. Oceanographic Setting

3.1.2.1 Wave climate

The coast of KwaZulu-Natal is affected by long southerly waves that are generated by eastward migrating cold fronts with low pressure zones moving to the south of Southern Africa (Smith et al., 2010). In comparison, northeasterly waves occur mostly as small amplitude wind waves that are superimposed on the southerly direction; these waves are dominant when the northeasterly wind is blowing over a considerable period of time (Rossouw, 1984). The KwaZulu-Natal coastline is impacted by extreme wave conditions associated with tropical cyclones and cut-off low (COL) storms (Smith, et al., 2010). The majority of the tropical cyclones move away from the continent in a south-easterly direction, and track back towards the Indian Ocean. It are these cyclones that occasionally remain semi-stationary south of Madagascar and cause the largest waves in the region (Mather & Stretch, 2012).

The South African Coast is exposed to a consistently high wave energy, with the wave height and wave period diminishing slightly northwards of the east and west coasts (Cooper, 2001). This renders the entire coastline as predominantly high energy, swell dominated environment. In particular, the wave climate of Durban was examined by Corbella & Stretch (2012). The average significant wave height is 1.68 m, the average wave direction as 130^{o} and the average peak period as 10.0 seconds. On record, the largest wave event took place in autumn and had a significant wave height of 8.5 m and an estimated return period of 32-61 years (Corbella & Stretch, 2012).

3.1.2.2 Tides

The tidal range for the South African coast is mostly uniform; the majority of the areas experience a spring tidal range of 1.8 m to 2 m rendering the coast as microtidal (tidal range < 2 m) (Davies, 1980; Cooper, 2001). In addition, Durban experiences mean the neap in the range between 0.6 m to 0.8 m. Extreme astronomical tides, storm surges and barometric surges enhance wave run-up levels and are responsible for widespread erosion that coincides with large wave events along the KZN coast (Smith et al., 2010). During the March 2007 event, the highest astronomical tides were recorded at 2.3 m above MSL in the Durban region (Mather & Stretch, 2012).

3.1.2.3 Currents

Oceanographically, the east coast shelf of southern Africa is dominated by the Agulhas Current, (Goodlad, 1978). The Agulhas Current is a vigorous geostrophic current that forms the western boundary of South Indian Ocean subtropical gyre (Martin & Flemming, 1986). The current flows polewards and forms off the northern Natal/Mozambique coast as result of the confluence of water that follows flow paths in areas of Madagascar and in the Mozambique Channel (Ramsay, 1994). The core of the current is located just offshore of the shelf break. Here the waters significantly affect the shelf, and as a consequence the inshore velocities of the Agulhas Current may attain velocities of 3 m/s where the shelf is most narrow (Ramsay, 1994; Lutjeharms, 2006). Offshore of Durban (Fig 3.2), the current core is located 15-100 km seaward at a depth of 1000 m and attains a current width of 100 km (Pearce et al., 1978).

The current transports suspended and bed load sediment onto the shelf and controls the physiological and biological processes of the shelf, which are responsible for producing the various sedimentological and biological features observed (Martin & Flemming, 1986; Ramsay, 1994). Where coastal offsets exist, inshore return currents form in the lee that flow counter to the poleward Agulhas Current (Lutjeharms, 2006). These create relatively vigorous south to north directed flows.

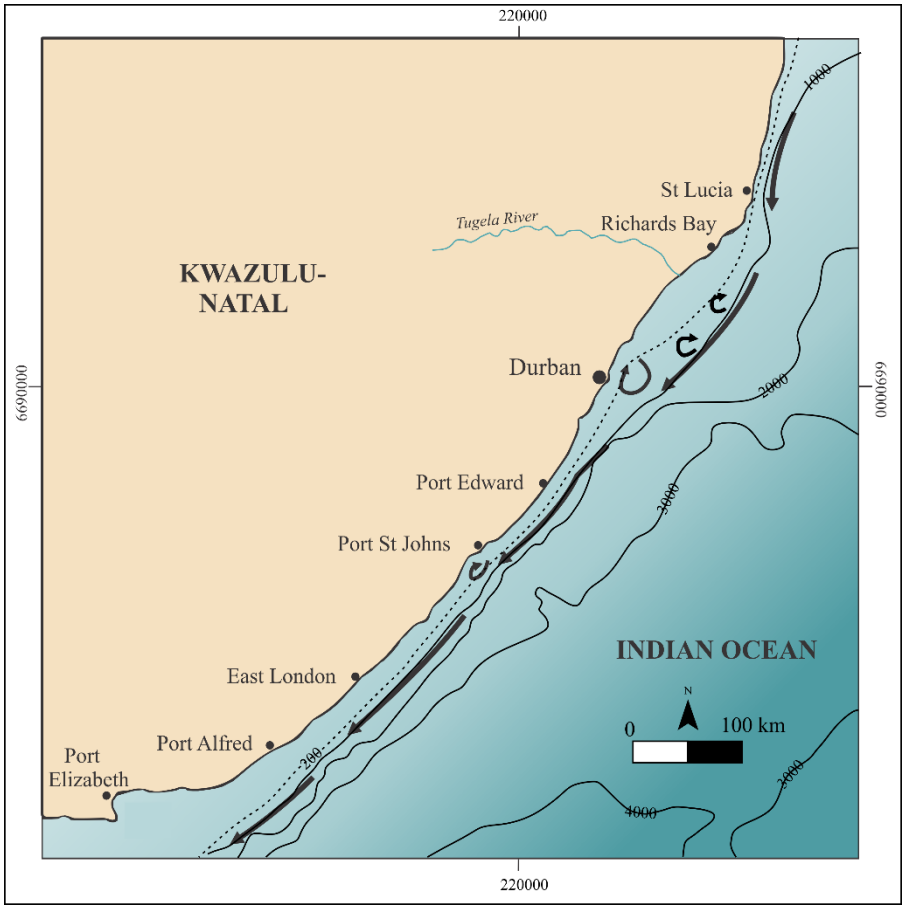

Figure 3.2: Geographic location of the northern Agulhas Current, indicating the path of the current (black arrows) following the continental slope. Isobaths are in meters (black lines) (Lutjeharms, 2006). Note the current reversals associated with the lees of coastal offsets.

3.1.4. Continental Shelf Morphology

When compared to the global average of ~ 50 km (Shepard, 1963), the continental shelf of the Durban region is much narrower (~ 18 km) (Green and Garlick, 2011). The shelf break occurs at a water depth of approximately 100 m and represents the gradual transition from outer continental shelf to steeply dipping basin sediment of the upper continental shelf (Green, 2009). Goodlad (1986) sub-divides the continental shelf of eastern South Africa into three morphological zones, with the Durban shelf constituting the narrowest section of the central region (Martin & Flemming, 1988)

The southeast African inner-shelf is marked by an active zone whereby terrigenous material is deposited and transported (Cawthra, et al., 2012). The inner to mid shelf consist of subaqueous dunes and the outer shelf is characterized by terrigenous gravels that are dominantly carbonate-rich with subordinate sediment drapes (Flemming, 1980). The sediment dispersal along the continental shelf is controlled by four main factors: the morphology of the upper continental

margin, wave regime and wind-driven circulation, the influence of the Agulhas Current, and sediment supply (Flemming, 1981, Smith et al, 2010).

3.1.5. Coastal Geomorphology

The east coast of South Africa is a high-energy, wave dominated (operating 40% of the year) environment that comprises coarse-grained reflective and intermediate beaches (Rossouw, 1984; Smith et al., 2010). Reflective beaches are narrow and steeply sloping, and consist of coarser sand in comparison to dissipative beaches. The intermediate types are identified by the presence or absence, form and nature of sand bars and rip currents in the surf zone. On these beaches, the nearshore zone is characterized by nearshore bars that are semi-continuous and parallel to the shore (Smith et al., 2010).

The geomorphology along the KZN coastline varies in accordance to the underlying geology of the region, the amount of sand within the coastal zone and the shape that these sand bodies have assumed (Cooper, 1994a). These geomorphological types range from rocky coasts that are typically encountered along the south of the coast (south of Uvongo) to a number of headland bound bays containing sandy beaches (Copper, 1991a,b), some of which form barriers across river mouths (Cooper, 2001).

Isipingo beach is situated between two pronounced headlands to form a sandy embayment (Cooper, 1991b). Both these headlands are large outcrops of beachrock and aeolianites that are resistant to erosion, the northern of which is termed Reunion Rocks. Cooper (1991b) monitored aerial photography of the area and noticed that the sandy embayment is a result of the obstruction of the headlands to the littoral sand transport, on what was a previous linear sandy shoreline (Cooper, 1991b). At the rear of the beach, a wide sand dune has been eroded by the retreating beach. The removal of sand from the undermined dune has delivered sediment onto the beach (Cooper, 1991b).

3.2. Regional and Local Geology

3.2.1 KwaZulu-Natal Basins

The offshore basins of the east coast of South Africa are fundamentally controlled by major crustal lineaments that dictate the differences in sedimentary histories of the basins (Dingle et al., 1983). According to Dingle et al. (1983) there are two contrasting styles observed, one on the North and the other on South. The sedimentary basins to the north of ~ 30^{o} S constitute part of a series of large compartmented grabens that trend approximately north to south and extend

from Cape St. Lucia to southern Mozambique. In contrast, south of ~ 30° S, the depocentres are confined to regions that are adjacent to and beyond the continent-ocean boundaries, which define the southern Natal Valley/Transkei Basin, bounded by the eastern edge of the Mozambique Ridge (Dingle et al., 1983).

The Durban Basin and Zululand Basin (Fig 3.3) are the two offshore basins that are located between Port Shepstone and Mozambique. The study area for this research forms part of the Durban Basin.

3.2.1.1 Durban Basin

The Durban Basin covers 10 000 km^2 and extends to the 2500 m isobath along the east coast of South Africa, between Port Shepstone and the Zululand Basin (Broad et al., 2006). Sedimentation in the basin was initiated prior to the break-up of Gondwana and originally formed an intracratonic basin (Dingle et al., 1983; Broad et al., 2006). According to Broad et al (2006), the Durban Basin is described as a structurally-complex rift basin that is located north of the termination of the Agulhas Falklands Fracture Zone.

The Tugela Cone (a subaqueous delta) borders the basin, located seaward of the continental shelf, and prograded into the Natal Valley area of the Mozambique Chanel since the Early Cretaceous (Goodlad, 1986). As described from boreholes and seismic investigations of the Durban harbour, Cretaceous strata are overlain by Cenozoic deposits (Leuci et al., 2002; Perritt et al., 2003). The top surface of the Cretaceous strata is located at a depth of 21-37 m below the harbour floor; the strata dip at 1^0-2^0 to the east and form a thickening wedge in a seaward direction (Leuci et al., 2002; Perritt et al., 2003).

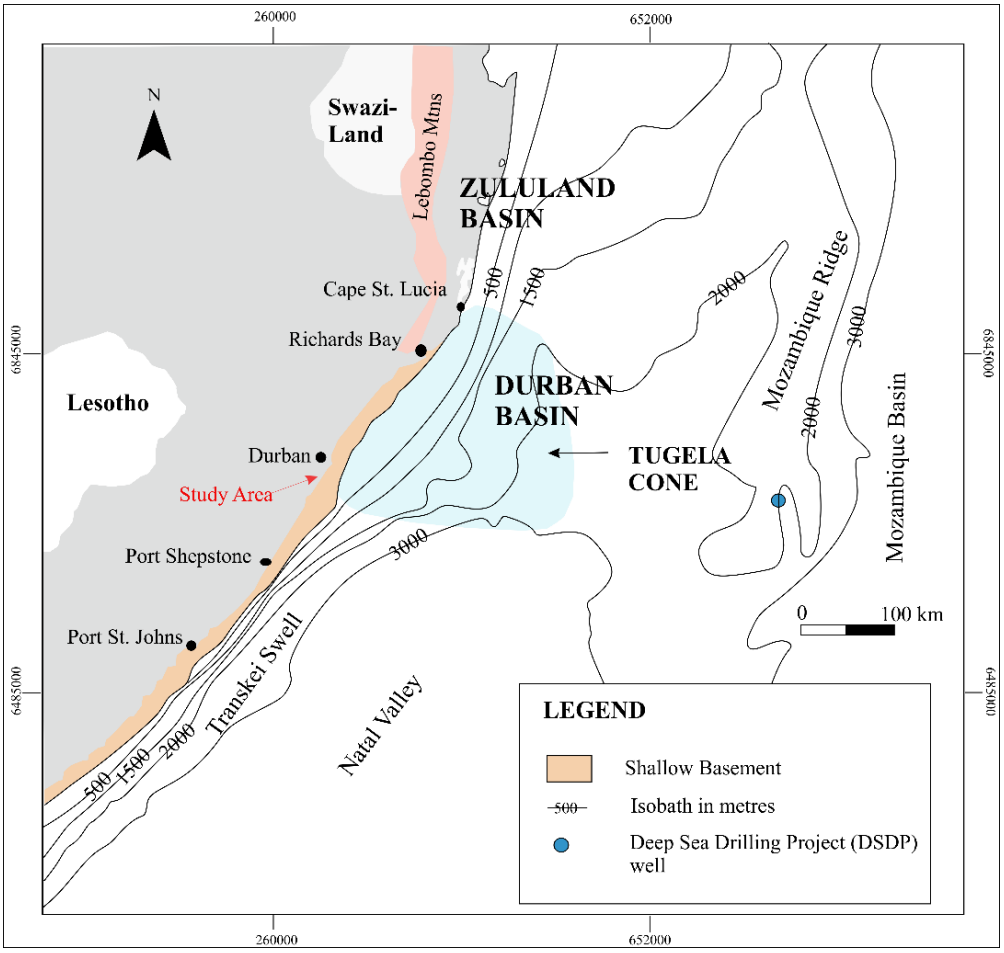

Figure 3.3: Regional context of the Durban and Zululand Basins

3.2.2 Cretaceous Deposits

The early Cretaceous Period was dominated by the tectonic movement of the Falkland microplate from its original position, south of the Durban Basin (Watkeys, 2006; Davids, 2009). The sediments of the Zululand Group were the first to be deposited on the newly formed continental margin, and crop out along the eastern flank of the Lebombo Ridge in Maputaland (Dingle et al., 1983). Mesozoic sediments up to 2000 m and dipping at 1^0-5^0 towards the east, have been documented by drilling on the coastal planes of Zululand, however, offshore, 4000 m of sediment are expected in the Durban Basin (Broad et al., 2006).

No significant Cretaceous deposits have been preserved along the KwaZulu-Natal coastline south of Cape St Lucia because the sedimentation patterns during the early Cretaceous were dependent on the relative accommodation space, which is controlled by sea-floor subsidence, still-stand, or the uplift of various parts of the continental margin of southern Africa (McMillan, 2003).

Upper Cretaceous units have been documented from numerous boreholes, despite there being no actual Cretaceous outcrop, including those drilled in the Durban Harbour and observed through seismic profiling (Dingle et al., 1983; Green and Garlick, 2011). The Upper Cretaceous transgression preceded southwards from St. Lucia (Coniacian age) to Durban (Santonian age) and westwards across the shelf beneath the Tugela Cone (Cenomanian age). Around Durban, post Cretaceous deposits subsequently covered all the Cretaceous units (Richardson, 2005).

3.2.3. Post Cretaceous/ Cenozoic Sequences

3.2.3.1 Tertiary Deposits

The Tertiary Period is characterised by two episodes of crustal uplift and the subsequent erosion of the landscapes, which had resulted in periods of river rejuvenation, escarpment retreat and non-preservation of sedimentary sequences as substantial amounts of sediment were bypassed and deposited in offshore basins (King & Maud, 1964; Hobday, 1982; Partridge et al., 2006). Significant deposits of Tertiary strata in KwaZulu-Natal (with the exception of Maputaland coastal plain) are observed on the continental shelf and continental slope, and occur as a seaward-thickening sedimentary prism dominated by the input of the Tugela River (Dingle et al., 1983).

3.2.3.2. Quaternary Deposits

The coast of KwaZulu-Natal is characterised by a continuous coastal plain that extends from Durban to Mozambique. Quaternary deposits comprise a Holocene sediment veneer, Pleistocene dune cordons of the Bluff Formation and deeply weathered, decalcified sand of the Berea Formation (SACS, 1980; Visser, 1989). Offshore KwaZulu-Natal, three Pleistocene to recent sequences unconformably overlie Cretaceous and Tertiary seaward dipping aged strata, as described by Martin & Flemming (1986).

Pleistocene deposits of the southeast coast of southern Africa are defined by coastal and offshore dune cordons of aeolianites and calcarenites; the remnants of coastal dune cordons that formed during periods of high sea-level, while offshore equivalents formed during lower sea levels and are preserved as coast-parallel reefs (Fig 3.5) (Martin & Flemming, 1988; Ramsay, 1994). At Durban, partially cemented calcareous sandstones and unconsolidated clay rich sands are preserved as the Berea and Bluff Ridges, and the Isipingo Formation, which all unconformably overlie Cretaceous-age rocks (Fig 3.4).

The Bluff Ridge is described as a compound dune comprising lithified aeolian sands of various ages and younger dune sands that are banked against a Pleistocene aged coastal dune complex, and overlain by Holocene sand (Cooper and Flores, 1991). Subsequent dating of the Bluff Ridge yielded an age of 182 000 ± 18 000 years B.P., however this age does not represent the initial age of sedimentation because of the possibility of numerous phases of cementation preserved (Ramsay et al.,1993; Ramsay & Cooper, 2002).

The Berea Ridge is limited to the narrow coastal belt where a single ridge, approximately one kilometre wide, is present adjacent to the shoreline. These NE-SW trending ridges are prominent landmarks in Durban and characterise the coastal zone of KwaZulu-Natal (Jermy & Mason, 1983; McCarthy, 1967). The Berea Ridge hosts a laterally extensive basal conglomerate that represents a beach deposit, over which aeolian sands were deposited and preserve large cross-bedded foresets (Jermy & Mason, 1983).

The Isipingo Formation, of the Maputaland Group, occurs as a rocky shoreline along the Bluff in Durban, and is dated as late Middle Pleistocene to Holocene (Roberts et al., 2006). The Formation incorporates aeolianites truncated by last interglacial-aged beaches that are calcified, as well as dune deposits. In certain regions, aeolianites have been planed by changes in sea level (Cawthra et al., 2012). On the northern portion of Bluff, the Formation extend 100 m below sea level, whereas in the southern portion it has a depth of 37 m below sea level. Therefore, the Isipingo Formation is equivalent to the Bluff Formation at the Bluff (Fig 3.4).

Unconsolidated Holocene sediment forms the deposits of recent sand accreted as beaches and dunes that extend along a narrow coastal belt and cover the seaward margin of the Bluff Ridge (Roberts et al., 2006) The bulk of the Holocene-age deposits are found offshore and blanket the inner and mid-shelf, forming an unconsolidated sediment wedge that attains a thickness of 25 m (Flemming, 1981; Martin and Flemming, 1986; Flemming and Hay, 1988; Birch, 1996; Ramsay et al., 1996; Green and Garlick, 2011).

On the continental shelf between Durban and Port Elizabeth, the nearshore zone is wave-dominated and is characterized by a Holocene sediment wedge that varies in thickness across different locations (Flemming, 1980). Within this wedge, sediment transported as bedload is dispersed across the region in which the carbonate component is added to constitute part of the bioclastic particles (Flemming, 1981). The bedload sediment is most probably transported by the wave-driven currents and wave-action. The nearshore sediment wedge progrades in the seaward direction until sufficient current strength entrains the sand. The transport of the

bedload sediment keeps the nearshore wedge in a dynamic equilibrium with the prevailing energy regime and any excess sand will become removed (Flemming, 1981). This lateral facies development is representative of the typical response pattern observed along the southeast coast of South Africa. Deviations from this pattern may be induced by the interaction between hydrodynamic factors and morphological features of the continental shelf. The development of the sand wedge in the nearshore zone may only occur if there are no topographic barriers obstructing its seaward growth. In the presence of barriers, the sediment is blocked behind to produce a vertical wedge rather than a horizontal one, therefore the absence or presence of these barriers are controlling factors in determining the escape of sediment offshore (Flemming, 1981).

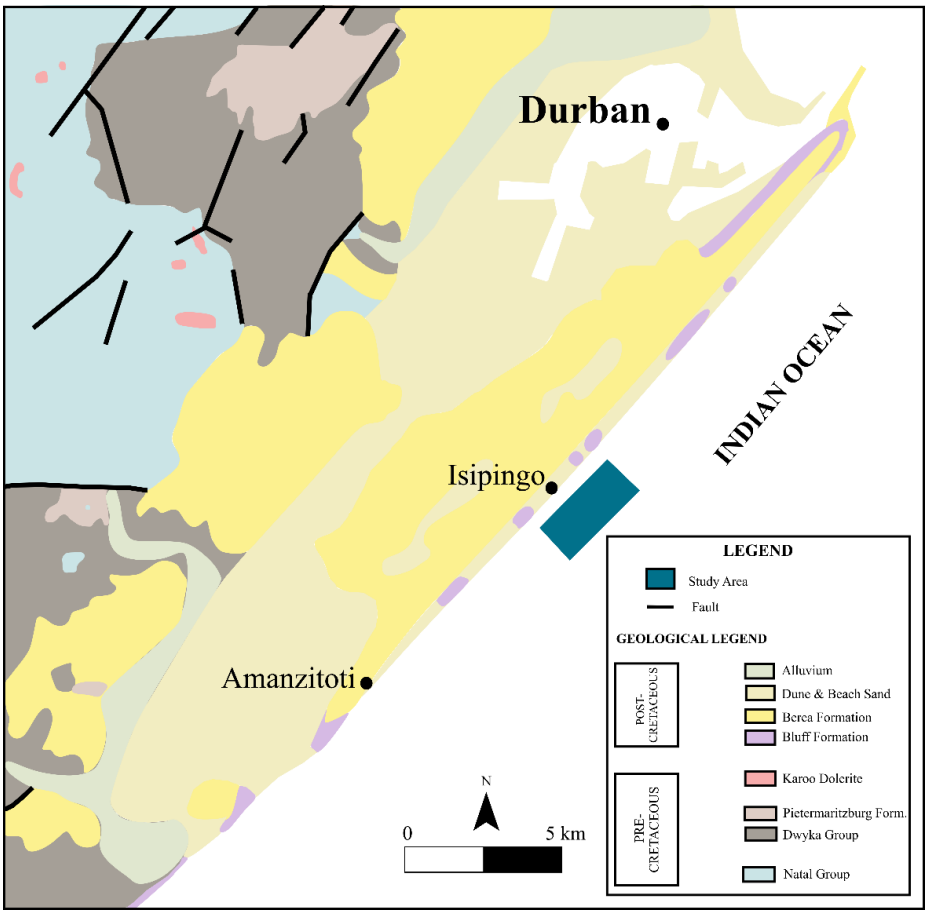

Figure 3.4: Onshore geological map of KwaZulu-Natal in relation to detailed study area (modified from the Council for Geoscience and King, 1962)

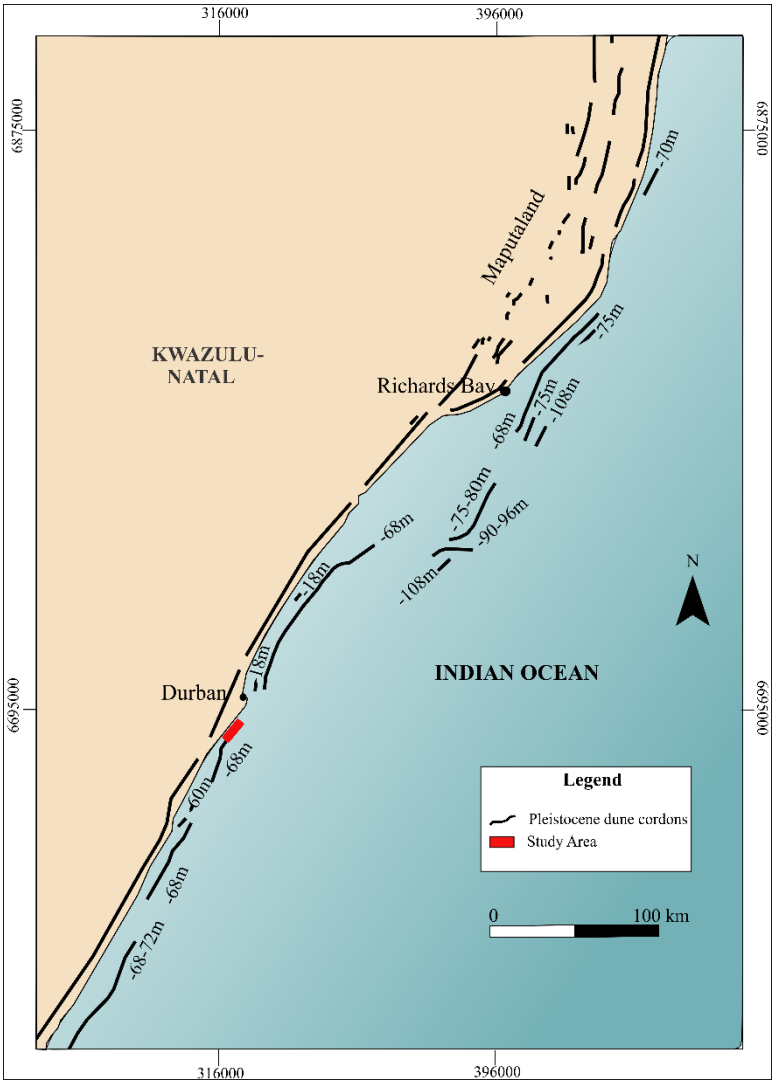

Figure 3.5: Distribution of consolidated aeolian cordons on the continental shelf and the Maputaland coastal plain in KwaZulu-Natal (modified from Martin & Flemming, 1987; 1988)

Chapter 4: Method and Materials

4.1. Geophysical Data Collection

The collection of geophysical data was a fundamental part of this research project, providing georeferenced seafloor data that served as a baseline for which other data types may be incorporated. The various types of data were combined to allow for final geomorphological interpretation and employed in the third-generation wave model SWAN (Simulation WAves Nearshore) to simulate the wave field of the survey area.

Multibeam bathymetric data were collected during two surveys. Survey 1 was completed before the winter season on the 12th April 2017 and 28th June 2017. The bathymetric grids produced during this survey allowed for the characterisation of the nearshore morphology of Isipingo embayment and implemented in wave modelling.

Bathymetric data for Survey 2 were collected after the winter season on the 8th and 12th of September 2017 and takes into consideration storm events occurring during the time frame between the two surveys. The datasets were used to analyse the morphological changes during a winter season and evaluate changes and mobility of characteristic bedforms and their relationships to wave induced forcing.

The acquisition hardware comprised four separate units: GPS system for navigation and positioning, a motion referencing device (for the vessel's heave, pitch and roll), a multibeam echosounder and sound velocity probe. All instruments were interfaced to the survey computer that acquired navigation and bathymetric data using *Hypack Hysweep* software.

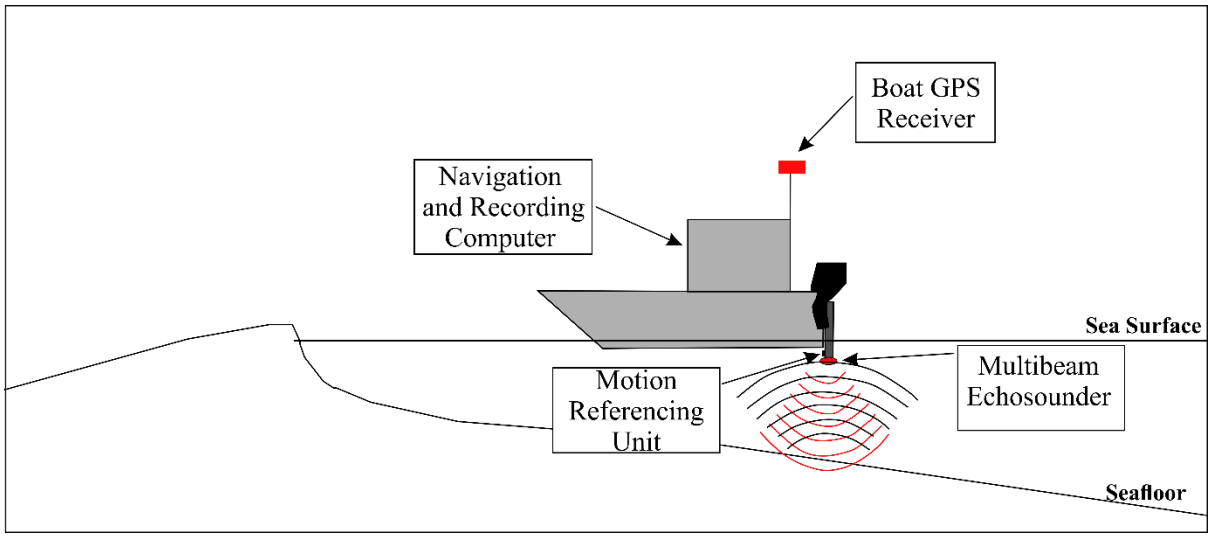

Figure 4.1: Diagrammatic representation of data acquisition method (modified after DeWitt et al., 2007)

4.1.1. Navigation and Co-ordinate System

Navigation and positioning was obtained through a Differential GPS system, with the base station on land being the Durban station of the South African TrigNet GNSS network, broadcasting the corrections through the Ntrip protocol, and a mobile GPS unit on board of the vessel. This composed of a dual antenna Vector VS330 GNSS Compass. The GPS system receives Real Time Kinematic (RTK) corrections from the base station and provides millimetre accuracy in real time. This allowed for a positioning accuracy of approximately 1 cm vertical and 2 cm horizontal direction. Positional data was received in geodetic datum WGS84 longitude and latitude. These data were converted into a projected co-ordinate system, which is ideally suited for geological mapping. All processed data and maps produced in this study used the Universal Transverse Mercator (UTM) projection, Central Meridian 33^0 East (Zone 36 South) on the WGS84 spheroid.

All soundings and co-ordinates were acquired on a survey computer using the software Hypack 2017. The program acquired, synchronised and transformed positional data, as well as displayed the vessel in real time, which allowed the survey track lines to be predetermined and planned for the entire survey area. A total of 80 shore-parallel tracklines were spaced at a 20 to 40 m intervals parallel to the shore of the Isipingo embayment, covering an area of 1.35 km x 2.80 km (Fig 4.2). The survey lines where planned for an overlap between swaths of more than 50%.

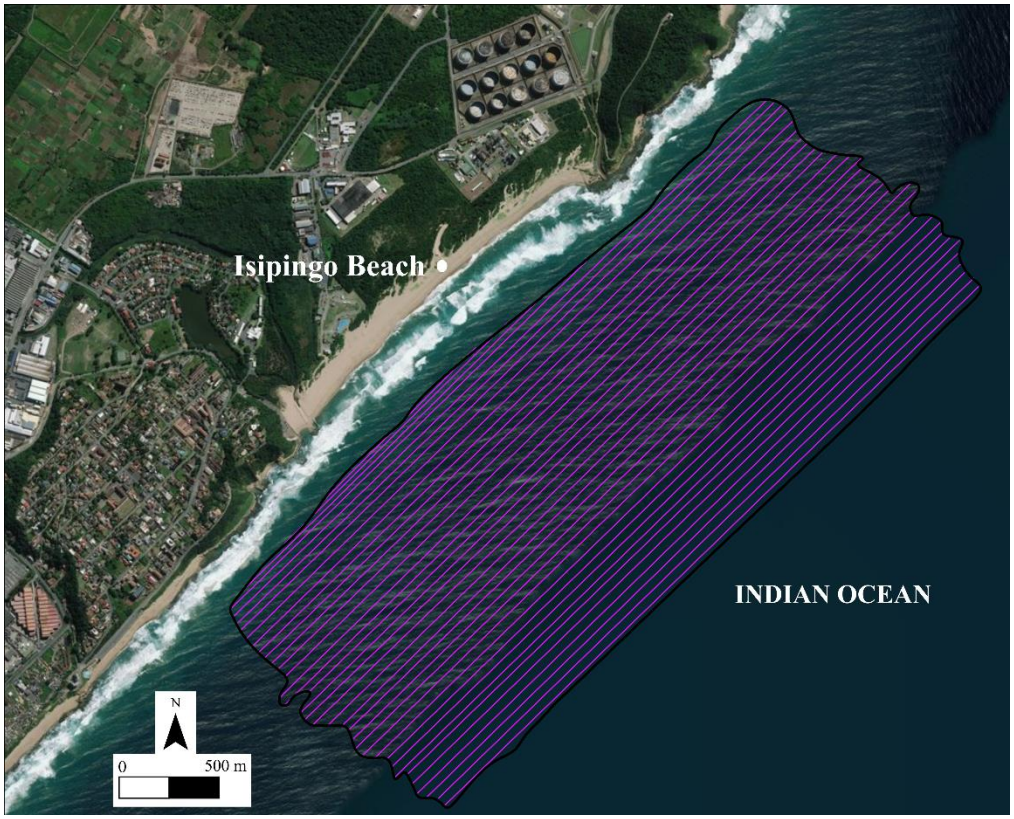

Figure 4.2: Survey tracklines (purple line) constructed parallel to coast for both Survey 1 and Survey 2

4.1.2. Multibeam Echo-sounder, Motion Reference Unit and Sound Velocity

The R2 SONIC 2024 and Reson 8101 were used to map the seafloor: and these meet the requirements of the US Army Corps Engineers (USACE) and the International Hydrographic Organisation (IHO) special order standards for hydrographic surveying. The first leg of Survey 1 was completed using the R2 SONIC 2024 system, which operates at a frequency of 200 kHz-400 kHz and has the firmware to simultaneously collect backscatter data in the traditional sidescan-sonar or Snippet format. The Reson 8101 was used during the second leg of Survey 1 and to complete the entirety of Survey 2, and performed at a frequency of 240 kHz.

Teledyne TSS Dynamic Motion Sensors (DMS) and F180 were utilised in addition to the multibeam echosounders to provide real time motion measurements of the vessel roll, pitch and heave. The information from the sensor is used in the post- processing of the data. Although the motion sensors reasonably compensated for the vessel motion, they are still exposed to constant drift, hence require visual monitoring during the survey and are subjected to alteration in the post-processing stage.

The sound velocity profiles were obtained using the Valeport Sound Velocity Profiler (SVP) (Survey 1) and Teledyne Odom Digibar Pro (Survey 2) which measured the temperature, salinity and depth of the water column at intervals of 0.5 m, and transformed it into sound velocity based on established constants. The sound velocity is required to correct the bathymetry data to account for changes in the velocity of sound on the water column in post-processing procedures.

Table 4.1: Summary of geophysical surveys and the equipment used at the Isipingo embayment, KwaZulu-Natal.

Survey	Cruise Date	Multibeam Echosounder	Sound Velocity Profiler	Motion Referencing Unit
Survey 1	12/04/2017	R2 SONIC 2024	Valeport SVP	F180
	28/06/2017	Reson 8101	Valeport SVP	DMS
Survey 2	08/09/2017	Reson 8101	Teledyne Odom Digibar Pro	F180
	12/09/2017	Reson 8101	Teledyne Odom Digibar Pro	F180

4.2. Geophysical Data Processing

A number of approaches exist to process multibeam bathymetric datasets. The processing may be interactive, with an operator-based processing method that may be performed in a subjective manner, or it may be semi-automated by using custom standardised filters (Huvenne et al., 2007). It is however essential that processing is carefully performed in order to make accurate seafloor interpretations. The simplest processing method includes the use of simple depths and angle gates, this allows for soundings at shallower or deeper water to be rejected at reasonable limits, based on the knowledge of the surveyed area or the outer beams where refraction is significant (Calder & Mayer, 2003). The more complex procedures involve the identification of soundings that do not correctly measure the depth, hence removing them from consideration. (Calder & Mayer, 2003).

4.2.1. Bathymetric Data

The process of producing a bathymetric grid involves several phases of processing the navigational data collected. Data processing consisted of cleaning and filtering of the raw data, noise reduction, and editing and visualization using the *Hypack Hysweep* 2017 software suite. *Hypack Hysweep* provides for the calibration, data collection and data processing of multibeam data within the Hypack package.

The multibeam transducer specifications are loaded through 64 bit *Hypack Hysweep MBMAX*, which applies corrections that may have not been applied during the survey. The raw data are edited by applying corrections, such as tide, draft and ray bending to the soundings to find the corrected depth or elevation (Hypack, 2016). The data allows for the import of a variety of data formats including XYZ formats, filled matrix (.*MTX), GSF format files and HS2 or HS2X format files. Hysweep facilitates the processing of raw multibeam data to a final XYZ file via a three-phase editing process:

The first stage reviews navigation tracklines, roll-pitch-heave, tide-and-draft, and sound velocity profile information. These tracklines are edited, the "True Heave" is applied, corrections were applied to eliminate heave drift, and tides are recomputed using RTK tides.

Stage 2 involves operator-based analysis and editing of swath data, whereby geometric filters were applied to remove any outliers. To improve data quality and depth accuracy of the collected MBES data, the beams were trimmed to 55^{o} either side of the nadir.

The third stage is area-based editing that allows points to be grouped into cells in which filters are applied based on the distributional z value of each cell. A sophisticated statistical filter called CUBE (Combined Uncertainty and Bathymetric Estimator), which is a standard feature in Hysweep, was applied to provide near-automated editing of data by cleaning and binning the data into suitable data density cells. These binned data were exported as an XYZ file.

Lastly, the TIN (Triangular Irregular Network) model program in Hypack Hysweep was applied to edited XYZ data files to create surface models by connecting adjacent data points in optimized triangles. The extracted TIN model may be saved as various files in the project directory.

The multibeam bathymetric maps were produced using the XYZ data of the TIN model. Gridding of the Z value was carried out in ArcMap version 10.3, a Geographic Information System (GIS) in which the final rasters were generated having a resolution of 1 m. The software

was used to combine, catalogue, analyse and display different datasets throughout the research project.

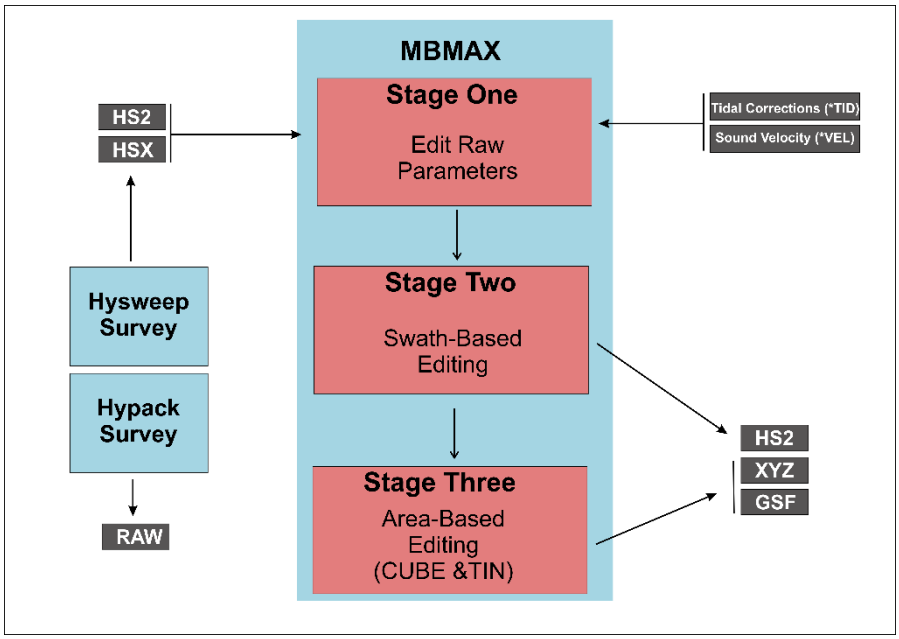

Figure 4.2: Overall data flow and procedure for geophysical data processing

4.3. Wave Modelling

4.3.1. SWAN Model Description

Simulating WAves Nearshore (SWAN) is a third-generation wave model that has been developed by the Delft University of Technology (Booij et al., 1999). The model is a freely available open source model that is commonly used by scientists and engineers for research and consultancy purposes (Holthuijsen, 2007). The waves in SWAN are described by the two-dimensional wave action density spectrum, even under non-linear conditions. The rationale is based on the possibility of predicting, with reasonable accuracy, the second-order moment even when nonlinear phenomena dominate (Booij et al., 1999). SWAN solves the time-dependant spectral action equation that accounts for refraction, depth shoaling, nonlinear transfer of energy through wave-wave interaction, and wave energy dissipation as result of bottom friction, whitecapping and depth-induced breaking (Guillou, 2013).

The model considers action density spectrum $N(\sigma, \theta)$ rather than the energy density spectrum $E(\sigma, \theta)$, because in the presence of ambient currents the action density is conserved whereas the energy density is not (Booij et al., 1999).

4.3.2. Model Setup

Offshore wave data were transferred to conditions in the nearshore of the Isipingo embayment using a nested modelling scheme. For this study, SWAN was run in stationary mode i.e. time is not considered in the calculations and waves are assumed to propagate instantaneously across the entire modelling domain, with the nested scheme composed of two computational grids. Model predictions were initialized at the boundaries of the the larger grid with the input parameters from the wave buoy data. SWAN was implemented to simulate the wave field, orbital motions and bed shear stresses over a range of statistically calculated wave conditions that included the mean conditions, 90%, 95% and 99% (extreme storms) exceedance levels. These parameters encompass the expected average conditions, moderate to strong storms, as well as extreme storms.

4.3.2.1. Computational Grids

The SWAN simulations require a defined computational area over which various wave conditions are to be modelled, with the equations being computed in the grid nodes. The parameters defined in the computational grid are related to the origin coordinates, length and resolution of the domain the X and Y dimensions (Fig 4.3). The nested modelling scheme allowed the model to be run on a coarse grid covering a regional scale, and on a nested fine grid covering the nearshore region.

The offshore computational grid (Fig. 4.4a) was defined by a uniform, regular (rectangular) grid, which covered an area of 10 km by 6 km from the Isipingo coastline, including ~0.5 km of land in the embayed region. This area covers approximately 11633 m latitude (301348 to 312981 m S) and 10678 m longitude (6673344 to 6684022 m E). The grid resolution was set as 50 m x 50 m, which implies 200 and 120 grid cells in the x- and y- direction respectively. SWAN's computational capabilities are set at a maximum resolution of 250 km x 250 km, hence the specified resolutions are well within SWAN's limitations. This 50 m mesh was sufficient to model the transfer of wave energy in deep water to shallow water, with the main zone of interest occurring at 30 m depth.

The input boundary conditions for the finer nearshore grid were determined from the computations in the coarse offshore grid. A regular structured grid with a 5 m resolution was used to represent the computational domain of the nearshore, matching the bathymetric grid

that is representative of the bottom conditions of the region. The nearshore computational grid is smaller than the regional grid, covering an area of 1.2 km x 2.8 km with 249 grid cells in the x directions and 554 grid cells in the y direction (Fig. 4.4b). For the purpose of this study, the chosen grid spacing was sufficient to achieve the project objectives since the main area of interest is the nearshore occurring at depths of 3 m to 30 m.

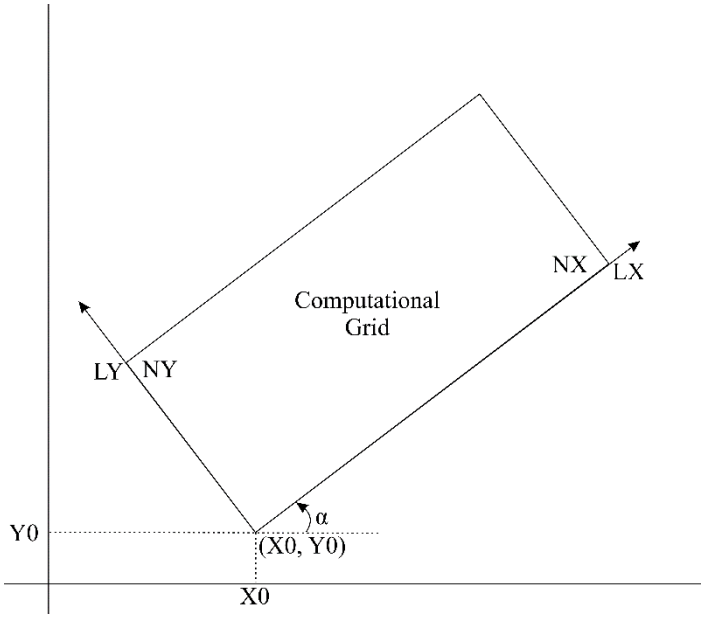

Figure 4.3: Computational grid set up, with coordinates of the origin (X0) and (Y0), the orientation (α) and the grid point numbering of the computational grid with respect to the coordinates system used.

4.3.2.2. Bathymetric Grids

The bathymetric grids are read as an input grid file in SWAN, which is sufficiently large to cover completely the computational grid and is representative of the bottom conditions of the study area. The nested modelling scheme requires bathymetric grids for both the offshore and nearshore computational grids. The regional run was performed on bathymetric data collected by Marine Geosolutions and Subtech in 2010. Single beam and multibeam bathymetry datasets from the above surveys were combined and resampled to a resolution of 50 m and read as a bottom file (*BOT file) in SWAN. The nearshore scheme was modelled on data collected from Survey 1 for this research project, which was resampled to a resolution of 5 m to allow for computational efficiency.

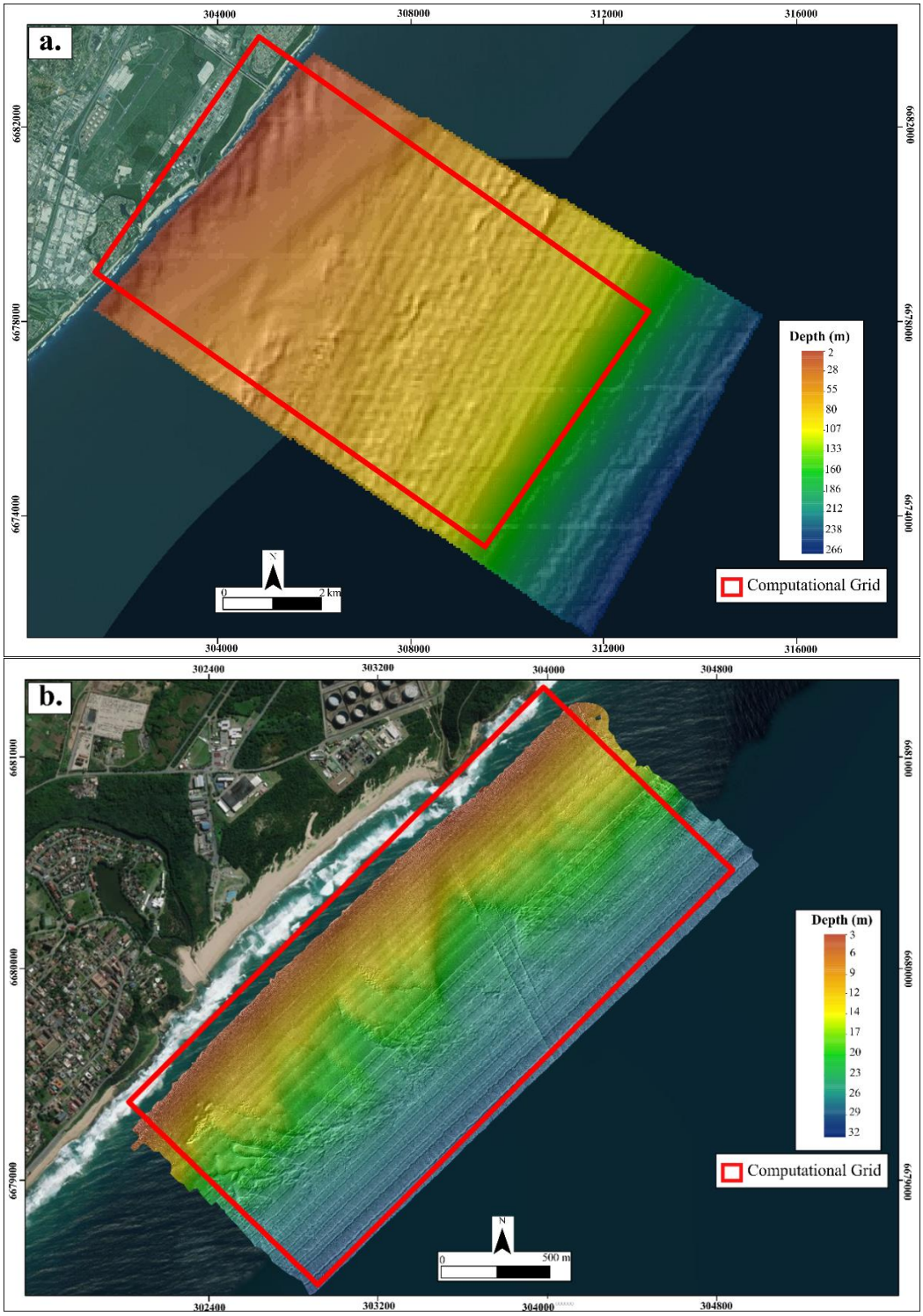

Figure 4.4: Offshore (a.) and nearshore (b.) bathymetric grid and computational grid used in SWAN model

4.3.2.3. Boundary Conditions

Wave data for this study were obtained from a directional Datawell Waverider buoy presently operational off Durban. The CSIR Waverider is located in 30 m water depth off the Bluff, about

1.7 km from the shore at a longitude and latitude of 31.0767^0 and 29.884^0, respectively. Wave data analysed in this study was collected on an hourly basis between 23/08/2007 and 31/07/2017. The nearshore wave parameters implemented in SWAN were computed over a range of statically calculated offshore wave conditions, including the mean, 90%, 95% and 99% exceedance levels that represent an increase from fairweather conditions (mean) to the extreme storms (99% exceedance levels). The significant wave height, mean wave period, wave direction and directional spreading were computed from the wave buoy dataset for each varying condition by determining the mean values and respective quantiles (90%, 95% and 99%) (Table 4.2).

The wave conditions implemented in the model run for the offshore computation are used directly to run SWAN for the nearshore simulation by the use of nesting commands, without the need for any further details regarding the wave spectra and parameters.

4.3.2.3.1. March 2007 Storm Event

Besides the wave conditions based on the statistical analysis of the wave records from the wave buoy, the March 2007 storm event has been identified as the largest storm event on record for the KwaZulu-Natal coast (Corbella & Stretch, 2012). Extreme conditions were observed between 19th and 20th March 2007, when a large cut off low-pressure system remained stable off the KZN coast, causing severe erosion along approximately 350 km of the KwaZulu-Natal coastline (Corbella & Stretch, 2012). Taking into consideration the importance and impact of the storm event on the coastline of KwaZulu-Natal, the storm and its respective 10 and 100 year recurrence intervals were modelled independently in SWAN.

Input wave boundary conditions for the storm were obtained from Corbella & Stretch (2012). The significant wave height was recorded as 8.5 m, with a peak period of 16.6 s (Table 4.4.1) that coincided with an extreme high tide of 2.2 m above chart datum. The wave direction and directional spreading were not presented by Corbella & Stretch (2012), hence these values were assumed to be consistent with the conditions experienced under the 99% exceedance levels. A wave direction of 194° and directional spreading of 45.76° were used as inputs to the SWAN model.

Further analysis into the wave field of the storm event required the consideration of the 10 and 100 year recurrence intervals for the storm parameters. The specific return periods become of

importance for coastal hazard analysis (Corbella & Stretch, 2012). The wave boundary conditions were provided by Corbella & Stretch (2012) using a copula model that simulated events by incorporating the dependence between the significant wave height, duration and peak period. The wave and directional spreading assumed to coincide with the values calculated for the 99 % exceedance levels (Table 4.2).

Table 4.2: Wave parameters calculated from wave buoy datasets as well as for the 2007 storm event and respective 10 and 100 year recurrence intervals and implemented in SWAN

Wave Conditions	Significant Wave Height (m)	Wave Peak Period (sec)	Wave Direction (°)	Spreading Direction (°)
Mean	1.68	9.96	131	28.83
90%	2.30	14.20	166	34.02
95%	2.58	14.29	171	37.60
99%	3.21	16.60	194	45.76
2007	8.50	16.60	194	45.75
10 year	8.60	16.60	194	45.75
100 year	9.80	16.60	194	45.75

4.3.2.4. Physical Processes

There are several wave transformation and propagation processes that can be activated/deactivated in SWAN. The simulations for this study were run in third-generation mode in SWAN and accounted for the following physical processes:

- Non-linear triad wave-wave interaction which is an important process in coastal zones and takes into consideration the generation of wave coupling and generation of double waves (Holthuijsen, 2007)
- Bottom friction dissipation using the empirical JONSWAP expression according to Hasselmann et al. (1973) of 0.067 m^2/s^3
- Breaking dissipation was activated to account for depth-induced breaking and to determine the wave height to water depth ratio. The default bore-based model was provided by Battjes & Janssen (1978), who suggested a depth-induced wave breaking parameter of (γ) 0.78.
- Diffraction is not included in the default computations of SWAN and needed to be activated for the study region.

- Whitecapping accounts for energy dissipation when the maximum wave steepness of H_{max}/L = ~0.14 is exceeded (Holthuijsen, 2007). This dissipation process has a small impact on the simulation output for this study.

4.3.2.5 Output Requests

The nearshore wave field was computed for the varying wave conditions and included the output variables:

- Significant wave height (Hs)
- Peak wave period (Tp)
- Wave direction (DIR)
- Peak wave direction (PDIR)
- Bottom orbital velocity (Urms)

4.3.2.6. Bed Shear Stress

Modelling wave-induced potential sediment entrainment and transport under varying wave conditions is achieved by evaluating the threshold bed shear stresses that are based upon the modified Shields parameters for coarse sediment (cf. Soulsby, 1997). The spatial variability of bed shear stresses is dependent on the bottom orbital velocity amplitude, which SWAN outputs as the root-mean-square orbital motion near the bottom (U_{rms}). The threshold bed shear stress for initiation of sediment transport (T_{cr}) is evaluated for coarse sand (d_{50}= 0.5 to 2 mm) and fine gravel (d_{50}= 2 to 8 mm), with the T_{cr} values of 0.63 N/m^2 obtained for the mean class value of coarse sand (d_{50} = 1.2 mm) and 4.00 N/m^2 for fine gravel (d_{50} = 5 mm) (C. Loureiro, pers. comm). Bed shear stresses under waves (T_{ws}) are considered in terms of a flat, non-rippled bed whereby only the wave-skin friction component is required to determine the hydrodynamic forcing acting on the bed and the driving potential for sediment transport and entrainment. For the entire modelling domain, T_{ws} was computed using the bottom orbital velocity (U_w) modelled by SWAN and the wave friction factor (f_w) according to Soulsby (1997):

$$T_{ws} = \tfrac{1}{2} p f_w U_w^2$$

where *Tws* is the bed shear stress (N/m^2), p is the density of seawater (1027 kg/m^3), U_w is the U_{rms} computed by SWAN and f_w calculated by using Soulsby's (1997) formulation:

$$f_w = 1.39(A/z_0)^{-0.52}$$

where A is the semi-orbital excursion ($U_w T/2\pi$) and z_0 is the bed roughness ($d_{50}/12$) in meters.

4.4. Morphological Changes

The high-resolution bathymetry collected in April 2017 and September 2017 were compared to assess the morphological changes that occurred in the nearshore over the winter period. These changes encompass storm events that had occurred. To analyse the changes between the subsequent surveys, post-winter bathymetry was subtracted from pre-winter bathymetry using the mathematical tools available in ArcMap 10.2. The resulting bathymetric change map shows morphological changes as areas of erosion, deposition and no change. Morphological changes were classified by an interval size of 0.5 m, with areas of erosion ranging between -2.9 m to -0.5 m and accretion defined in the range of 0.5 m to 5 m. Morphological changes in the category of ± 0.5 m are considered regions of "no change" to account for survey inaccuracies. Such inaccuracies were encountered during the second leg (28/06/2017) of Survey 1, when collecting bathymetric data in the offshore region of the study area. Instrumental limitations of the motion referencing unit caused a roll and yaw error that could not be removed during post-processing of data. These errors became more pronounced at depths greater than 19 m. Polygons were digitized to indicate the major variations in the location and patterns of morphological features that were identified in this study during the discussed time frame.

Chapter 5: Results

5.1. Bathymetry

High resolution multibeam bathymetry data from the Isipingo embayment spans a depth range (referenced to mean sea-level, MSL) from 3 m in the shallowest surveyed in the surf zone, to a maximum depth of 33 m in the offshore region (Fig. 5.1.1). The seafloor of the study area is characterised by varying bathymetric gradients (Fig.5.1.2) that range from gently sloping seafloor (0^o to 4^o) to moderately sloping seafloor (4^o to 8.5^o). The shallower region (3 m -12 m depth) is defined by seafloor gradients that range from 0^o to 8^o, with the steeper regions located towards the northeastern (NE) headland. Deflections in the contour pattern and areas of steeper slopes are observed at 11 m to 24 m water depth and flatten seaward. The cross-sectional profiles (Fig 5.1.1) indicate the general bathymetric trend of the embayment. Overall, the bathymetric configuration of the study area is relatively regular, with bedforms of varying scales formed along the unconsolidated sediment cover. These range from ridges to dunes and are discussed below from a hierarchical perspective based on Ashley (1990).

5.1.1. Outcrop

A prominent outcrop occurs in the inshore area of the embayment (Fig. 5.1.3), taking the form of irregular seafloor relief. The most prominent outcrop section occurs adjacent to the southern headland of the embayment, approximately 400 m from the shoreline at water depths of 14 m to 17 m. This outcrop is distinguished by pinnacles that rise to a height of ~3 m with particularly rugged relief, expressed as areas of irregular and variable slope values (Fig. 5.1.2.). Smaller scattered outcrop sections occur at slightly shallower depths of 12 m to 15 m. Each of these outcrops are associated with some degree of sediment scouring around their edges, resulting in a steeper slope (4^o to 8^o) on the seaward side of the outcrops compared to the surrounding seafloor (1^o to 5^o).

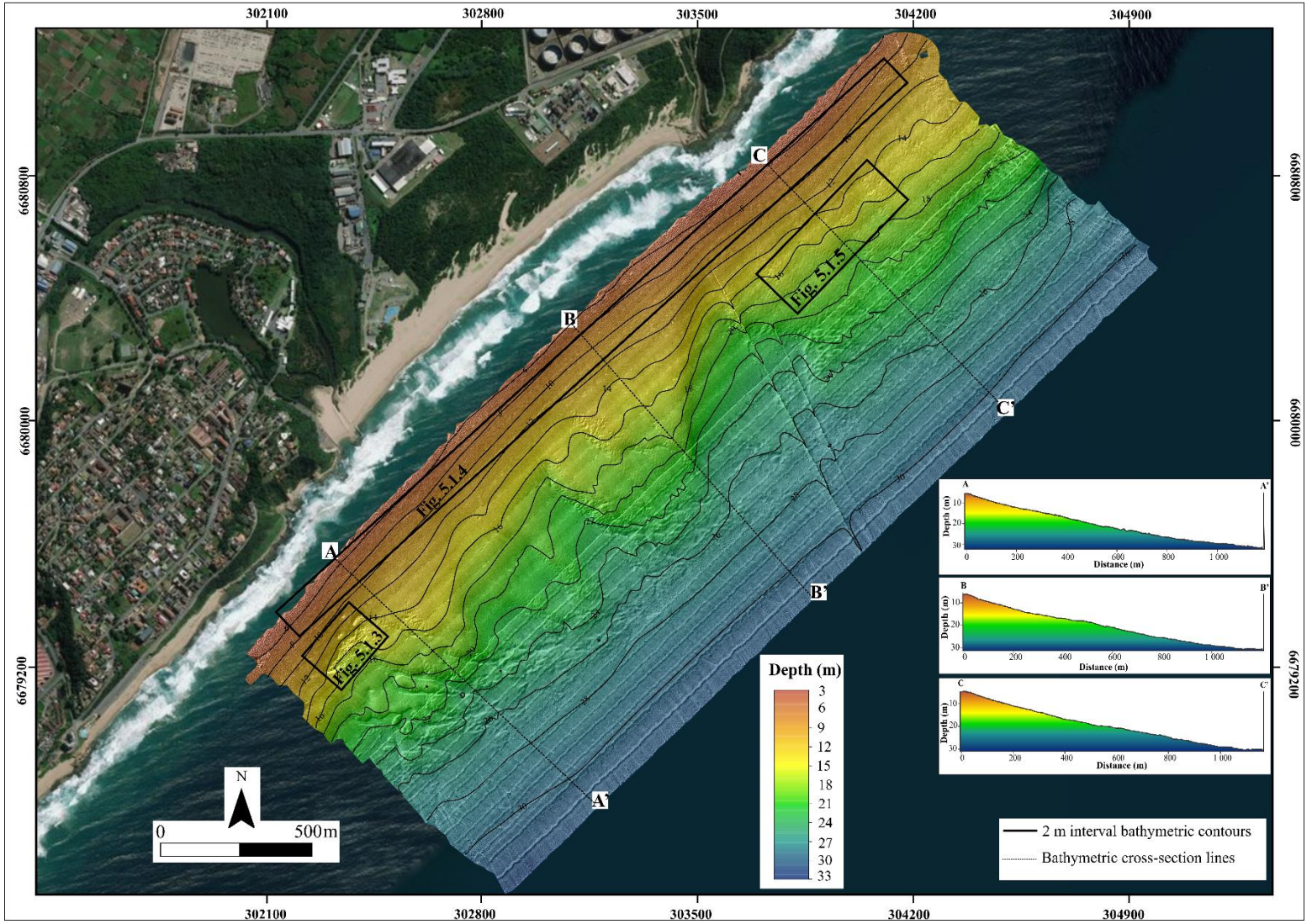

Figure 5.1.1: Bathymetry of the Isipingo embayment, KwaZulu-Natal. Coordinates in UTM 36S.

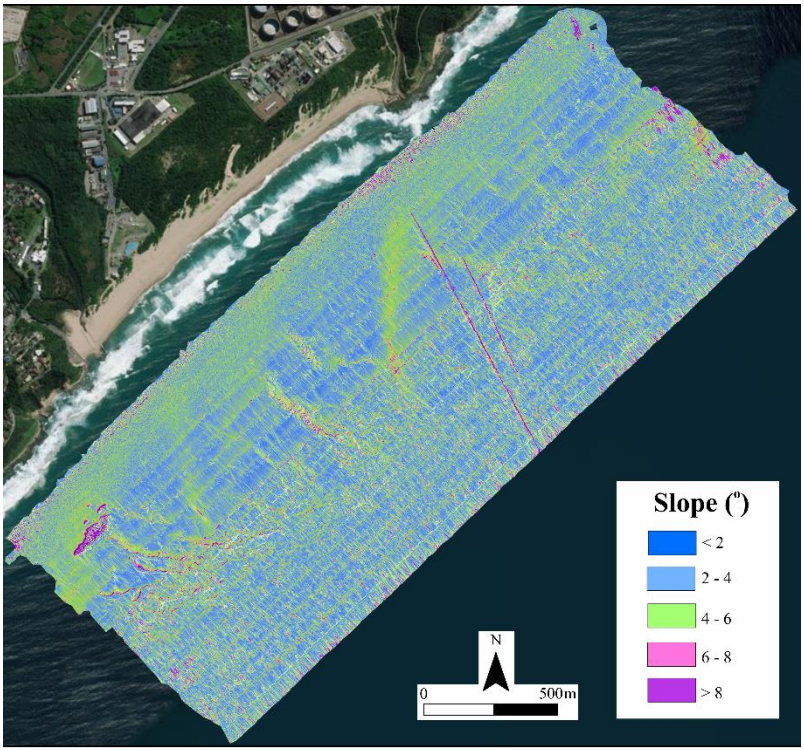

Figure 5.1.2. Slope map of the seafloor of the Isipingo embayment

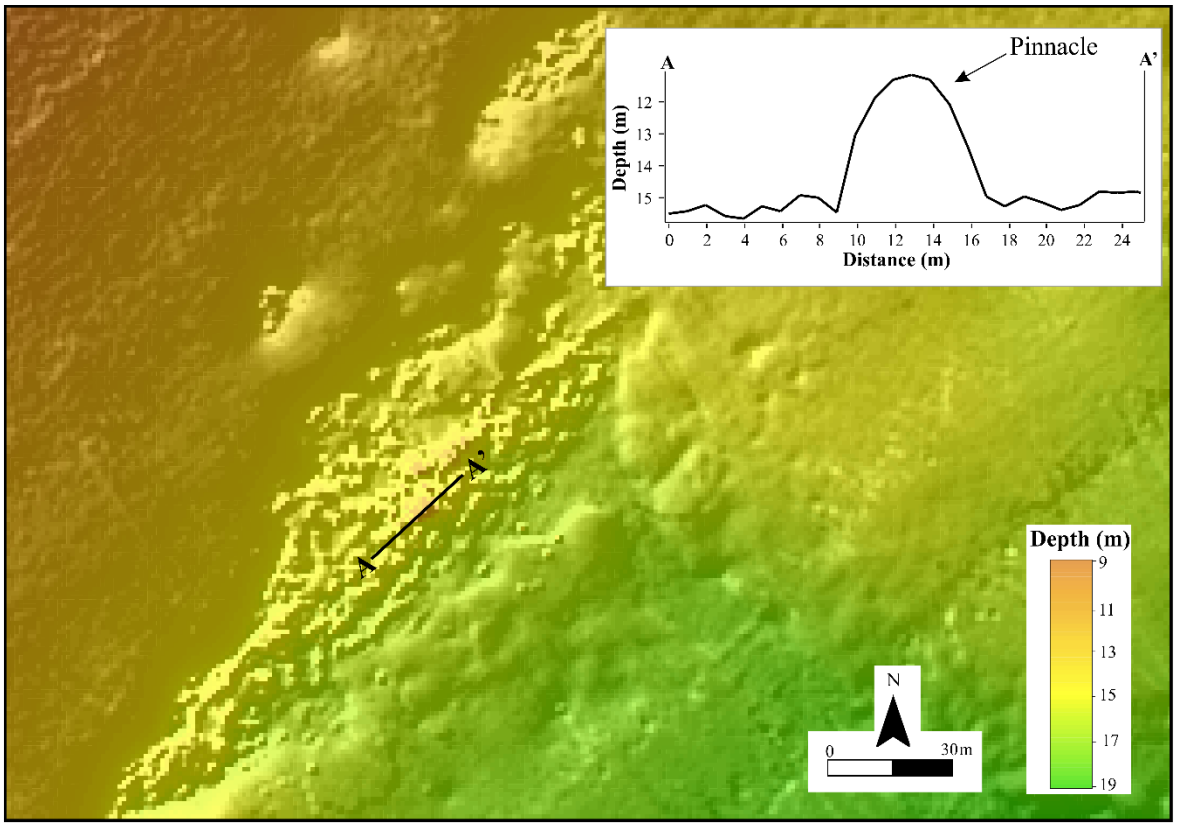

Figure 5.1.3. Bathymetry of the outcrop area with accompanying bathymetric cross-sectional profile

5.1.2. Small Subaqueous Dunes

The inshore region of the survey area is defined by a series of small dunes that extend from the inshore survey limits to depths of ~ 10 m (Fig. 5.1.4a). The dune long-axes trend southwest-northeast (shore parallel), with amplitudes (η) of 0.05 m to 0.2 m, and wavelengths (λ) of 2 m to 6 m. These features are most prominent closest to the shore and gradually flatten and widen with depth. The small dunes in the embayment (Fig. 5.1.4 Profiles C & D) have the smallest amplitudes (η= 0.05m) and wavelengths (λ= 3 m); whereas small dunes located towards the NE headland (Fig 5.1.4. Profile E) are significantly larger (η= 0.2 m, λ= 6 m). The small dunes are characterised by sharp crests, although round-crested varieties are also present but mostly uncommon. These are orientated 4^0- 8^0 north-south, which is sub-parallel to the shoreline.

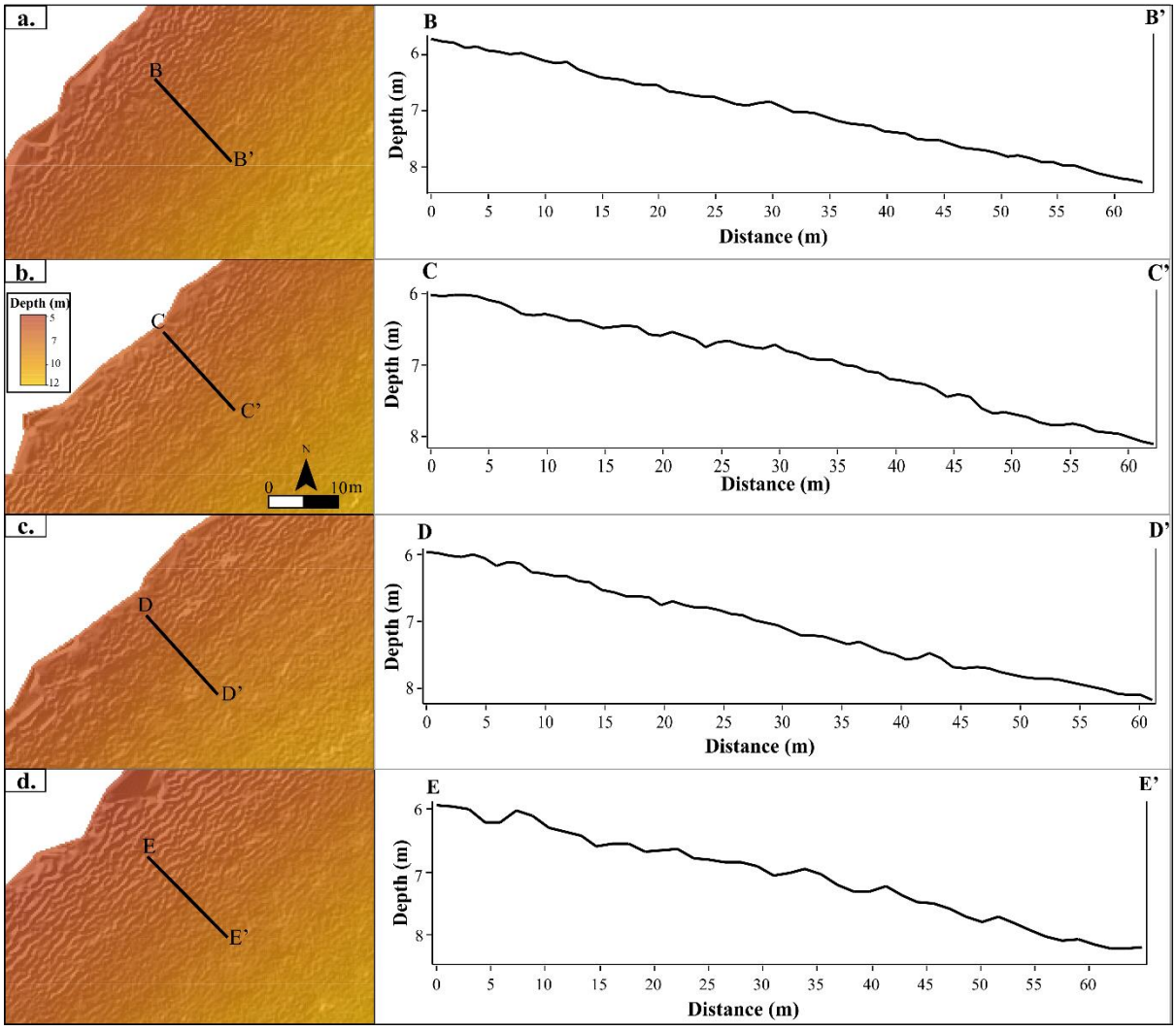

Figure 5.1.4: Cross-sectional locations through the small subaqueous dune fields with accompanying bathymetric cross-section profiles

5.1.3. Very large Subaqueous Dunes

A series of very large subaqueous dunes occur throughout the study area, but become more prominent towards the north-eastern end of the embayment, offshore the northern headland (Fig. 5.1.1). These bedforms are characterised by an average wavelength of 200 m and amplitudes that vary from 1 m to 1.3 m. In contrast, to the shore parallel dunes, the crests of the subaqueous dunes are orientated perpendicular to the coastline at an angle of 270° to 327°. The irregular surface of the bathymetric profiles across the subaqueous dunes shows that smaller bedforms are superimposed on the larger dunes (Fig. 5.1.5.). These smaller scale bedforms have, on average, wavelengths and amplitudes of 17.5 m and 0.2 m respectively, categorising them as small subaqueous dunes that are orientated shore-normal.

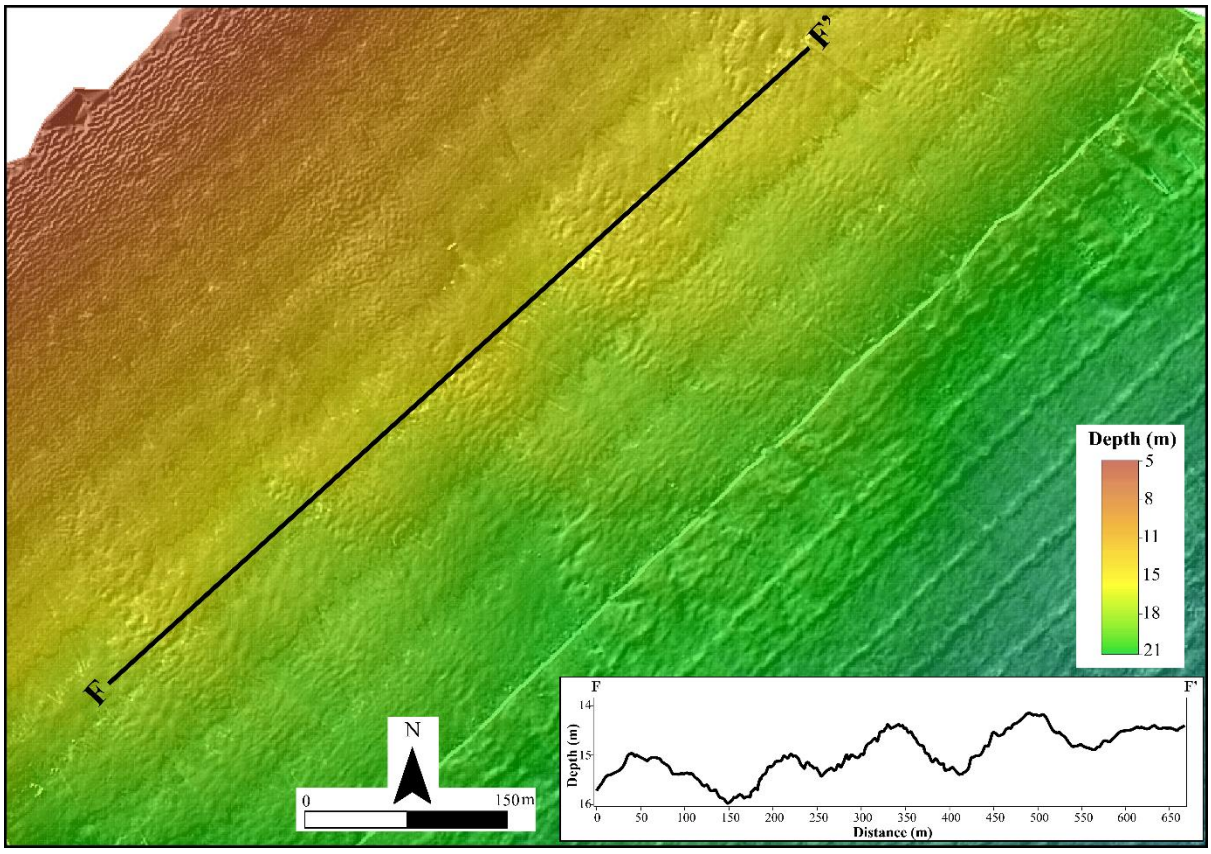

Figure 5.1.5: Subaqueous dunes with accompanying bathymetric cross-section profile. Note the superimposed smaller dunes on the larger wavelength features.

5.1.4. Shoreface-Connected Ridges

Shoreface-connected ridges (SFCR's) form prominent bathymetric highs and occur from depths of between 9 m and 24 m (Fig. 5.1.6). These features occur regionally and are not strictly associated with the embayment. Two SFCR's have been identified in the main embayment,

each varying in size and configuration, with an alongshore spacing of up to 1 km between their successive crests. Overall, the SFCR's are on the order of 400 m to 500 m in wavelength, with amplitudes of ~ 1 m in the shallow regions. However, these can reach up to 3 m as the depth increases. They are sigmoidal in shape, located at a water depth of 6 m - 20 m and extend in a seaward direction forming a 30^{o}- 40^{o} (NNW-SSE trending) angle with the coastline. The most prominent ridge feature aligns with the northern headland of the embayment.

5.1.5. Rippled Scour Depressions (RSD's)

The surface morphology of the southwestern region of the Isipingo embayment is characterised by several shore-normal to shore-oblique rippled scour depressions (RSD's). These features comprise elongate depressions in the seafloor that host smaller ripple sets. The RSD's occur at water depths of 13 m - 27 m (Fig. 5.1.6.) where approximately 35 RSD's can be identified in the study area. RSD's can be subdivided as follows: 1) RSD's that occur in the southwestern region of the Isipingo embayment, which are associated with outcrop (Fig. 5.1.7a). 2) RSD's in the central area of the embayment, located to seaward of small subaqueous dunes (Fig. 5.1.7b).

The RSD's of the first group are located approximately 0.7 km from the shoreline and occur seaward of the outcrop. These are up to 90 m long and 80 m wide, with a length to width ratio averaging 1, while other varieties of RSD's are characterised by a length of 60 m and a width of 18 m (L/W ratio of ~3.5 m). The depth of these features can range from a few centimetres (30-60 cm) up to nearly 1m, with an approximate interval spacing of 90 m between features. The depressions narrow towards the outcrop, where the gradient is higher than the surrounding seafloor, and progressively become wider and more widely spaced towards the southeast (seaward).

The second group are characterized by smaller RSD's that merge into the subaqueous dune fields (Fig. 5.1.7b). At a depth of 13 m to 27 m, in the centre of the embayment, the seabed is characterised by a series of asymmetrical dunes that are focused in elongate clusters that trend coast-oblique to near coast-perpendicular. The clusters occur as seafloor depressions within the embayment, each cluster spaced ~ 200 m to 650 m apart, and are often found in association with areas of dunes. The dunes have mean amplitudes of 0.2 m and wavelengths of 13 m, their straight crests and broad troughs orientated approximately east-northeast and aligned

perpendicular to the trend of the seafloor depression. The RSD's associated with the dunes are distinguished by an approximate length and width of 9 m and 6 m respectively, with an average L/W ratio of 1.5, and are spaced at ~ 15 m intervals. These depressions have similar depth ranges as the first group associated with the outcrop, and are similarly orientated. Other occurrences of RSD's were observed in association with the SAPREF pipelines, in water depths of 24 m.

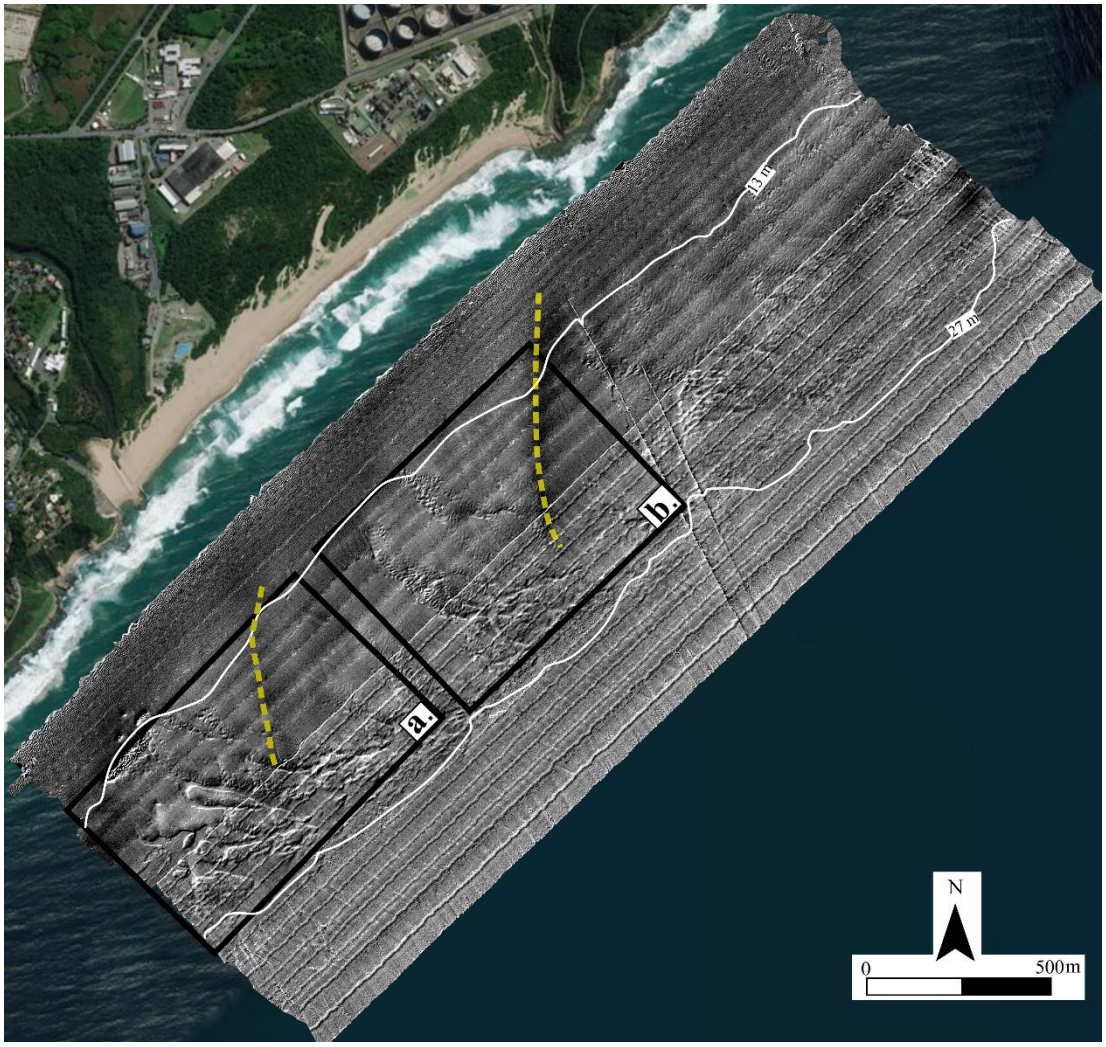

Figure 5.1.6: Hillshaded bathymetry indicating the location of rippled scour depressions (RSD's) between the 13 m and 27 m isobaths, as well as shoreface-connected ridges (SFCR's) denoted by the dotted yellow lines

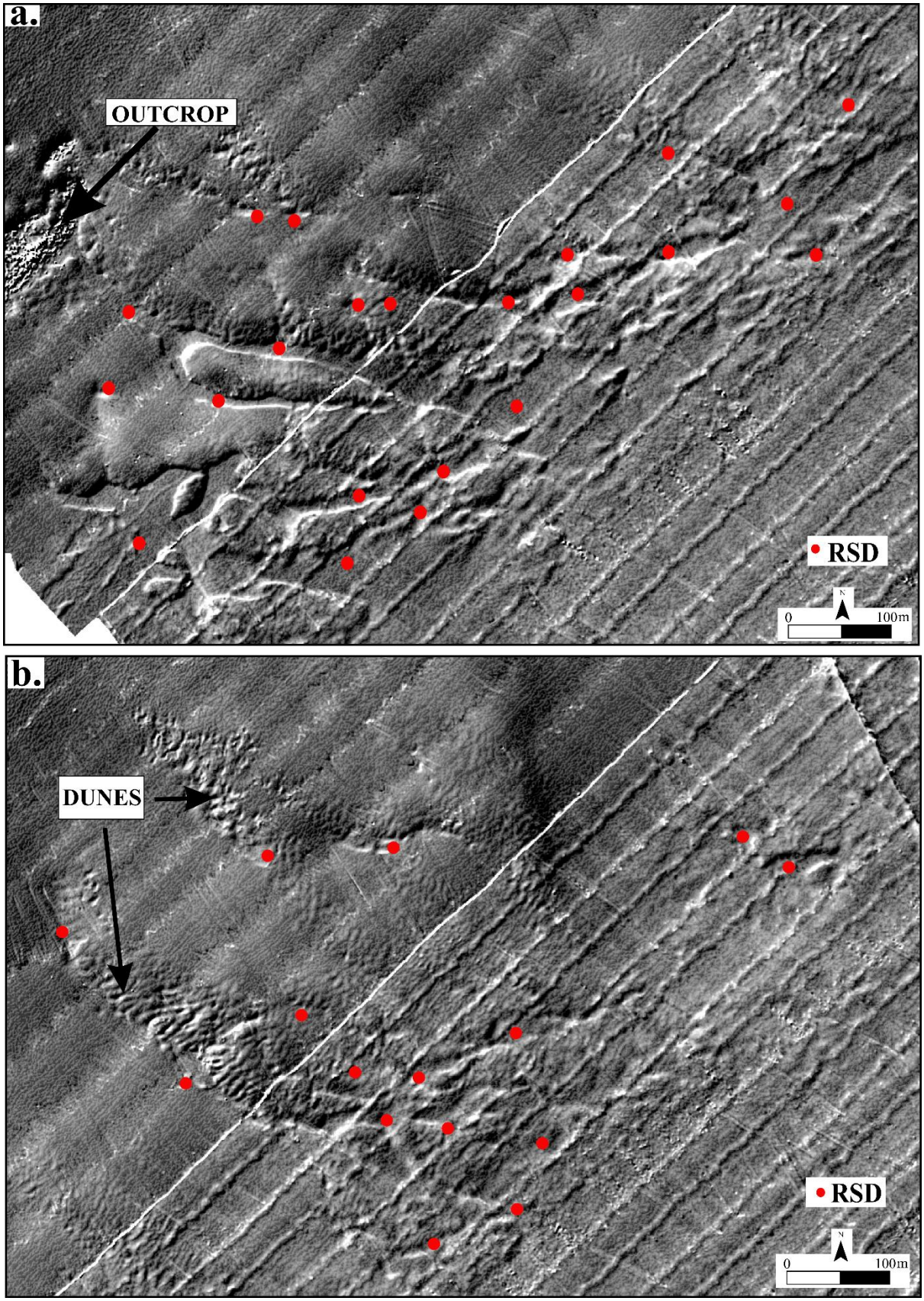

Figure 5.1.7: Rippled scour depressions associated with outcrop (a.) and rippled scour depressions associated with dunes (b.)

5.2. Wave Modelling

The numerical wave model SWAN was used to simulate wave conditions for the mean, 90%, 95% and 99% exceedance levels, as well as applied to March 2007 storm event and the storm parameters for the estimated 10 and 100 year recurrence intervals. The results show the spatial variability of the nearshore wave field and provide insight into the potential entrainment and transport of coarse sediment.

5.2.1. Modelled Wave Conditions

5.2.1.1. Mean Conditions

For the average wave conditions, the modelled wave field in Isipingo embayment is characterized by an expected increase in *Hs* as waves propagate from deeper water to shallower water depths due to the increased shoaling and interaction between the waves and the seabed (Fig 5.2.1). The wave period (Fig. 5.2.3) does not exhibit significant spatial variation (Tp = 8.3 s) under the mean wave conditions, specifically from a depth of 30 m to 6 m. However, within the shallowest regions of the embayment (6 m to 4 m), the wave period decreases to ~ 6 s. A dominant wave direction (Fig. 5.2.4) of 134° is reasonably consistent across the modelling domain, indicating the diminished effect of wave refraction and a prevalent southeasterly wave direction. The nearshore wave field under the mean wave conditions is spatially homogenous throughout the embayed region and is characterised by an average H_s of 1.6 m, average wave period of 8.23 s, and mean wave direction of 134°.

5.2.1.2. 90% and 95% Exceedance Levels

High-energy events are computed based on the 90% and 95% percentiles of the significant wave height distribution, which are representative of moderate and severe storm conditions, respectively. The 90% and 95% exceedance levels are discussed collectively based on the comparable modelled results of these simulations (Fig.5.2.1). SWAN simulations indicate an average *Hs* for these conditions in the range of 2.40 m - 2.60 m, with the modelled wave heights not varying more than 0.2 m between both these two exceedance levels. The highest values of H_s are observed along the central area of the embayment, with the results demonstrating more clearly the impact of shoaling on the shallower sections. The larger wave heights occur along

the shallower regions associated with the shoreface connected ridges and along the northeast (NE) and southwest (SW) headlands as a result of wave focusing (Fig.5.2.1). Based on the modelled results, the variation in the nearshore bathymetry exerts the main influence on the spatial variability in *Hs*. Wave heights increase when propagating over nearshore bedforms as a result of increased bottom roughness. This is most notable on the NE portion of the study area over the large subaqueous dunes and on the shoreface-connected ridges, associated with the areas of steeper seabed gradients. Within the region of the rippled scour depressions, H_s increases over these bedforms and declines in the area of the outcrop. Model simulations show south-easterly wave propagation, with the average wave direction (Fig. 5.2.4) 153°. At water depths of 30 m to 12 m, the peak wave period (Fig. 5.2.3) is spatially uniform and has a maximum value of ~12 s. The wave period decreases with decreasing water depth and reaches a minimum value of 7 s closest to the shore, landward of the breaking zone.

5.2.1.3. 99% Exceedance Levels

Extreme storm events were analysed based on the 99% exceedance level from the 10 year-long wave record. These events are characterized by average H_s values of 3.14 m across the entire domain and exhibit largest spatial variability (Fig. 5.2.1). Notably, the significant wave height peaks in areas over the most prominent nearshore large-scale bedforms due to wave shoaling. Waves are predicted to shoal at a depth of ~ 18 m, 550 m from the shoreline and the wave heights continue to increase up to a distance of 200 m offshore and only then start to decrease due to breaking at ~ 5 m water depth (Fig 5.2.2). Shoaling occurs over a longer distance (450 m) for the 99th exceedance levels in comparison to the mean conditions, where waves only shoal for a distance of ~ 280 m prior to breaking (Fig 5.2.2). Waves approach from a more southerly direction for this scenario, so upon reaching the shoreface-connected ridges the wave heights tend to increase and decrease as they pass the ridges and move into deeper water again. Regarding the spatial distribution of the peak wave period (Fig. 5.2.3), longer waves (T_p ~14 s) occur at depths of 30 m to 15 m, reducing from 12 to 8 s over a wide area with shallower water depths. The shortest wave periods are associated with depths of 4 m. The spatial distribution of wave period is consistent under the varying wave conditions, with a mean T_p of 13.2 s recorded for the 99% exceedance level.

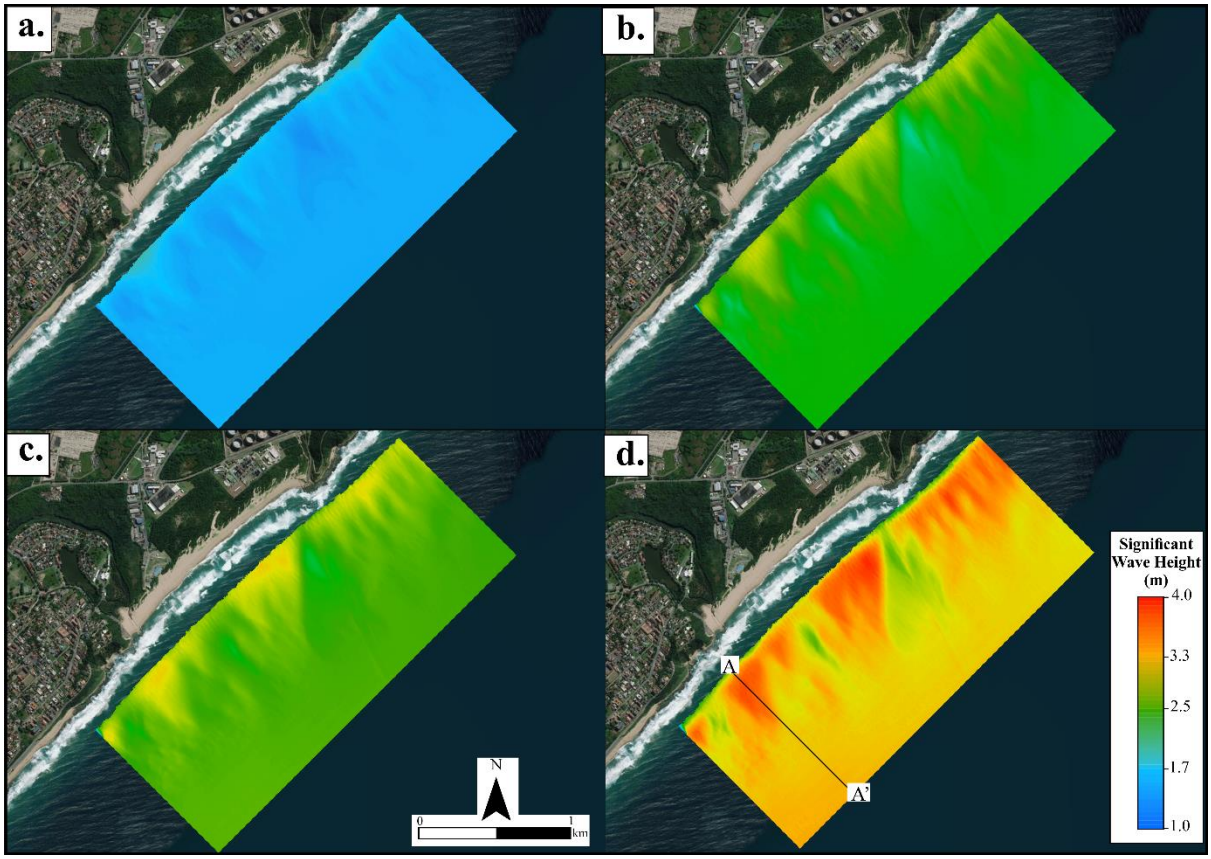

Figure 5.2.1: Significant wave height modelled under mean conditions (a.), 90 % (b.), 95 % (c.) and 99 % (d.) exceedance levels

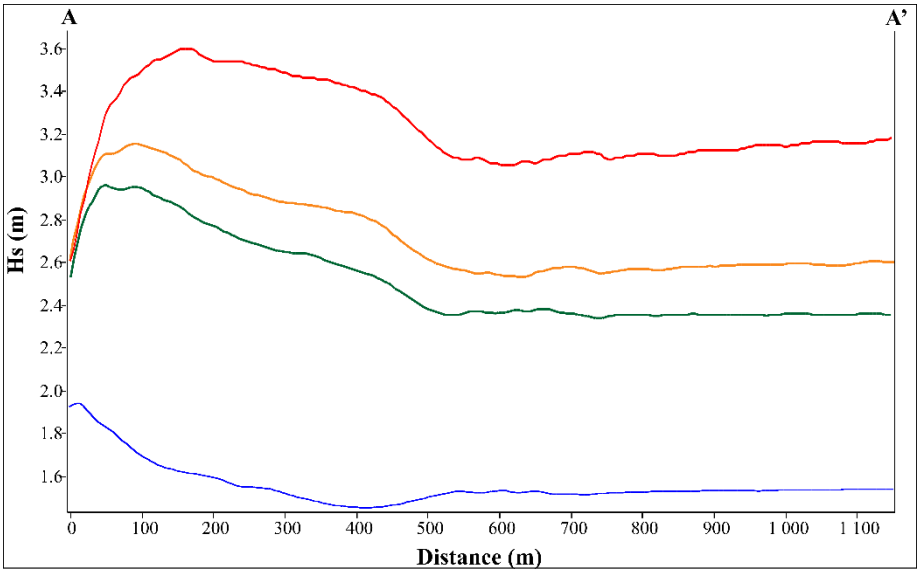

Figure 5.2.2: Significant wave height trend under mean conditions (—), 90% (—), 95% (—) and 99% (—) exceedance levels

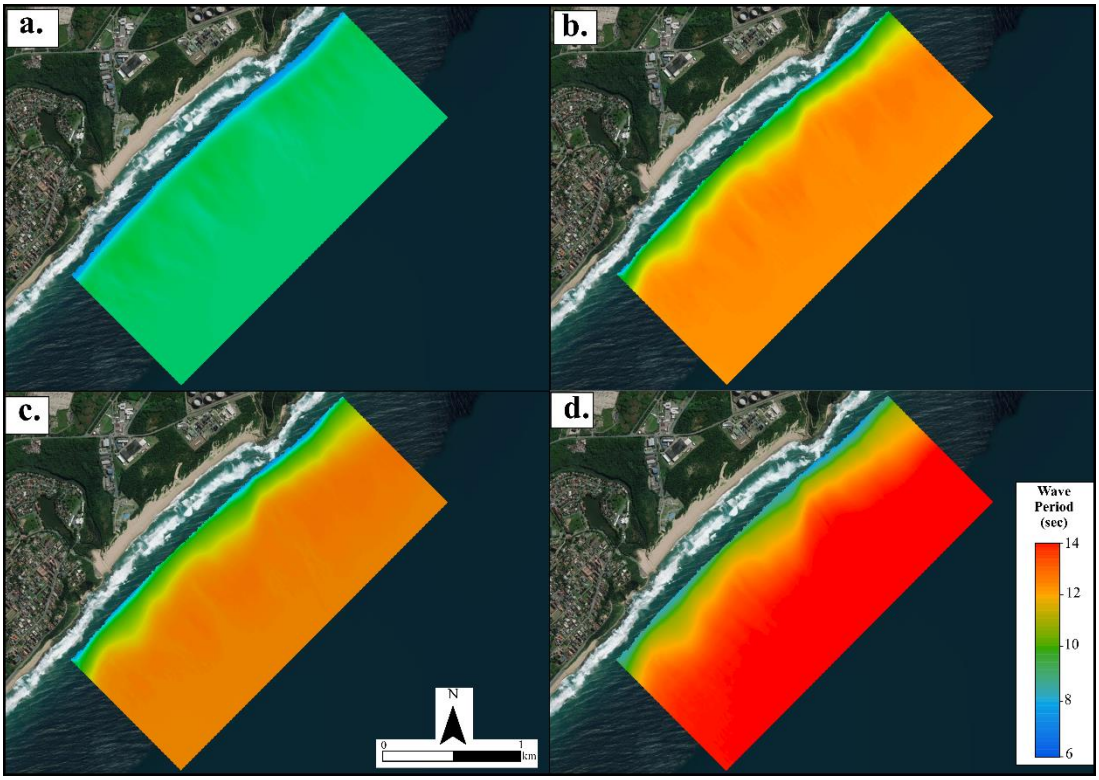

Figure 5.2.3: Peak wave period modelled under mean conditions (a.), 90 % (b.), 95 % (c.) and 99 % (d.) exceedance levels.

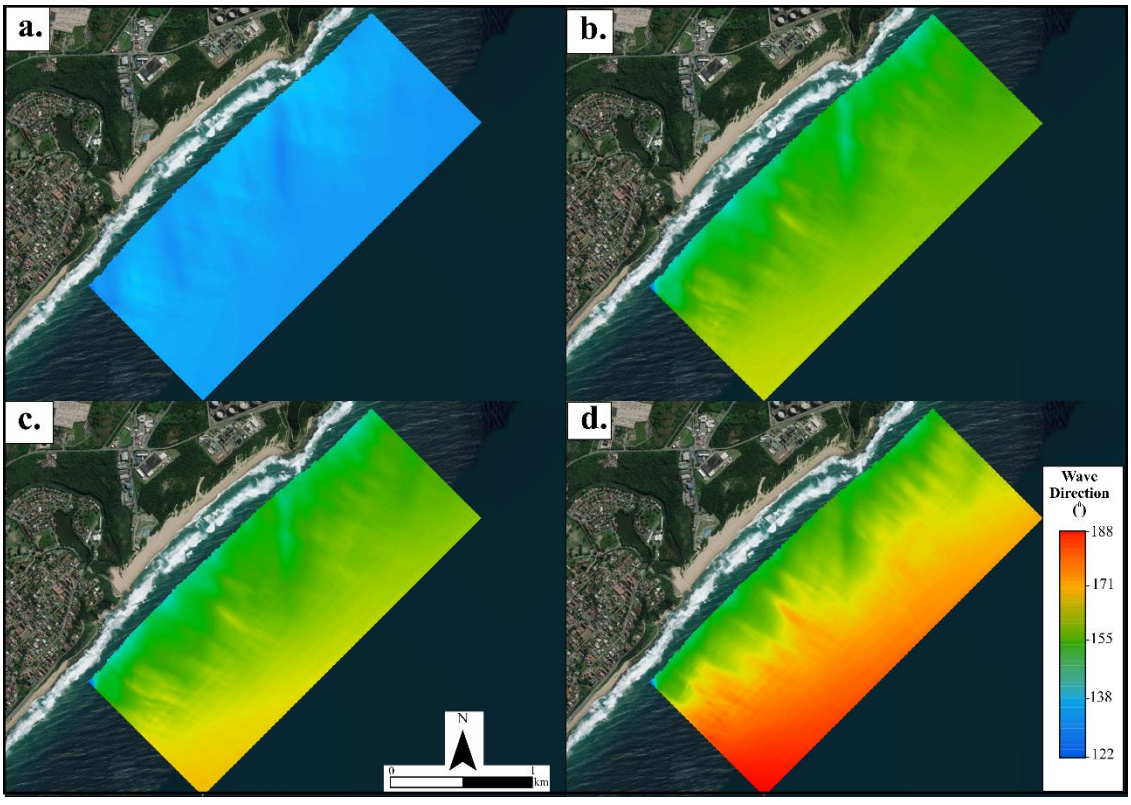

Figure 5.2.4: Wave direction modelled under mean conditions (a.), 90 % (b.), 95 % (c.) and 99 % (d.) exceedance levels.

5.2.2. Bottom Orbital Velocity

Under average wave conditions, the bottom orbital velocity is fairly uniform for the modelling domain and attains a mean value of 0.21 m/s with the velocity increasing from depths of 6 m to 4 m (Fig. 5.2.5). The bottom orbital velocity exhibits large spatial variability when simulated under the wave conditions for the 90% and 95% exceedance levels. Moderate to severe storm events drive an average U_{rms} of 0.38 m/s and 0.41 m/s respectively, and U_{rms} follows the spatial distribution of prominent nearshore bedforms where the velocity peaks over these features and attains maximum velocities (~0.9 m/s) along the shallowest regions and close to the headlands. Notably, the modelled extreme storm events (99th exceedance level) produce the greatest spatial variability in bottom orbital velocity with a mean value for the entire are of 0.52 m/s. Velocities increase towards the shore, with the higher velocities associated with shallower depths close to the embayment headlands and spatially dependant on the larger nearshore bedforms. This is most notable over the SFCR's, the large subaqueous dunes and in the region of the RSD's. The bottom orbital velocities closely mirror the significant wave heights under each wave condition and the bathymetry of the study area

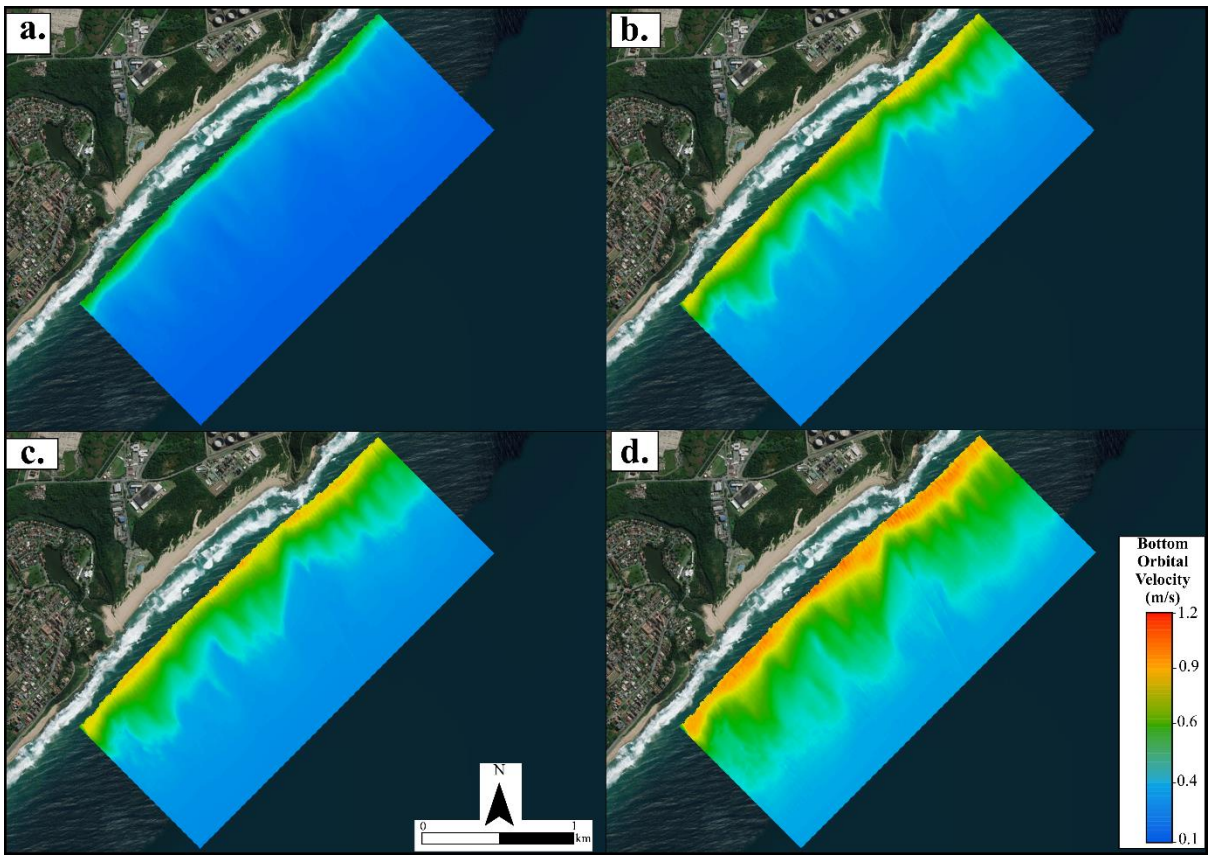

Figure 5.2.5: Bottom orbital velocity modelled under mean conditions (a.), 90 % (b.), 95 % (c.) and 99 % (d.) exceedance levels.

5.2.3. Bed Shear Stress

The modelled bed shear stresses under waves are analysed to evaluate the hydrodynamic forcing acting on the seabed and the potential entrainment and transport of coarse sand (d50 = 1.25 mm) and fine gravel (d50 = 5 mm), which are the dominant sediment types in the area. The bed shear stress for the mobilisation and entrainment of coarse sand is evaluated against a threshold value of 0.62 N/m^2. Figure 5.2.6 displays the spatial variability of the bed shear stresses modelled under mean to extreme wave conditions. The bed shear stresses under the modelled wave conditions have the potential to mobilize coarse sand over the entire area. Moderate to severe storm events produce large bed shear stresses across the entire modelling domain, which peaks over seabed features and in the shallower regions on the study area. The bed shear stresses simulated for extreme storm events are responsible for the larger potential entrainment and mobilisation of coarse sand across the entire study area, particularly in the shallow section associated with wave breaking and higher bottom orbital velocities.

A threshold value of 4 N/m^2 was used to examine the transport and entrainment of fine gravel under each modelled wave condition. Mean wave conditions have the potential to mobilize fine gravel for depths shallower than 9 m. Moderate to severe storm events produce greater bed shear stress across a larger area, which extends from a depth of 19 m to 3 m (Fig. 5.2.7.). The bed shear stresses produced by the extreme storm events (99% exceedance levels), display the greatest spatial variability for water depths shallower than 23 m. As noted for the conditions associated with the 90%, 95% and 99% exceedance levels, the bed shear stresses for fine gravel increase over the nearshore bedforms (notably the SFCR's, large subaqueous dunes and RSD's) and reach their peak value at depths of ~5 m. Referring to Figure 5.2.6 and 5.2.7, coarse sand tends to be potentially mobilized under all wave conditions, but the bed shear stress threshold for fine gravel is only exceeded in approximately 13 % of the total area during mean wave conditions. For storm events coarse sand is potentially entrained and transported across the entire study area, while the area of potential fine gravel mobilisation increases from 41 % and 63 % for severe and extreme storms, respectively.

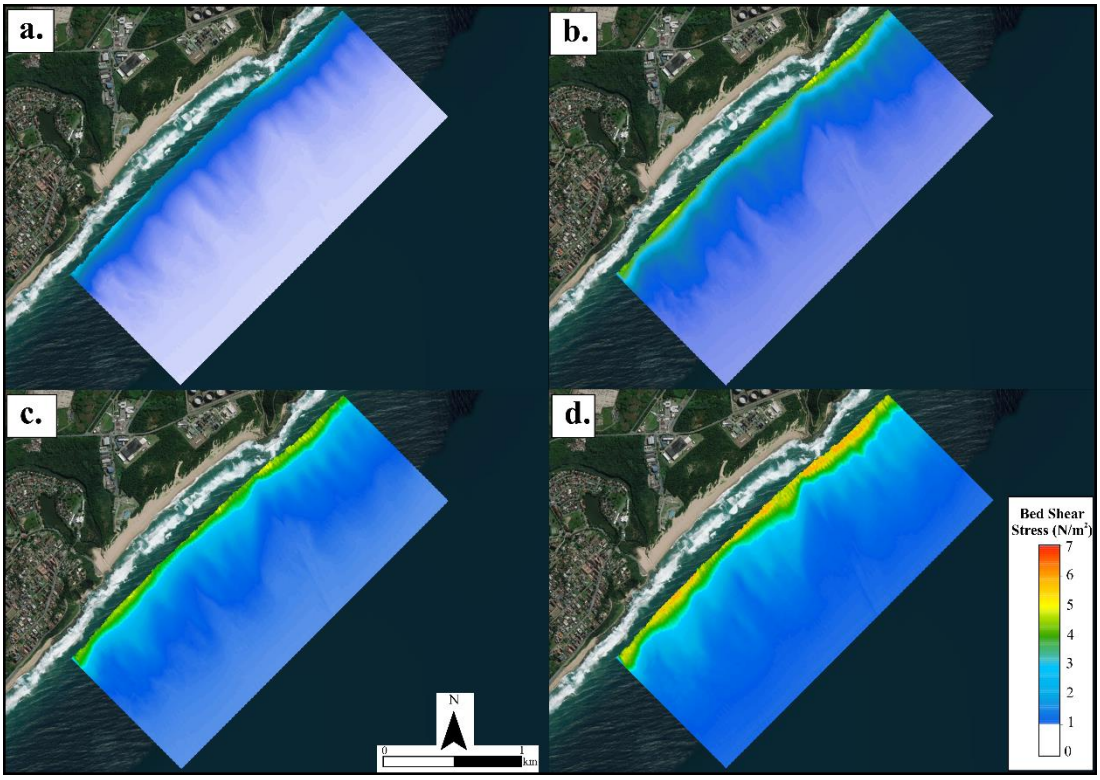

Figure 5.2.6.: Bed shear stress under modelled wave conditions considering coarse sand. Areas below the threshold for sediment entrainment of 0.63 N/m^2 are blanked out

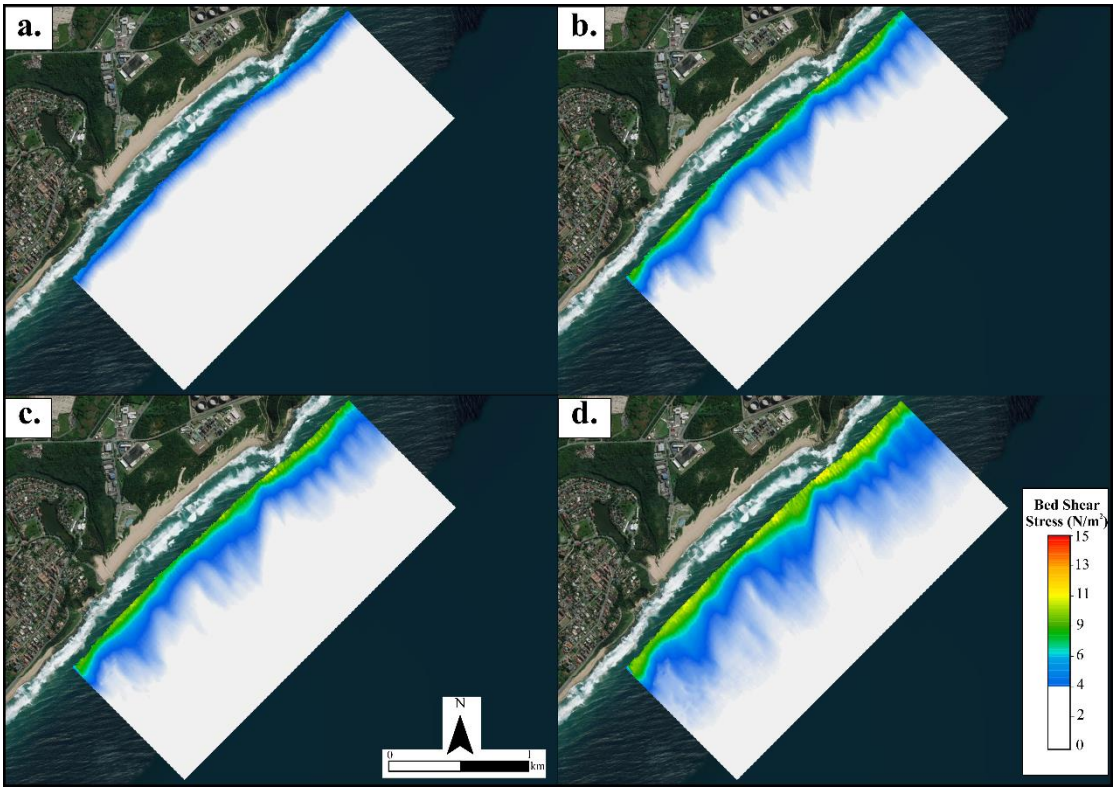

Figure 5.2.7.: Bed shear stress under modelled wave conditions considering fine gravel. Areas below the threshold for sediment entrainment of 4.00 N/m^2 are blanked out

5.2.4. Modelled Storm Events

5.2.4.1. The March 2007 Storm

Results from the modelled wave field during the peak conditions of the March 2007 storm, depicted in Figure 5.2.8, show the spatial variability of the significant wave height, bottom orbital velocity and bed shear stress for coarse sand and fine gravel. The H_s in Isipingo ranged between 1 m and 8 m (average of 6.9 m), consistently decreasing in a cross-shore direction and with less spatial variability alongshore, indicating that the magnitude of the storm forcing is so large that the control of the bathymetry is less noticeable. This storm event drives the most significant spatial variation in the bottom orbital velocities with the values ranging between 0.5 m/s to 1.2 m/s. In comparison to the 99 % exceedance levels, where the maximum U_{rms} is observed closer to shore, the wave orbital velocity for the 2007 storm peaks over nearshore bedforms and diminish at depths closer to the shore. The bed shear stresses indicate potential for coarse sand and fine gravel entrainment and transport across the entire area. For both sediment types, bed shear stresses increase landwards from the deepest regions of the study area and reach their maximum values over prominent seabed features.

5.2.4.2. 10 and 100 Year Storms

The model results for the storm conditions associated with the 10 and 100-year storms estimated by Corbella and Stretch (2012) based on the March 2017 event are presented in Figures 5.2.9 and 5.2.10. The spatial variation of the significant wave height for both the 10 and 100-yr storms is similar to the one described for the 2007 storm event, with decreasing wave heights towards the shore. The values and spatial distribution of modelled bottom orbital velocities and bed shear stresses are consistent for both the 10 and 100-year storms, exhibiting a strong association between the spatial variability of the significant wave height and increasing magnitudes as wave heights increase. As observed under all the modelled wave conditions (Fig 5.2.9 and 5.2.10), the bathymetric variability has a strong influence on the bottom orbital velocity as well as on the potential entrainment and transport of coarse sediment. The modelled 10 and 100-year storm wave field illustrates the nearshore conditions for events with larger wave heights, but the wave period and S-SE direction remains constant for all storm events (i.e. the 99 % exceedance and March 2007 Storm) across the entire modelling domain of the Isipingo embayment.

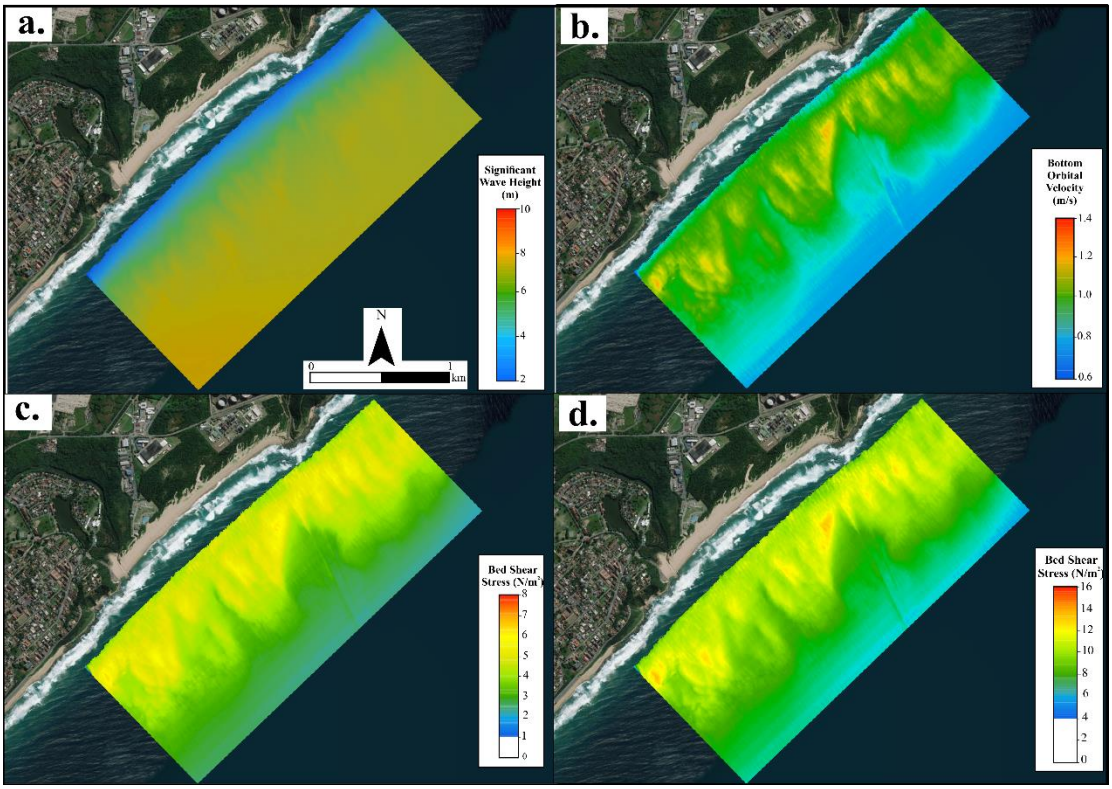

Figure 5.2.8.: Significant wave height (a) bottom orbital velocity (b) and bed shear stresses for coarse sand (c) and fine gravel (d) modelled for the March 2007 storm event.

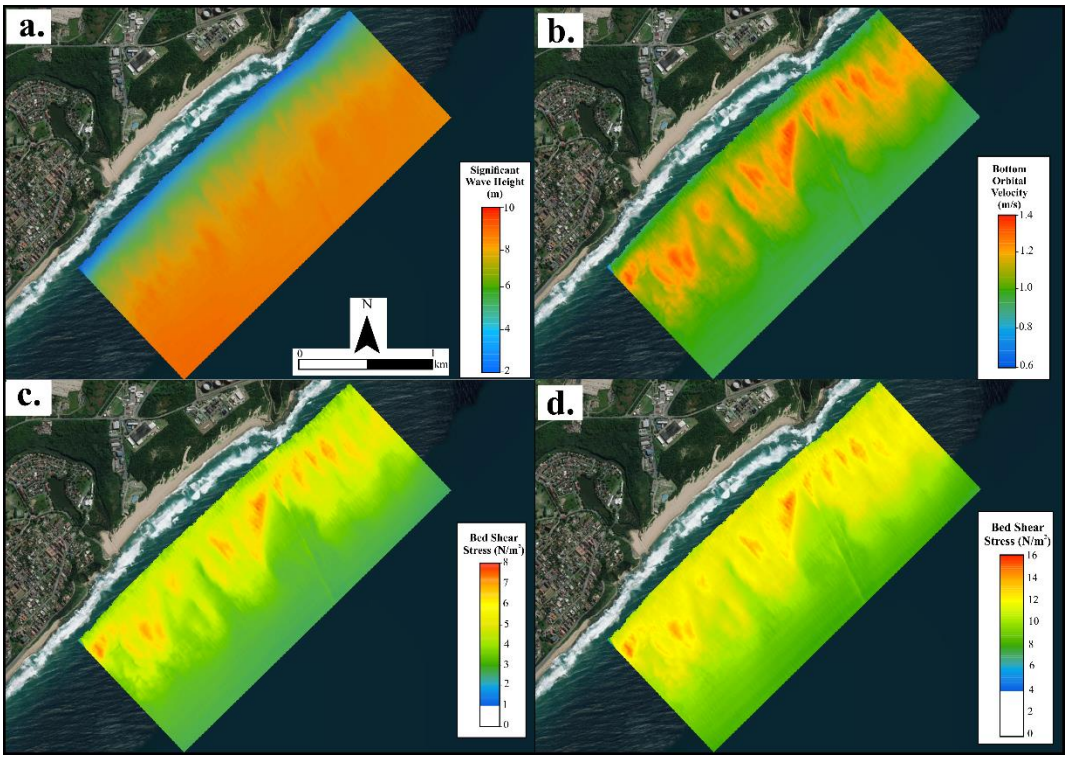

Figure 5.2.9.: Significant wave height (a), bottom orbital velocity (b) and bed shear stresses for coarse sand (c) and fine gravel (d) modelled for the 10 year recurrence interval of the March 2007 storm event.

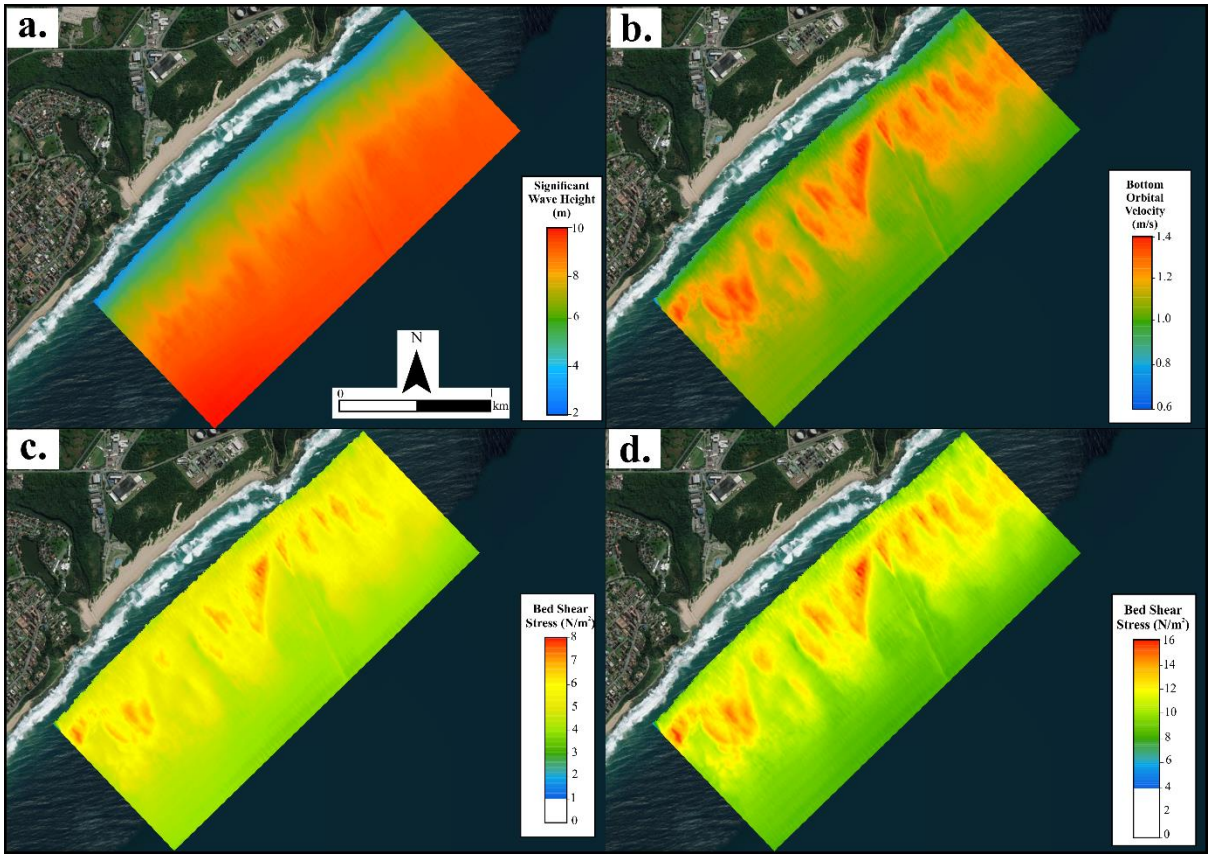

Figure 5.2.10. : Significant wave height (a), bottom orbital velocity (b) and bed shear stresses for coarse sand (c) and fine gravel (d) modelled for the 100 year recurrence interval of the March 2007 storm event.

5.3. Nearshore Morphological Changes

The morphological changes in the study area were determined by comparing the two bathymetric data sets representative of pre- and post-winter conditions. An assessment of the spatial and temporal changes to the seabed morphology is made for the Isipingo embayment.

Comparisons between the pre- and post-winter profiles along portions of the study area revealed differences in nearshore morphological changes that allow the evaluation of seafloor response to storm events of low-magnitude and short duration. The post-winter bathymetry illustrates the same main nearshore morphological features as previously identified from the pre-winter survey data (Fig. 5.3.1). These include the small dunes located in the inshore region, the large subaqueous dunes in the northeastern part of the embayment, a series of shoreface-connected ridges, and the 2 main groupings of RSDs, associated with the outcrop and with the subaqueous dune field.

The relatively gentle nearshore profiles exhibit minor variations during the 2017 winter season. As shown in profile A (Fig 5.3.1), accretion of approximately 1 m occurs at depths between 8 m and 4 m in the southern section of the embayment, with no significant changes seaward of this as these occur within the data uncertainty range of ±0.5 m. On the southern end of the embayment (profile B), small-scale (±0.2 m) morphological changes are observed indicating a relatively stable nearshore zone. Despite this general stability and absence of significant morphological changes in the central area of the embayment, up to 0.7 m of sediment were deposited within the rippled scour depressions associated with the subaqueous dunes (Fig. 5.3.1, profile E), between 12 m to 16 m depth. The alongshore profile over the RSD's (Fig. 5.3.1, profile F) associated with the outcrop, reveals deposition of up to 1 m of sediment along the margin of the depressions.

Profile C, located seaward of the NE headland, reveals 1 m to 2 m of erosion in the nearshore at depths ranging from 3 m to 8 m, with no significant changes at depths between 10 m to 14 m. Erosion of up to 1 m occurs at depths greater than 14 m. The alongshore profile over the large subaqueous dunes (profile D in Fig. 5.3.1) showed significant morphological variability during the winter season. As observed in the initial survey (Fig. 5.1.5), these dunes were superimposed by smaller bedforms, which become flattened during the winter as a result of erosion and accretion (± 0.6 m). The crests and troughs of the dunes migrated towards the northwest by ~ 0.4 m. The prominent ridge feature, forming a continuation from the northern headland, dominates the alongshore profile and is persistent in both the pre- and post-winter

surveys (Fig.5.31, profile D). The shore face-connected ridges have undergone no significant morphological changes in their alongshore orientation with little to no migration, indicating that these are semi-permanent features and not mobile on a seasonal scale.

Morphologic changes for the entire area were also evaluated by comparing the two high-resolution bathymetric grids (1 m x 1m resolution) and producing a surface difference map (Fig.5.3.2). The map presented indicates areas of erosion (0.5 m to 2.9 m) and areas of deposition (0.5 m to 2.5 m). Blanked areas of ± 0.5 m are considered regions of "no change" to account for data uncertainties. Such inaccuracies are more significant in the offshore area of Survey 1, due to the instrumental limitations with regards to motion reference unit used in the second leg of Survey 1. Hence, on the bathymetric difference map, morphological changes occurring at depths greater than 19 m are not taken into consideration.

The most substantial morphological changes were observed in the shallowest regions of the study area close to the NE and SW headlands. These comprise two distinct areas of erosion and deposition in the nearshore. The shallow zone along the NE headland, extending approximately 660 m into the embayment, experienced seafloor erosion from 0.5 m up to 2.95 m in extent. The erosion zone mostly forms a coast parallel scour that extends for 850 m in length and is 220 m wide. This zone of erosion occurs between 5 m and 14 m depth, with small patches occurring along the NE ridge to seaward. An area of significant accretion is situated adjacent to the SW headland, separated from the zone of erosion by an area of no significant changes. Here the seafloor accreted by up to 2 m during the winter season. The orientation and morphology of this accretion area is similar to the neighbouring erosion zone, but the size is smaller, covering a surface area of 0.06 km^2.

Minor, but still significant morphological changes, were also observed in the deeper areas between 9 m to 19 m. Here, localised and patchy regions of deposition and erosion are found and appear to be mostly restricted to the large bedform field and indicate migration of the nearshore bedforms. Within the region of the large subaqueous dunes (Fig. 5.3.3), localized areas of erosion and accretion occur almost sequentially to one another, suggesting an average migration of 0.42 m in a northwest direction for these bedforms during the winter season

The comparative analysis between bathymetric grids also identified significant morphological changes in the area of the RSD's. The movement and reconfiguration of these bedforms are most notable in the region associated with outcrop. Here, newly developed depressions are evident on the northeastern side of the outcrop, with alternating areas of erosion and deposition

of ± 1 m (Fig 5.3.4). A prominent zone of deposition (0.5 m to 1 m) is evident on the southwestern (seaward) region of the Isipingo embayment within the RSD's connected to the outcrop.

Smaller morphological changes in the areas of the RSD's that merge into the dunes occur between depths of 14 m to 16 m. Here, patches of smaller-scale deposition (0.5 m to 1 m) and erosion (-1 m to -0.5 m) are identified. As shown in Figure 5.3.5 (insets a and b) additional RSD's developed during the winter season on the north-eastern flank of the pre-existing depressions. The difference map indicates that the RSD's have a general erosion and accretion pattern characterized by deposition of sediment in pre-winter depressions and erosion on the northeast margin of these features to form additional RDS's during winter.

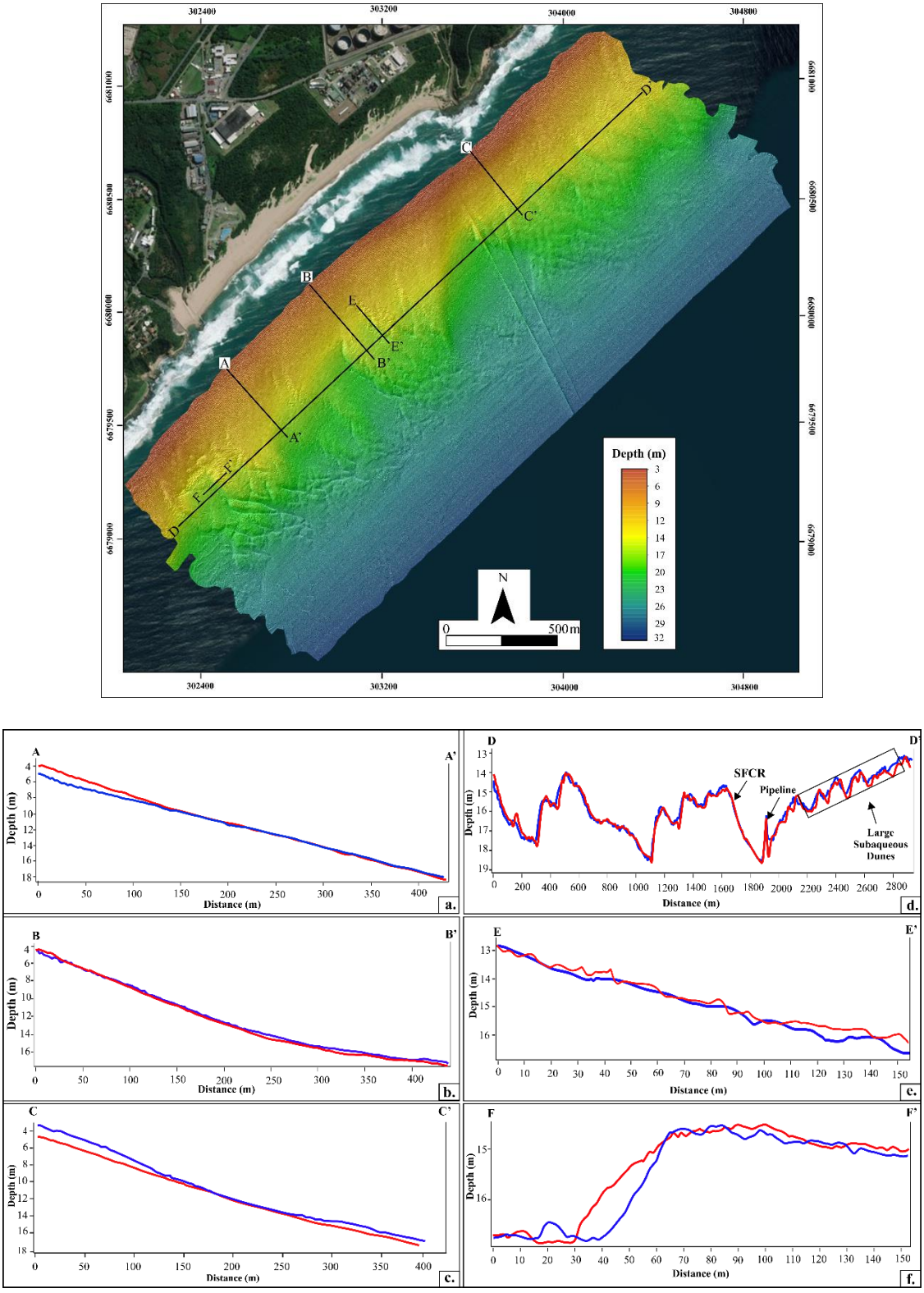

Figure 5.31: Post-winter bathymetry of the Isipingo embayment, with accompanying pre- (blue) and post-winter (red) cross-sectional profiles.

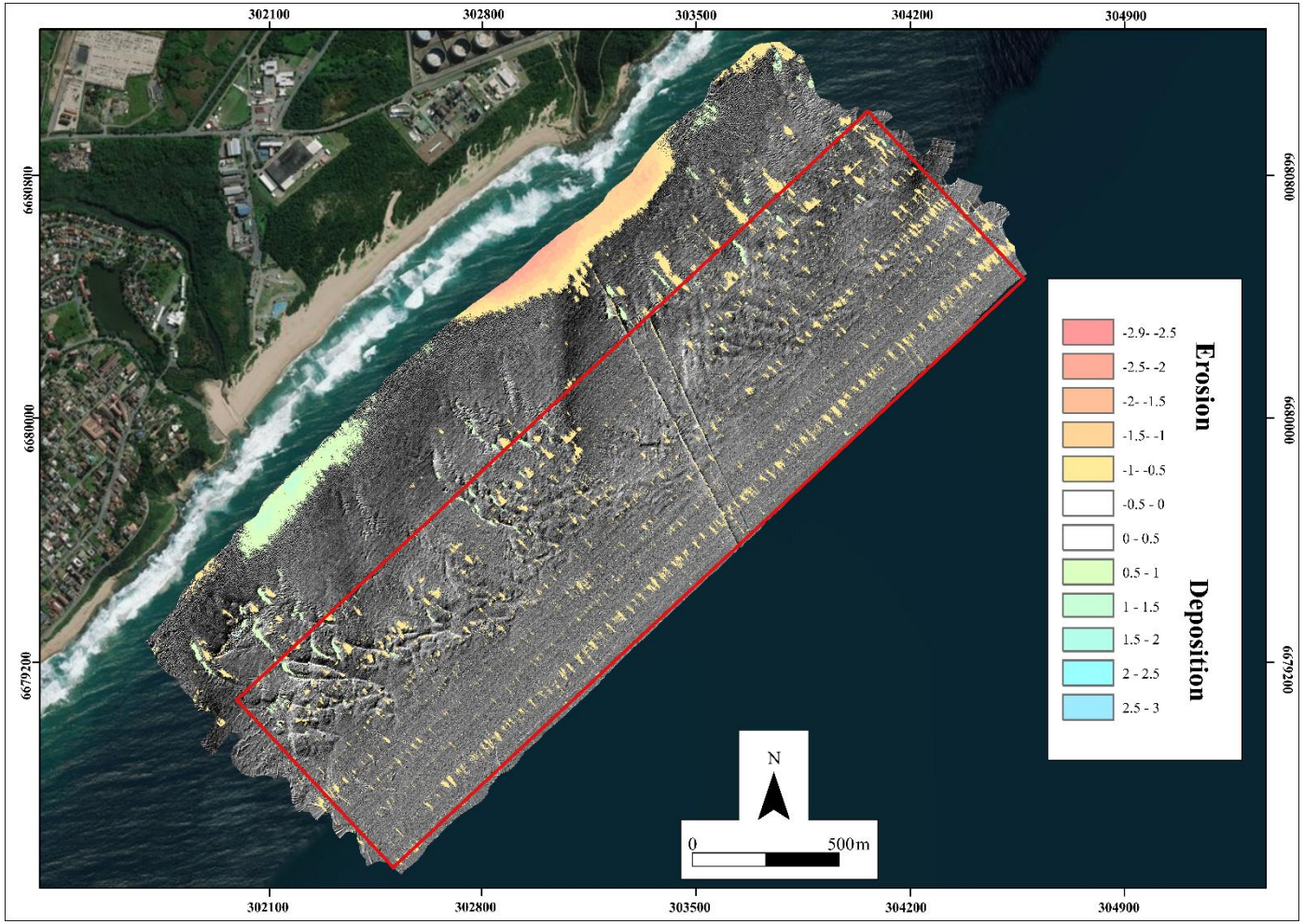

Figure 5.3.2: Bathymetric difference map for the 2017 winter season. Erosion and accretion (in meters) superimposed on the hillshaded post-winter bathymetry. The offshore area where morphological changes are not taken into consideration is indicated by the red box

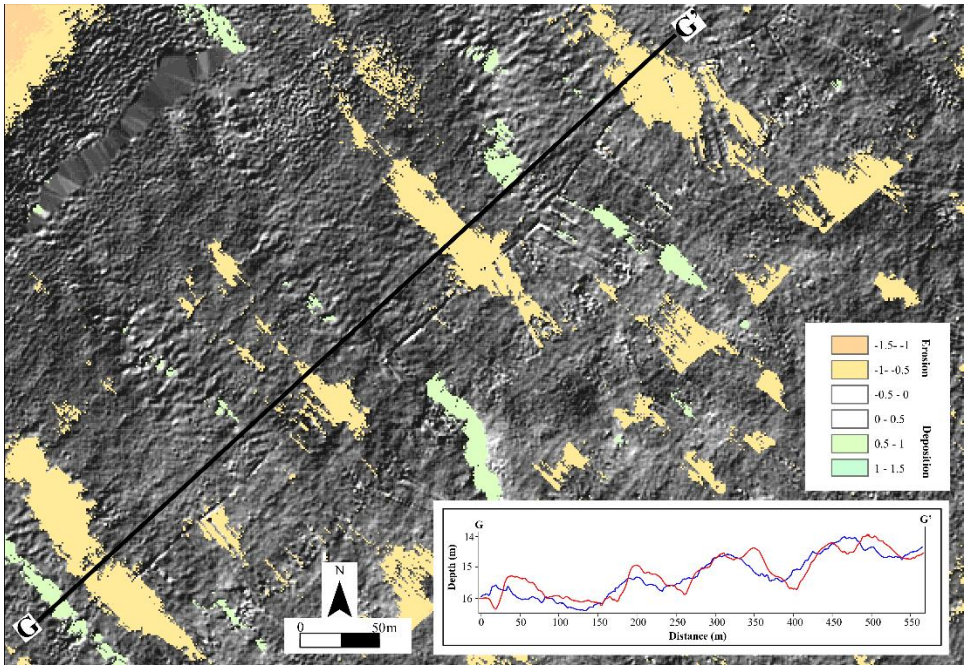

Figure 5.3.3: Bathymetric change map of the large subaqueous dunes, with the accompanying pre- (blue) and post-winter (red) cross-sectional profiles

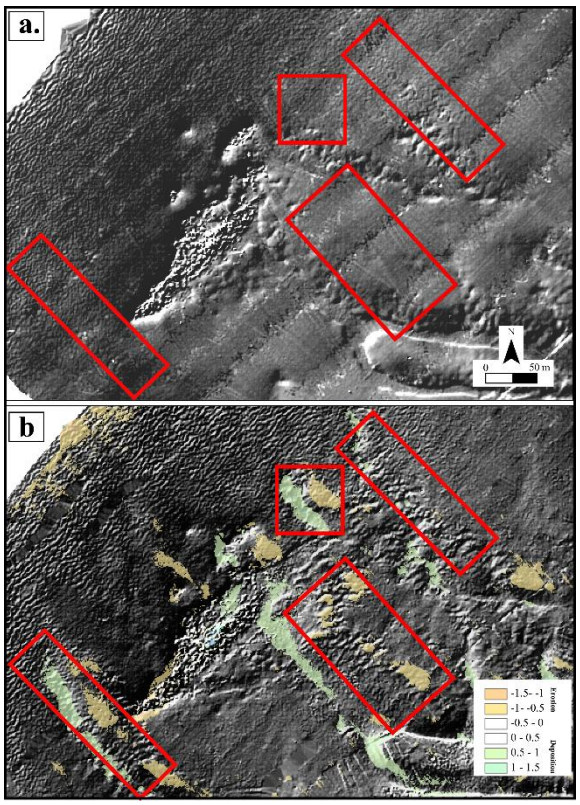

Figure 5.3.4: Hillshaded bathymetry of pre- (a) and post-winter (b) season showing significant morphological changes in the rippled scour depressions associated with the outcrop.

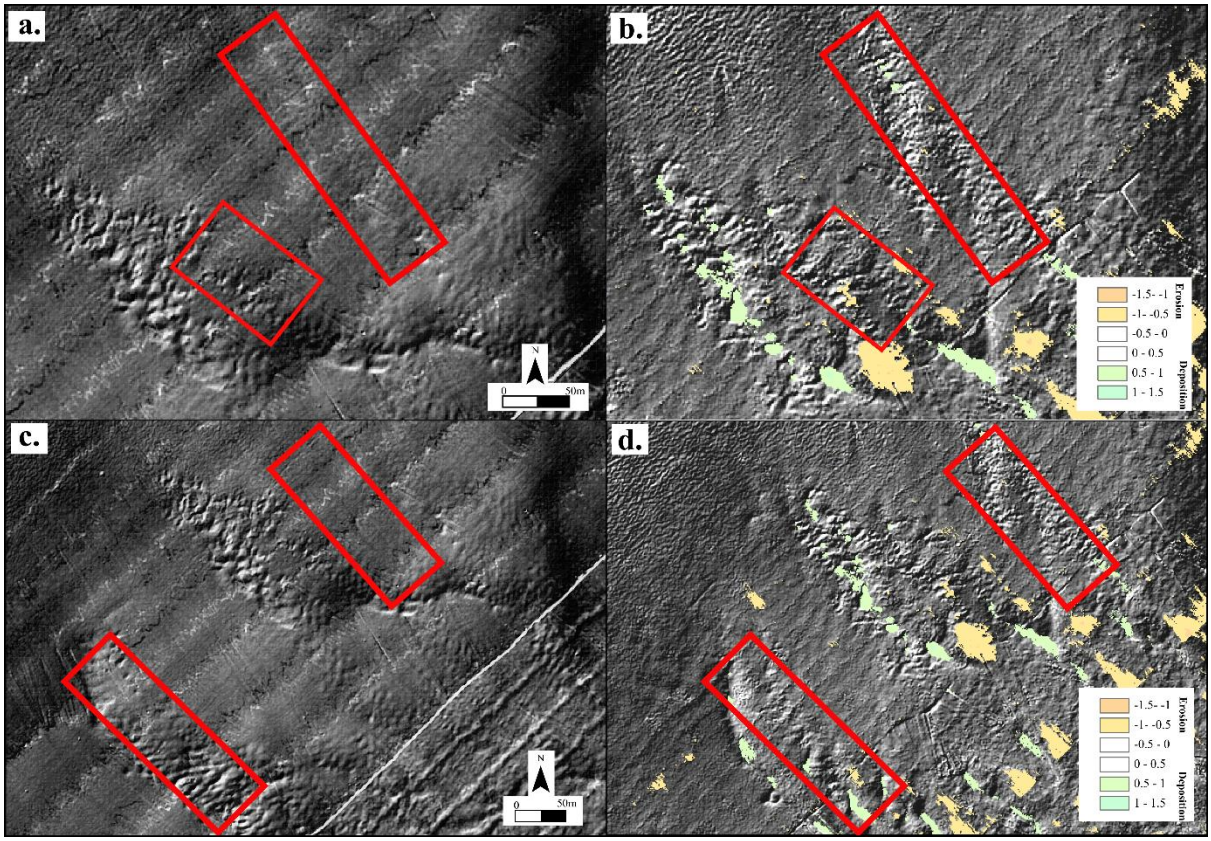

Figure 5.3.5: Hillshaded bathymetry of pre- (a, c) and post-winter (b, d) season showing the morphological changes of the dune associated RSD's.

Chapter 6: Discussion

High-resolution nearshore bathymetric surveying conducted at the Isipingo embayment before and after the 2017 winter season provides the opportunity to analyse in detail the seasonal nearshore morphological changes driven by winter storm events along embayments of the KwaZulu-Natal coast. Results from the wave modelling further provide insights about the wave induced forces in the study area, which assist in the interpretation of morphological changes and sediment transport pathways.

Factors controlling the movement of sediment under storm conditions are well documented by various authors (e.g. Komar, 1976; Wright & Short, 1984; Lee et al., 1998). These include the influence of nearshore morphology (Hequette et al, 2001), shoreline orientation (Kahn & Roberts, 1982; Jaffte et al., 1997), mean flows (Wright et al., 1991) wind-induced currents (Niedoroda et al., 1985; Xu and Wright, 1998), and nearshore sediment thickness (Backstrom et al, 2007). For this study, the variability in nearshore wave field and the patterns of morphological change appear to be controlled by the bathymetric configuration and the hydrodynamic mechanisms operating in the nearshore of the embayment that are influenced by geological inheritance.

6.1. Bathymetric control on wave field

It appears that the sequential changes in morphology and sediment accumulation/erosion are most likely driven by the nearshore wave field. Analysis of the modelled wave conditions and bed shear stresses indicate the strong influence of nearshore bathymetry on wave propagation and transformation in the nearshore region of the Isipingo embayment. Bathymetric features are well known to influence surface wave processes by causing wave refraction, reflection and wave-wave and wave-current interactions (Gomes et al., 2016). Conversely, the configuration of the bedforms and the morphological evolution of the nearshore depends on the relative contribution of propagating waves and the magnitude of the wave conditions.

Oscillatory flows associated with wave orbital velocities and the resulting bed shear stresses over nearshore morphology remains the most important mechanism for the mobilisation of sediment in the shoaling zone (Hequette et al., 2001). Nearshore bedforms play a role in sediment transport as they 1) increase the bed shear stresses, which increase the concentration of suspended sediment and 2) increase bed roughness, therefore influencing fluid velocity

gradients and sediment concentration profiles (Aagaard & Masselink, 1999). Bed shear stresses determine the velocity gradient close to the bed and the forces applied that mobilise sediment grains. Sediment entrainment and transport in the nearshore of wave-dominated settings is determined by waves rather than currents because the wave boundary layer is thinner than the current boundary layer. Therefore, the rougher the bed surface, the greater the wave orbital velocity and the more stress exerted by the wave motions on the seafloor (Aagaard & Masselink, 1999). Modelling results presented in this study indicate that the spatial variation and distribution of the bed shear stress is dependent upon the configuration (type) of bedform and the magnitude of the wave field. Consequently, the greater the energy of the wave conditions (i.e. as a result of major storm events) the greater the wave-induced forcing, which causes the change of the bedforms and the morphological evolution of the nearshore.

Bathymetric control on the spatial distribution of waves and sediment transport is discussed by Gomes et al (2016). The research highlighted the dependence of the location and intensity of wave breaking and alongshore variability in wave energy dissipation on morphological patterns on varying scales. Overall, the study found a strong correlation between the predicted spatial variability of wave breaking (using the non-hydrostatic SWASH model) and the nearshore morphological features. Analysis of the Isipingo bathymetry and the modelled nearshore wave field, under varying wave conditions, revealed this same strong correlation and dependence of the wave transformation processes and the spatial variability on the morphological features. Even though small morphological adjustments occur to all the main bedform types, these persist in a general sense between pre-and post-winter months and point to their long-term persistence and control on the wave dynamics in the region. Areas of wave focusing and increased orbital velocities have increased potential to experience preferential long-term erosion of the lower foreshore and beach.

6.1.1. Influence of shoreface-connected ridges

The shoreface-connected ridges observed in this study are similar to those described in a number of investigations performed on the inner continental shelf throughout the world (Duane et al., 1972; Swift et al., 1972, 1978; Swift & Freeland, 1978; Parker et al., 1982; Swift & Field, 1981; Figueiredo et al., 1982; Stubblefield et al., 1984; Hoogendoorn & Dalrymple, 1986; van de Meene & van Rihn, 2000). Although variable, the ridge features observed by these authors are typically orientated at an oblique angle of approximately 10° – 50° to the shoreline. The

SFCR's present at the Isipingo embayment follow this trend and are persistent features that that have undergone no migration during the time frame of this study. As documented by Trowbridge (1995), shoreface-connected ridges are formed by the convergence of sediment flux at the crest of the ridge and divergence at the ridge troughs. Details on the processes responsible for the formation and maintenance of these features have been analysed by various authors (e.g. Trowbridge, 1995; Calvete et al., 2001a, 2001b; Vis-Star et al.,2007; Nnafir et al., 2014a, 2014b).

Irrespective of the formative mechanisms, the modelled results indicate that the prominent SFRC's of the embayment tend to increase the H_s and the bed shear stresses acting on the seabed as a result of wave shoaling. The dominant wave-induced forcing under mean wave conditions is from the southeast, but becomes increasingly southerly during extreme storms (Fig. 5.2.4), as showcased by the as-yet unprecedented 2007 storm event. Consequently, there is an increase in the potential entrainment and transport of coarse sediment when waves approach along the ridges (i.e. ~ 160^o). Sediment entrainment and transport is evidenced by the bathymetric change map whereby the SFCR focus waves towards the NE headland causing an extensive erosional zone to occur in the shallower area. These findings are consistent with the analysis from Xu et al. (2016) and Safak et al. (2017), whose research focussed on the numerical simulations of idealized SFCR under varying wave magnitudes and directions. These studies revealed that 1) ridges have the potential to enhance wave energy when waves propagate along the ridge (i.e. the wave angle corresponds to the ridge orientation) compared to when waves propagate across the SFCR (i.e. when the wave angle is perpendicular to the ridge orientation) and 2) variation in wave direction will result in an opposite alongshore sediment transport gradients. Hence, the influence of SFCR's at Isipingo on sediment transport becomes more significant during storms conditions compared to mean conditions, not just by the magnitude but also by the direction of wave approach. Extreme storm conditions induce a more southerly wave direction, forcing waves to propagate along the ridge (rather a perpendicular) increasing the bed shear stresses and focusing waves towards the NE headland. This response is validated by the extensive erosional area seawards of the headland.

6.1.2. Rippled scour depressions

RSD' are commonly found in numerous nearshore environments around the world. Within the nearshore of the Isipingo embayment two types of RSD's have been identified as either

outcrop-controlled, or those associated with the subaqueous dune field. Both these types correspond to the definition of rippled scour depressions proposed by Cacchione et al. (1984), Hunter et al. (1998), Thieler et al. (1995) and Green et al. (2004). Nearshore rippled scour depressions have various origins but are ultimately formed as a result of the interaction between waves, mean currents and poorly sorted bed material in high-energy environments, such as that of the nearshore region (Murray & Thieler, 2004).

For the purpose of this study, RSD's are differentiated based on the classification introduced by Davis et al. (2013) due to the similarities in the morphology and spatial distribution of these features to those found along the Californian coast. This classification is modified from that proposed by Green et al. (2004) and classes RSD's based on their depth, proximity to bedrock and size. The classes are described as inshore, offshore, inshore rock-associated, offshore rock-associated, and "mega" RSD's (Davis et al., 2013). The inshore bedrock controlled rippled scour depressions of the Isipingo embayment are consistent with studies in Australia (Field & Roy, 1984) and Canada (Hequette & Hill, 1993). The outcrop contributes to the formation of the RSD's by focussing and channelling bottom currents, increasing flow velocity and resulting in the formation of RSD's. Outcrop-associated RSD's occur in an area where the near-bed orbital motion increases, since these features act as roughness elements that generate greater bed shear stresses relative to that of the surrounding seafloor. This enhances the entrainment and transport of coarse sediment. These RSD's are generally larger than RSD's found in the centre of the embayment, in addition they span a greater morphological variability. This is evident in pre-winter RSD's, with slightly larger and more abundant RSD's were identified in the area surrounding the outcrop. Such observations are shared with Davis et al (2013) where bedrock controlled RSD's were observed to be generally larger than those found in the sandy regions. Therefore, the presence of bedrock may not be necessary for the formation of RSD's but still plays an influential role in the formation and persistence of these features as well as the development of large expanses of RSD's.

Where RDS's are observed in areas where no outcrop is exposed, particularly in the central section of the embayment, they exhibit morphological characteristics more similar to those observed on the East Coast of the US (Goff et al., 2005) and Southern California (Davis, 2013). These studies suggest that those features that occur in the absence of outcrop are possibly generated by rip currents caused by large storm waves (Cacchione et al., 1984). The RSD's occur at a depth where increases in wave height due to shoaling lead to increasing wave orbital velocities, enhancing sediment flux in the region. This shoaling is linked to the bedforms and

SFCR's of the area, focussing the development of RSD's in these domains. Similar physical processes and conditions attributing to the development of RSD's as described in this study have been observed by Ferrini & Flood (2003). The creation of these sedimentary features were controlled by the increased stresses associated with waves and/ or current convergence on the seabed and driven by the hydrodynamics related to nearshore waves. Variations of the RSD's in the nearshore of Isipingo are driven by variable wave conditions during pre- and post-winter. In addition, the RSD's at the centre of the embayment appear to be generated and morphologically controlled by rip current activity, and in turn, these features act as a feedback mechanisms that bathymetrically control the strength and migration of the rips.

Despite the differences in their formation mechanisms, the morphological change results suggest that for both RSD types, there is erosion on the down-current side and deposition on the lee (Fig. 5.3.4), implying a south to north migration with the longshore drift regime . Such conditions for the formation of RSD's were observed on the coast of North Carolina where the net longshore drift is towards the south (Thieler et al., 1995) in contrast to the prevailing longshore drift direction discussed in this study.

6.1.3. Large Subaqueous Dunes

The bed shear stresses over large subaqueous dunes are important factors that influence sediment transport during dune migration (Bridge, 1981). Bed shear stresses increase over subaqueous dunes, given the interaction of wave orbital motions with the seabed bedforms, and this contributes to increased sediment transport. This results in areas of accretion and erosion as they migrate (Fig. 5.3.3). The migration pattern of these features, shown in Figure 5.3.1.D and 5.3.3, suggests longshore sediment transport in a northeasterly direction, perpendicular to the wave direction under mean conditions and oblique to the waves propagating under extreme storm events. The hydrodynamic modelling points to a limited spread in swell direction, and as such, limited changes to the longshore components. The nearshore here, although not fed by large rivers, likely has enough sediment transported by the vigorous wave-climate, to build large dunes, especially if the coastline is compartmentalised, such as in an embayment, and a resulting pocket of sediment is trapped in the nearshore. The flattening of the crests in the winter season points to periodic modification by larger swell events that limit the aggradation of the bedforms by scouring.

6.2. Geological Constraints and nearshore hydrodynamics

Nearshore currents may be divided into offshore currents, rip currents and longshore currents (Aagard & Masselink, 1999). These currents are generated by the dissipation of energy from breaking waves and wind action. The currents operating in the nearshore are also partially controlled by onshore geological constraints (i.e. headlands and coastal configuration) and nearshore bathymetric features (e.g. ridges, troughs, canyons). Consequently, because there is some degree of geological control on nearshore hydrodynamics, there will be geological influence in sediment transport and the resulting nearshore morphological evolution.

Nearshore geological control not only influences the nearshore wave field, but it also determines the accommodation space and sediment that is available to be transported. A prominent geological constraint at the embayed region of Isipingo is created by the NE and SW headlands, which have an impact on wave focussing and transformation. Headlands have a recognizable influence by modulating the shape of embayed beaches, determining alongshore variations in the nearshore wave field and contributing to topographically-induced nearshore circulation (Short, 2010; Gallop et al., 2011; Loureiro et al., 2012). The headlands at the Isipingo embayment have a small shadowing effect. Despite this, the NE headland appears to have a greater influence on the hydrodynamics, by constraining northerly-directed flows. The interaction between the incoming S-SSE waves and the embayment configuration drives an uni-directional longshore drift, which sets up local circulation creating topographic rips against the northeast headland (discussed below), which forces offshore sediment transport into the trough of the SFCR . Considering some shadowing effect by the SW headland alongside the presence of the outcrop and the bedform field immediately offshore of the headland, it is reasonable to assume that the wave-focussing that occurs in this area leads to a reduction in the wave forcing and bed shear stresses in the area immediately leeward, as evident in Fig. 5.2.7 to 5.2.1

6.2.1. Topographic rips and Mega rips

Topographic rips are rip currents that are controlled by topographic features (either natural or man-made) such as headlands, reefs or groynes and result from the alongshore variation in wave height due to the attenuation and refraction of waves around these features (Short, 1985). Within the surf zone, currents are deflected along the side of the obstacle in a seaward direction as a stronger topographically-controlled flow of water. Rips are generated by wave breaking

across the surf zone that creates a longshore a rip feeder current that feed into the topographic rips (Short, 2010).

Compared to the embayed beaches in Australia (Short, 2010), Brazil (Klein et al, 2010) and Portugal (Loureiro et al., 2012), Isipingo is a relatively linear, shallow embayed region (spans a length of 1500 m and width of 140 m) with the headlands causing little to no wave refraction and diffraction in the nearshore (see modelled results). However, topographic-rips predominately occur around the NE and SW headlands where waves are high enough to maintain active surf zones and drive energetic wave-induced currents (Fig. 6.1). An alongshore current moves parallel to the shore, landward of the sandbar revealed by the wave breaking patterns, being forced in a seaward direction against the of the NE and SW headlands. Here, the rip current dynamics are important mechanisms in the transport of sediment in the nearshore, similar to what has been identified from several other locations (e.g. Shepard et al., 1941; McKenzie, 1958; Short, 1985; Smith & Largier, 1995). Aerial imagery (Fig. 6.1.) shows that rip activity towards the SW headland is very limited during the winter and post-winter period. This suggests accretion has occurred and the rip current is no longer active, contrary to the pre-winter image where the rip is large and highly active. However, towards the NE headland, the rips are active, particularly when waves approach from S-SSE direction (Fig. 6.1). The increased rip induced erosion may explain the erosion in the NE region, while reduction in rip activity may have led to accretion in the SW section.

While no evidence for offshore deposition and channelling of sediment is presented in this study, it is hypothesised that the mega rips may play a role in the wave induced forcing of the area, and hence, the subsequent morphological evolution during major storms events (i.e. modelled by the 99 % exceedance level and March 2007 storm). Megarips are large-scale topographically- controlled rip currents that are generated in embayed beaches during high-energy wave conditions and responsible for the offshore deposition of sediment (Short, 2010). Modelled storms events suggest that the wave conditions in these setting may be conducive for generating megarips since the wave heights reached under 99 % exceedance levels and the March 2007 were 3.15 m and 6.9 m, respectively. Although no offshore deposition is observed in the morphological changes, a mega-rip may have to form against the NE headland, where a persistent rip is present, as waves approach from a S-SSE direction and allow for the water pilling against the beach to escape. This has been suggested by Smith et al. (2010), who during the March 2007, identified in various areas along the KZN coast that the March 2007 storm

event generated wave-driven megarips that eroded nearshore bars and transported eroded coastal sediment offshore.

6.2.2. Nonstationary rip currents

Previous studies of rips currents have focussed on the flows that are generated and controlled by the bathymetric variability of the surf zone (Long & Özkan-Haller, 2016). In particular, bathymetrically-controlled rip currents are characterised as "channel" or "focussed" rip currents that are relatively persistent in space and time, for a given wave regime and tidal elevation (Castelle et al., 2016). Focussed rips are a type of bathymetrically-controlled rip current that are forced by shoaling waves determined by morphological features in the shoaling zone and outer surf zone. Rip currents have also been identified to persist over much shorter-time scales and are referred to as "transient rips" (Smith & Largier, 1995; Johnson & Pattiarathch, 2004) and may be forced by spatial and temporal variations in the incident wave field that are associated with a specific wave group (Fowler & Dalrymple, 1990; Reniers et al., 2004a). Long & Özkan-Haller (2016) identified "non-stationary "rip currents whose formation and variability were more strongly controlled by the direction of incoming wave energy and less strongly controlled the nearshore bathymetry.

At Isipingo, there are two persistent rip currents approximately in the centre of the embayment, which align with the position of the non-bedrock controlled RSD's and located between the two shoreface-connected ridges (Fig 6.1). These bathymetric features appear to control the hydrodynamic forcing leading to the development of the focused rip currents. However, as displayed in Figure 6.1, these rips vary spatially and shift their alongshore position mainly towards the NE headland, with a spacing between them ranging from 100 m to 500 m. The nearshore wave field is dominated by waves approaching from the southeast under fair-weather conditions, and the south during storm events. This creates a strong alongshore variability in wave height, forcing the rip currents to migrate in the alongshore direction (e.g. Long & Özkan-Haller, 2016). Due to the migration of these rip current towards the NE headland, it is likely that these currents are a contributing mechanism responsible for the extensive erosion in the NE section of the study area. As a consequence, the absence of significant rips in the centre region and the focussing of the wave action towards the NE section explains the area of relative stability at the centre of the embayment, where no morphological changes occur between the extensive zones of erosion and accretion.

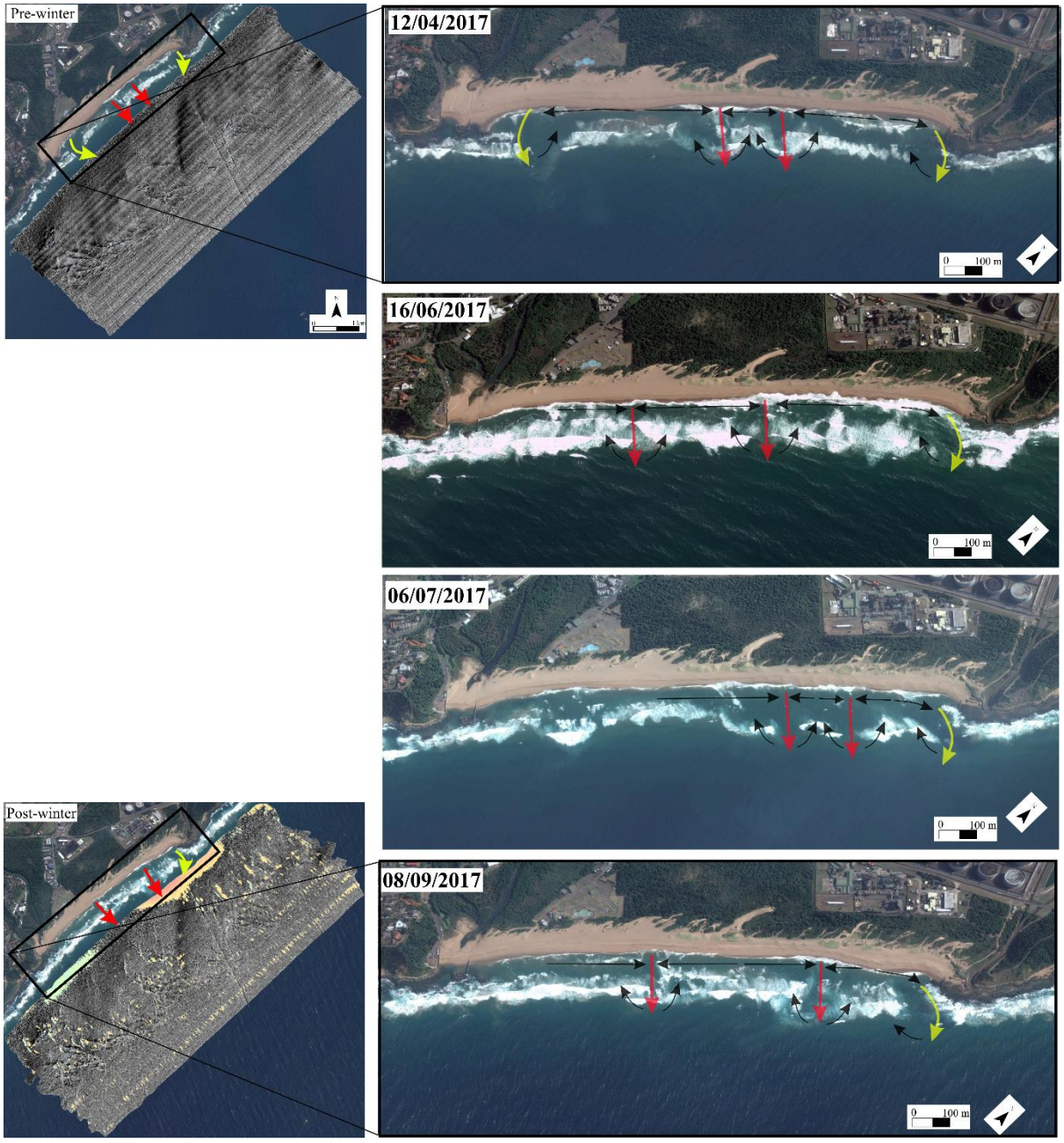

Figure 6.1. Topographically controlled rip currents (yellow arrow) and focussed rip currents (red arrow) operating at the Isipingo embayment during the pre- and post-winter season (Google earth image)

6.2.3. Beach Rotation

The most significant morphological changes of the embayment are exhibited as two extensive zones of erosion and accretion that are located shore-normal to the headlands. These zones occur in the areas of higher modelled wave-induced forcing and increased bed shear stresses acting on the seabed. As a consequence of the increased wave energy, the potential for sediment

entrainment and transport is enhanced, resulting in active erosion along the NE headland and localized accretion adjacent to the SW headland. This is separated by an area of no change. Morphological changes similar to those exhibited at Isipingo have been observed at several embayed beaches in Australia (Short et al., 1995; Short, 1999; Short & Trembanis, 2004; Ranasinghe et al., 2004) and Brazil (Klein et al., 2002) and are a result of the process of beach rotation. Beach rotation is the periodic shifting of sediment towards one end of an embayment and mainly occurs on beaches that are directly exposed to variable wave climate, which experiences changes in wave direction and longshore sediment transport (Short, 2010).

In previous location-specific studies, beach rotation has been typically attributed to the seasonal or oscillations in climate indices, which change the distribution of wave-approach angles (Ranasinghe et al., 2004; Thomas et al., 2011), or, in some locations, cross-shore processes explain majority of the variation observed on embayed beaches (Harley et al., 2011). Monitoring of the pre and post-winter shoreline position in Isipingo embayment (Fig 6.2a) as well as the morphological changes in the nearshore (Fig 6.2b) display an apparent rotation of the beach and the nearshore. However, the mechanisms responsible for this rotation are inconsistent with those attributed by the traditional beach rotation processes as explained by the above mention authors. Under fair weather wave condition, the nearshore zone of Isipingo is dominated by waves approaching from the southeast and this direction becomes more southerly during major storm events. Although there is a shift in wave direction, wave direction-forced beach rotation is not consistently supported by the results presented in this study as the change in direction is insufficiently variable to initiate such rotation. Instead, the rotation patterns may be a result of the nearshore cellular circulation mechanisms, particularly the topographically- controlled rip currents, which is not as straightforward as wave-direction forced beach rotation (Loureiro et al., 2012). Ratliff & Murray (2014) and Blossier et al. (2017) identified a new "breathing mode" as a process to explain the apparent rotation of the embayed beaches that are dominated by low-angle waves.

The breathing mode characterises the changes in shoreline curvature that are controlled by mechanisms that transport sand from the middle of the embayed beach to the edges and back (Ratliff & Muarry, 2014). The process is a critical driver of alongshore sediment transport and the resulting patterns on erosion and accretion along embayed beaches. The local breathing process at Isipingo transports sediment from the region perpendicular to the NE headland and moves it towards the SW headland. The resulting erosion and accretion patterns in the nearshore are controlled by the interaction between wave shadowing effects of the headlands

and the influence of the alongshore transport gradient. In previous studies, the apparent rotation of the beach is discussed in context of onshore rotation and confined to the region of the sandbars due to limitations in imagery of areas beyond these regions. However, multibeam data presented over a 5 month period in this study validate that apparent beach rotation (despite not being wave direction forced rotation) extends to the nearshore and mimics the same erosion and accretion patterns observed on the beach.

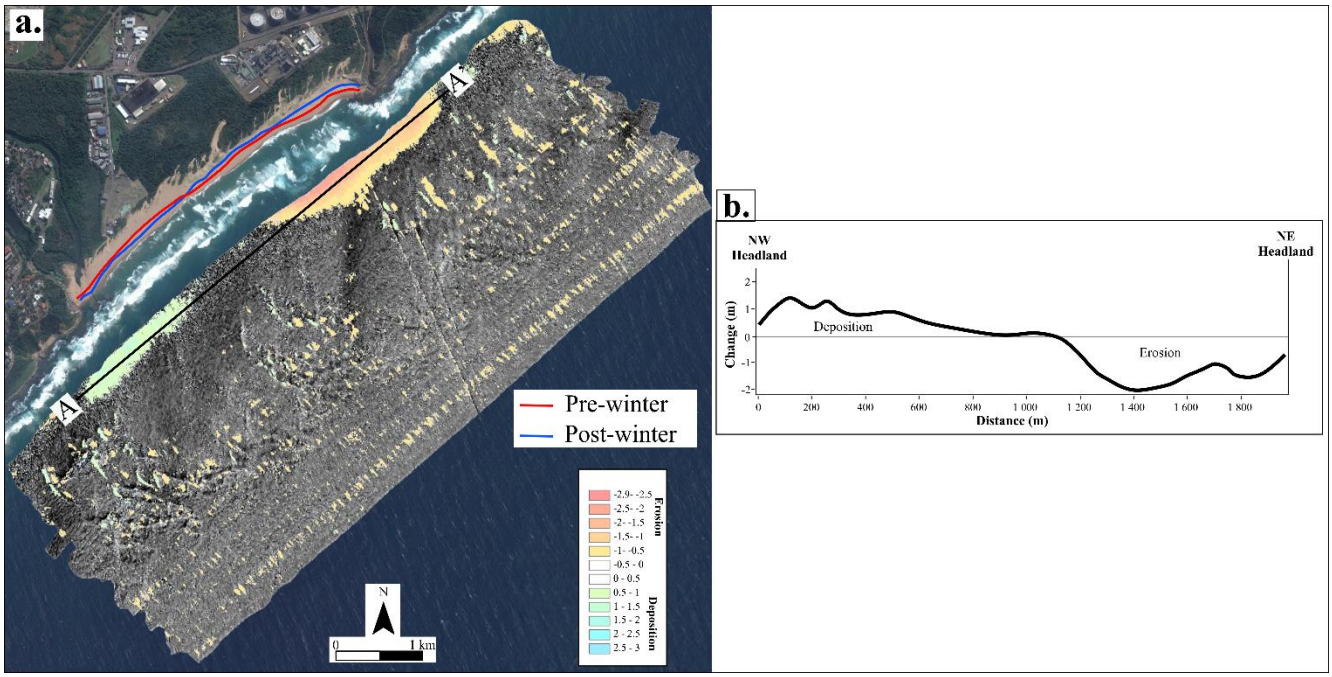

Figure 6.2: Bathymetric changes and shoreline position for the pre-and post-winter season (a) and nearshore morphological cross-section representing the general trend of nearshore sediment erosion and deposition (b)

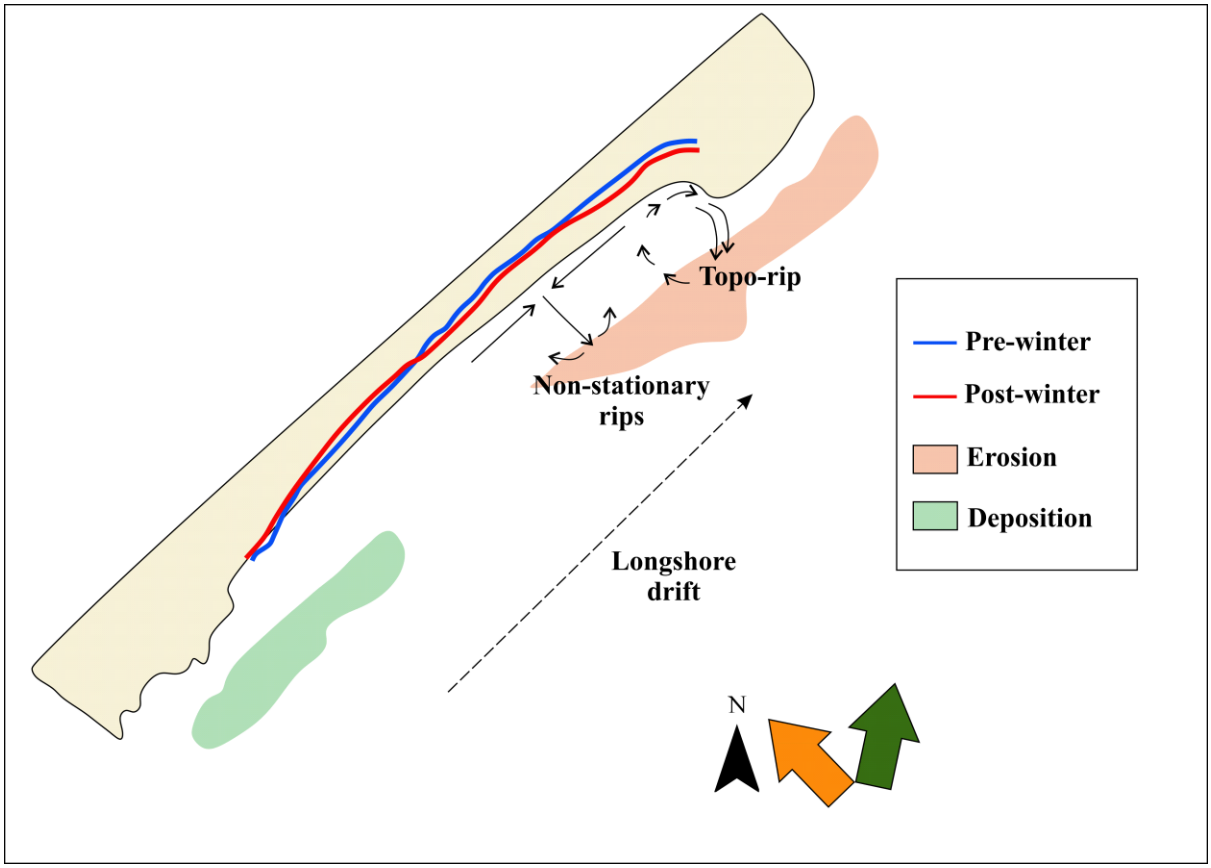

Figure 6.3: Schematic representation of the "breathing mode", rip currents and longshore drift of the study area. Orange and green arrows represent the wave direction under mean wave conditions and extreme storm events, respectively.

6.3. High-energy Morphodynamics

Modelling of extreme storm events, such as that of the 99 % exceedance levels and March 2007 event, indicate that the nearshore morphology is not the only mechanism controlling the hydrodynamics and the resulting changes that occur. It is well cited in literature that strong storm events generate morphological changes over a shorter time as compared to longer intervals during fair-weather conditions (Backstrom et al., 2009). A typical storm will involve the removal of sediment in the nearshore and transport it offshore to form sandbars, the offshore movement of sediment attributed to the bed-return currents (Russel et al., 1993). Additionally, during moderate wave conditions, there is a significant net shoreward transport of sediment with erosion in the nearshore and accretion further onshore (in the form of bars) (Lee et al., 1998). Storms at Isipingo are associated with significant wave heights that exceed 3 m, wave periods greater than 14 s and swells generally approaching form the south. Under these wave conditions the potential for sediment entrainment and transport is driven by intense bed shear

stresses and the combined interaction between waves and currents. An energetic wave field of the study area drives a greater degree of wave focussing on the NW and SW headlands (Fig. 5.2.1), generating a stronger longshore drift, likely resulting in greater morphological changes during storm events. This can be seen to some extent by the flattening of the bedform field crests (e.g. Fig. 5.3.3), the migration of the RSD's, refocusing of the main areas of erosion and accumulation, all of which were associated with a winter season that was relatively energetic.

Chapter 7: Conclusion

Morphological change in the coastal compartment of Isipingo, along the south coast of KwaZulu-Natal was monitored over the winter season from two high-resolution bathymetric datasets. Modelling of wave-induced forces revealed the spatial variation of the wave field and its influence on the morphological response of the nearshore. Spectral wave modelling results of the wave field and bed shear stresses agree with observed morphological change, with significant erosion and deposition occurring in the shallower regions (5 m to 14 m) of the study area and along the NE and SW headlands, respectively.

The variability in nearshore wave field and the patterns of morphological change appear to be controlled by the bathymetric configuration and the hydrodynamic mechanisms operating in the nearshore of the embayment, which are in turn influenced by geological inheritance. Despite the small morphological adjustments that occurred to the main bedform types, the configuration of the large-scale features (SFRC's, RSD's and large subaqueous dunes) was found to control the wave dynamics in the region by focusing waves and increasing wave orbital velocities in areas where erosion and deposition may occur. The morphological evolution is controlled by the geological constraints and nearshore hydrodynamics. The prevalent south to north longshore currents sets up a local circulation that creates toporips against the NE headland, forcing sediment removal and creating an extensive erosional zone. The shadowing effect of the SW headland contributes to the wave forcing and bed shear stresses in the area immediately leeward, likely contributing to the development of the area of accretion in the SW section of the embayment. The hydrodynamic forcing mechanisms of the non-bedrock controlled RSD's and SFCR's bathymetrically control the persistence of the non-stationary rip currents towards the NE headland of the embayment. The absence of significant rips in the centre region and the focussing of the wave action towards the NE section are most likely to explain the area of relative stability at the centre of the embayment. The apparent rotation of the beach and nearshore region is not driven by the classic understanding of beach rotation, which is based purely on variation in longshore sediment transport. Rather, a combination of processes that are driven by nearshore cellular circulation mechanisms and a breathing of the berm dictate this. This study illustrates a case that is often suspected but undocumented: the onshore beach rotation extends to regions beyond sandbars and into the nearshore.

The morphological evolution of the embayed nearshore region during storm events is controlled predominantly by an energetic wave field and its interaction with nearshore morphology, both of which control high-energy morphodynamics response. The study provides a framework to understand the interactive processes that drive the morphological responses of the nearshore in a geologically-constrained setting. The methods employed address scientific, industrial and environmental concerns that are relevant for the proposed engineering schemes of Durban, and show how detailed multibeam mapping is a significantly effective as a tool for accurately assessing coastal change and modelling the nearshore waves. Improvement to the type of equipment utilised during surveying would greatly enhance the accuracy of the bathymetric depth measurement. As consequence, this will allow for the assessment of nearshore morphological changes to extend to the regions further offshore in the coastal compartment of Isipingo.

Future research will entail extension of the period of analysis, including further surveys of the nearshore and the connecting beach. Detailed wave modelling for the of the winter season covered in this study and the associated storms during this period will improve on performed work and provide a better understanding of the wave induced forcing in the study area. Additionally, future work will involve grain size analysis in order to better detail bed shear stresses and the potential sediment motion for similar wave conditions at the Isipingo Embayment.

References

Aagaard, T., & Masselink, G. (1999). The surf zone. In: Short, A.D. (ed.), Handbook of Beach and Shoreface Morphodynamics. Chichester, U.K.: Wiley pp. 72–118

Aagaard, T., Greenwood, B., & Hughes, M. (2013). Sediment transport on dissipative, intermediate and reflective beaches. Earth-Science Reviews 214, 32–50.

Allen, J. R. (1988). Nearshore Sediment Transport. Coastal Geomorphology 78, 148-157.

Ashley, G. (1990). Classification of large-scale subaqueous bedforms: A new look at an old problem. Journal of Sedimentary Petrology 60, 160-172.

Backstorm, J.T., Jackson, D.W.T., & Cooper, J.A.G. (2007). Shoreface dynamics of two high-energy beaches in Northern Ireland. Journal of Coastal Research, Special Issue 50, 594–598.

Backstorm, J.T., Jackson, D.W.T., Cooper, J.A.G., & Malvárez, G.C. (2008). Storm-Driven Shoreface Morphodynamics on a Low-Wave Energy Delta: The Role of Nearshore Topography and Shoreline Orientation. Journal of Coastal Research 246, 1379-1387.

Battjes, J. A. & J. P. F. M. Janssen. (1978). Energy loss and set-up due to breaking of random waves. Proceedings on the 16th Conference Coastal Engineering (Hamburg), New York, ASCE 569–587

Bellec, V.K., Reidulv, B., Leif, R., Slagstad, D., Oddvar, L., & Dolan, M. (2010). Rippled scour depressions on continental shelf bank slopes off Nordland and Troms, Northern Norway. Continental Shelf Research 30, 1056–1069.

Birch, G.F. (1996). Quaternary Sedimentation off the East Coast of Southern Africa (Cape Padrone to Cape Vidal). Bulletin of the Geological Survey of South Africa, Council for Geoscience 118, 55.

Blossier, B., Bryan, K.R., Daly, C.J., & Winter, C. (2017). Spatial and temporal scales of shoreline morphodynamics derived from video camera observations for the island of Sylt, German Wadden Sea. Geo-Marine Letters 37 (2), 111-123.

Booij, N., Ris, R., & Holthuijsen, L. (1999). A third generation wave model for coastal regions, part 1, model description and validation. Journal of Geophysical Research 104 (4), 7649–7666.

Bowen, A., Inman, D., & Simmons, V. (1968). Wave “set-down” and “set-up”. Journal of Geophysical Research 73 (8), 2569–2577.

Bretherton, F., & Garrett, C. (1969). Wave trains in inhomogeneous moving media. Proceedings of the Royal Society of London 302, 529–554.

Bridge, J.S. (1981). Bed shear stress over subaqueous dunes, and the transition to upper-stage plane beds. Sedimentology 28, 33-36

Broad, D. S., Jungslager, E. H. A., McLachlan, I. R. and Roux, J. (2006). Offshore Mesozoic Basins. In: Johnson, M. R., Annhauser, C. R. and Thomas, R. J. (eds.), The Geology of South Africa. Geological Society of South Africa, Johannesburg/Council for Geoscience, Pretoria, pp. 553-571.

Brown, C.J., & Blondel, P. (2009). Developments in the application of multibeam sonar backscatter for seafloor habitat mapping. Applied Acoustics 70 (10), 1242 -1247.

Brown, C.J., Todd, B., Kostylev, V., & Pickrill, R. (2011). Image-based classification of multibeam sonar backscatter data for objective. Continental Shelf Research 31, 110-119.

Buckley, M., & Lowe, R. (2013). Evolution of nearshore wave models in steep reef environments. Coastal Dynamics 249-260

Cacchione, D.A., Grant, W.D., & Tate, G.B. (1984). Rippled scour depressions on the inner continental shelf off central California. Journal of Sedimentary Petrology 54, 1280–1291.

Calder, B., & Mayer, L. (2003). Automatic processing of high-rate, high-density multibeam echosounder data. Geochemistry, Geophysics, Geosystems. Technical Brief 4(6), 1-22

Calvete, D., Falqués, A., de Swart, H.E., & Walgreen, M. (2001a). Modeling the formation of shoreface-connected sand ridges on storm-dominated inner shelves. Journal of Fluid Mechanics 441, 169–193.

Calvete, D., Walgreen, M., de Swart, H.E., & Falqués, A. (2001b). A model for sand ridges on the shelf: effect of tidal and steady currents. Journal of Geophysical Research 106 (C5), 9311–9325.

Castelle, B., Scott, T., & McCarroll, R.J. (2016). Rip current types, circulation and hazard. Earth-Science Reviews 163, 1-21.

Casulli, V. & G.S. Stelling. (1998). Numerical simulation of 3D quasi-hydrostatic free-surface flows. Journal of Hydraulic Engineering 124(7), 678-686.

Cawthra, H.C., Neumann, F.H., Uken, R., Smith, A.M., Guastella, L.A., & Yates, A. (2012). Sedimentation on the narrow (8 km wide), oceanic current-influenced continental shelf off Durban, Kwazulu-Natal, South Africa. Marine Geology 323(325), 107–122.

Chen, W., Demirbilek, Z., & Lin, L. (2009). Coupling Phase-Resolving Nearshore Wave Models with Phase-Averaged Wave MKomaodels in Coastal Applications. Estuarine and Coastal Modeling 528-600.

Chester, R. (2009). Marine geochemistry (2nd Edition). Oxford: John Wiley & Sons, 345.

Cooper, J.A.G., (1991a) Shoreline Changes on the Natal coast: Mkomanzi River mouth to Tugela River mouth. Natal Town and Regional Planning Commission Report, 77. 12-48

Cooper, J.A.G., (1991b) Shoreline Changes on the Natal coast: Tugela river mouth to Cape St Lucia. Natal Town and Regional Planning Commission Report 76. 12-49

Cooper, J. A. G. (2001). Gemorphological variability among microtidal estuaries from the wave-dominated South African coast. Geomorphology 40(1–2), 99– 122

Cooper, J.A.G., & Flores, R.M. (1991). Shoreline deposits and diagenesis resulting from two Late Pleistocene highstands near + 5 and + 6 metres, Durban, South Africa. Marine Geology 97, 325-343.

Cooper, J.A.G., & Pilkey, O. (2004). Longshore Drift: Trapped In An Unexpected Universe. Journal of Sedimentary Research 74(5), 599–606.

Corbella, S. and Stretch, D.D. (2012). The wave climate on the KwaZulu-Natal coast of South Africa. Journal of the South African Institute of Civil Engineering: Technical Paper 54 (2). 45-50.

Cowell, P., Hanslow, D. & Meleo, J. (1999).The Shoreface In: Short, A. Handbook and Beach and Shoreface Morphodynamics. Chichester: John Wiley & Sons, pp. 40-71.

Clarke, L.B., Werner, B.T., 2004. Tidally modulated occurrence of megaripples in a saturated surf zone. Journal of Geophysical Research 109, C1012, 1-15.

Clifton, H.E. (1976). Wave-generated structures - a conceptual model. In: Davis, R.A & Ethington R.L (eds.), Beach and Nearshore Processes. Special publication: Society of Economic Palaeontologists and Mineralogists, 24, 26--148.

Dally, W. (2006). Surfzone Processes. In: M. Schwartz (ed.), Encyclopaedia of coastal science. Washington: Springer Science & Business Media, pp. 929-935.

Dalrymple, R.W., & Hoogendoorn, E.L. (1997). Erosion and deposition on migrating shoreface-attached ridges, Sable Island, eastern Canada. Geoscience Canada 24, 25–36.

Dalrymple, R., MacMahan, J., Reniers, A., & Nelko, V. (2011). Rip Currents. Annual Review of Fluid Mechanics 551-581.

Dartnell, P., & Gardner, J. (2004). Predicting Seafloor Facies from Multibeam Bathymetry and Backscatter Data. Photogrammetric Engineering & Remote Sensing 70(9), 1081–1091.

Davids, S. (2009). Tugela Licence Area. Petroleum Agency South Africa 2009 Licence Round 15.

Davidson-Arnott, R.G.D. (2010). Introduction to Coastal Processes and Geomorphology. Cambridge University Press, 78-112

Davidson-Arnott, R. (2013). Nearshore bars. In: Shroder, J., & Sherman, D. (eds.), Treatise on Geomorphology. San Diego,CA: Academic Press, 10, 130–148 .

Davis, R. (1978). Beach and Nearshore zone. In: Davis, R (ed.) Coastal Sedimentary Environments. New York: Springer Science & Business Media, 237-285

Davis, R., & Hayes, M. (1984). What is a wave-dominated coast? Marine Geology 60, 313-329.

Davis, A.C.D., Kvitek, R.G., Mueller, C.B.A., Young. M.A., Storlazzi, C.D., & Phillips, E.L. (2013). Distribution and abundance of rippled scour depressions along the California coast. Continental Shelf Research 69, 88-100.

Demirbilek, Z., & Panchang, V. (1998). CGWAVE: A Coastal Surface Water Wave Model of the Mild Slope Equation. Technical Report CHL-98-26, US Army Corps of Engineers Waterways Experiment Station, Vicksburg, MS 39180.

Dingle, R.V., Siesser, W.G., Newton, A.R., 1983. Mesozoic and Tertiary geology of southern Africa. AA Balkema, Rotterdam, 375.

Duane, D.B., Field, M.E., Meisburger, E.P., Swift, D.J.P., & Williams, S.J. (1972). Linear shoals on the Atlantic inner continental shelf, Florida to Long Island. In: Swift, D.J.P., Duane,

D.B., Pilkey, O.H. (eds.), Shelf Sediment Transport. Dowden, Hutchinson, and Ross, pp. 447–498

Dugan, J., Morris, W., Vierra, K., Piotrowsk, C., Farruggia, G., & Campion, D. (2001). Jetski-Based Nearshore Bathymetric and Current Survey System. Journal of Coastal Research,17(4), 900-908.

Dyer,K.R., & Huntley, D.A. (1999). The origin, classification and modelling of sand banks and ridges. Continental Shelf Research 19, 1285–1330.

Ebersole, B. A., & Dalrymple, D. (1980). Numerical Modelling of Nearshore Circulation. Coastal Engineering Proceedings 1(17), 2710-2724.

Elko, N., & Homan, R. (2014). The past and fiuturre of nearshore processes research: reflections on the Sallenger years and a new vision for the future. Shore and Beach 82 (3), 30-31.

Ferrini, V., & Flood, R. D. (2005). A comparison of Rippled Scour Depressions identified with multibeam sonar: evidence for sediment transport in inner shelf environments. Continental Shelf Research 25,1979 –1995.

Field, M.E., & Roy, P.S. (1984). Onshore transport and sand body formation: evidence from a steep high-energy shoreface in southeastern Australia. Journal of Sedimentary Research 54, 1292–1302.

Figueiredo, A.G., Sanders, J.E., & Swift, D.J.P. (1982). Storm-graded layers on inner continental shelves: examples from southern Brazil and the Atlantic coast of the central US. Sedimentary Geology, 31, 171–190.

Flemming, B. W. (1980). Sand transport and bedform patterns on the continental shelf between Durban and Port Elizabeth (Southeast African continental margin). Sedimentary Geology 26. 179-205

Flemming, B. (1981). Factors Controlling Shelf Sediment Dispersal along the Southeast African Continental Margin. Marine Geology 41, 259-277.

Flemming, B. W., and Hay, R. (1988). Sediment distribution and dynamics on the Natal continental shelf. In: Schumann, E. H. (ed.), Coastal Ocean Studies off natal, South Africa. Lecture Notes on Coastal and Estuarine Studies, 3, 47–80.

Fowler, R. E., &. Dalrymple, R. A. (1990). Wave group forced nearshore circulation, In: Edge, B.J. (ed.), Proceedings of 22nd International Conference on Coastal Engineering, New York: American Society of Civil Engineering, pp. 729–742,

Gallagher, E.L., Elgar, S., Thornton, E.B. (1998). Observations and predictions of megaripple migration in a natural surf zone. Nature 394, 165–168.

Gallop, S.L., Bryan, K.R., Coco, G., & Stephens, S.A. (2011). Storm-driven changes in rip channel patterns on an embayed beach. Geomorphology 127, 179-188.

Garnaud, S., Leueuer, P., & Garlan, T. (2005). Origin of rippled scour depressions associated with cohesive sediments in a shoreface setting (eastern Bay of Seine, France*)* Geo-Marine Letters 25, 34–42.

Gibbs, A., Santos, P., van der Westhuysen, A., & Padilla, R. (2013). Nearshore wave prediction system: enhancing marine forecasting capabilities during high impact events. Proceedings at the 38th NWA Annual Meeting, Charleston, 1-13.

Goodlad, S. W. (1986). Tectonic and sedimentary history of the mid-Natal Valley (SW Indian Ocean). Joint Geological Survey/University of Cape Town, Marine Geoscience Unit Bull 15.415

Goff, J.A., & Kleinrock, M.C. (1991). Quantitative comparison of bathymetric survey systems. Geophysical Research Letters 18 (7), 1253-1256

Goff, J.A., Mayer, L.A., Traykovski,P., Buynevich,I., Wilkens,R., Raymond,R., Glang, R., Evans,R.L., Olson,H., & Jenkins,C. (2005) .Detailed investigation of sorted bedforms, or "rippled scour depressions" within the Martha's Vineyard Coastal Observatory, Massachusetts. Continental Shelf Research 25, 461–484.

Gomes, E.R., Mulligan, R.P., Brodie, K.L., & McNinch, J.E. (2016). Bathymetric control on the spatial distribution of wave breaking in the surf zone of a natural beach. Coastal Engineering 116, 180-194.

Graber, H., & Madsen, O. (1988). A finite-depth wind-wave model, part 1: model description. Journal of Physical Oceanography, 18, 1456-1483.

Green, A.N. (2009). Sediment dynamics on the narrow, canyon-incised and current-swept shelf of the northern KwaZulu-Natal continental shelf, South Africa. Geo-Marine Letter, 29, 201-219

Green, A.N., & Garlick, G.L. (2011). Sequence stratigraphic framework for a narrow, current-swept continental shelf: the Durban Bight, central KwaZulu-Natal, South Africa. Journal of African Earth Sciences 60, 303-314.

Green, M., Vincent, C., & Trembanis, A. (2004). Suspension of coarse and fine sand on a wave-dominated shoreface, with implications for the development of rippled scour depressions. Continental Shelf Research 24, 317–335.

Guillén., J., & Hoekstra, P. (1997). Sediment Distribution in the Nearshore Zone: Grain Size Evolution in Response to Shoreface Nourishment (Island of Terschelling, The Netherlands). Estuarine, Coastal and Shelf Science 45, 639-652.

Guillou, N. (2013). Effects of bed-sediment grain-size distribution on wave height predictions in the English Chanel. Coastal Dynamics, 769-780.

Harley, M. D., Turner, I. L., & Short, A. D. (2015), New insights into embayed beach rotation: The importance of wave exposure and cross-shore processes. Journal of Geophysical Research: Earth Surface 120, 1470–1484.

Hasselmann, K., Barnett, T.P., Bouws, E., Carlson, H., Cartwright, D.E., Enke, K., Ewing, J.A., Gienapp, H., Hasselmann, D.E., Kruseman, P., Meerburg, A., Müller, P., Olbers, D.J., Richter, K., Sell, W., & Walden, H. (1973) . Measurements of wind-wave growth and swell decay during the Joint North Sea Wave Project (JONSWAP). Deutsche Hydrographische Zeitschrift Suppl A8 (12) 95.

Hequette, A., & Hill, P.R. (1993).Storm-generated currents and offshore sediment transport on a sandy shoreface, Tibjak Beach, Canadian Beaufort Sea. Marine Geology 113,283–304

Hequette, A., DesRosiers, M., Hill, P.R., & Forbes, D.L. (2001). The influence of coastal morphology on shoreface sediment transport under storm-combined flows, Canadian Beaufort Sea. Journal of Coastal Research 17(3), 507–516.

Hobday, D.K. (1982). The southeast African Margin. In: Nairn, A.E.M., &. Stehli, F.G (eds.), The ocean basins and margins, volume 6 – the Indian Ocean. Plenum Press, New York 149-183

Holland, K.T., & Elmore, P.A. (2008). A review of heterogeneous sediments in coastal environments. Earth-Science Review 89,116–134.

Holman, R., & Haller, M. (2012). Remote Sensing of the Nearshore. Annual Review of Marine Sciences 5, 95-113.

Holthuijsen, L. (2007). Waves in oceanic and coastal waters. New York: Cambridge University Press.

Hoogendoorn, E.L., & Dalrymple, R.W. (1986). Morphology, lateral migration and internal structures of shore-face connected ridges, Sable Island Bank, Nova Scotia, Canada. *G*eology 14, 400–403.

Hsu, T.J., Elgar, S., & Guza, R.T. (2006). Wave-induced sediment transport and onshore sandbar migration. Coastal Engineering 53, 817-824

Hughes Clarke, J. (2012). Optimal use of multibeam technology in the study of shelf. In: Li, M., Sherwood, C., & Hill, P. (eds.), Sediments, morphology and sedimentary processes on continental shelves: advances in technologies, research, and applications (Special Publication 44 of the IAS). Chichester: John Wiley & Sons, 109, pp. 1-28

Hughes Clarke, J., Mayer, L., & Wells, D. (1996). Shallow-Water Imaging Multibeam Sonars: A New Tool for Investigating Seafloor Processes in the Coastal Zone and on the Continental Shelf. Marine Geophysical Research 18(6), 607-629.

Huvenne, V. H. (2007). Detailed mapping of shallow-water environments using image texture analysis on side scan sonar and multi-beam backscatter imagery. In: Proceedings of the 2nd underwater acoustic measurements conference 2007 (on CDROM), Heraklion, Greece 879-886.

Iacono, C.L., & Guillen, J. (2008).Environmental conditions for gravelly and pebbly dunes and sorted bedforms on a moderate-energy inner shelf (Marettimo Island, Italy, western Mediterranean). Continental Shelf Research 28,245–256.

Inman, D. L. (2002). Nearshore Processes. Scripps Institution of Oceanography.1-7.

Inman, D., & Jenkins, S. (2006). Budget of sediment. In Schwartz, M. Encyclopaedia of Coastal Science. Washington: Springer Science & Business Media, pp 412-413.

International Hydrographic Organization. (1998). IHO Standards for Hydrographic Surveys (4th Edition). Monaco: International Hydrographic Bureau. 1-5.

Jaffe, B.E., List, J.H., & Sallenger, A.H. (1997). Massive sediment bypassing on the lower shoreface offshore of a wide tidal inlet—Cat Island Pass, Louisiana. Marine Geology 136, 131–149.

Jermy, C.A. and Mason, T.R. (1983). A sedimentary model for the Berea Formation in the Glenwood Tunnel, Durban. Transactions of the Geological Society of South Africa 86, 117-125.

Johnson, D., & Pattiaratchi, C. (2004), Transient rip currents and nearshore circulation on a swell-dominated beach, Journal of Geophysical Research, 109, 1-20.

Jury, M.R., & Melice, J.-L. (2000). Analysis of Durban rainfall and Nile river flow 1871–1999.Theoretical and Applied Climatology 67, 161–169.

Kahn, J.H., & Roberts, H. (1982). Variations in storm response along a microtidal transgressive barrier-island arc. Sedimentary Geology 33, 129–146.

King, L.A. (1962). The post-Karoo Stratigraphy of Durban. Transactions of the Geological Society of South Africa 65, 95-99.

King, L. A., and Maud, R. R. (1964). The geology of Durban and its environments. Bulletin of the Geological Survey of South Africa 42, 55.

Klein, A.H.F., Ferreira, O., Dias, J.M.A., Tessle, M.G., Silveira, L.F., Benedet, L., de Menezes, J.T., & de Abreu, J.G.N. (2010). Morphodynamics of structurally controlled headland-bay beaches in southeastern Brazil: A review. Coastal Engineering 57, 98-111.

Klein, A.H.F., Filho, L.B., & Schumacher, D.H. (2002). Short-Term Beach Rotation Processes in Distinct Headland Bay Beach Systems. Journal of Coastal Research 18 (3), 442-458.

Komar, P.D. (1976). Beach Processes and Sedimentation. Englewood Cliffs, New Jersey: Prentice Hall. pp. 554.

Konicki, K.M. & Holman, R.A. (2000). The statistics and kinematics of transverse bars on an open coast. Marine Geology 169, 69–101.

Lark, R., Marchant, B., Dove, D., Green, S., Stewart, H., & Diesing, M. (2015). Combining observations with acoustic swath bathymetry and backscatter to map seabed sediment texture classes: The empirical best linear unbiased predictor. Sedimentary Geology 328, 17-32.

Larson, M., Kubota, S., & Erikson, L. (2004). Swash-zone sediment transport and foreshore evolution: field experiments and mathematical modeling. Marine Geology 212, 61–79.

Lee, G., Nicholis, R.J., & Birkemeier, W.A. (1998). Storm-driven variability of the beach-nearshore profile at Duck, North Carolina, USA, 1981–1991. Marine Geology 148, 163–177.

Leuci, R., Perritt, S. and Miller, W. (2002). Island View Channel and Basin bathymetric and seismic survey. Council for Geoscience Internal Report 2002-0117, 20.

Long, J.W., & Özkan-Haller, H.T. (2016), Forcing and variability of nonstationary rip currents, Journal of Geophysical Research: Oceans 121, 520-539

Longuet-Higgins, M. (1970). Longshore currents generated by obliquely incident sea waves. Journal of Geophysical Research 75(33), 6778-6789.

Longuet-Higgins, M.S., & Stewart, R.W. (1964) Radiation stresses in water waves: a physical discussion with applications. Deep Sea Research 11, 529–563.

Loureiro, C., Ferreira, O., & Cooper, J.A.G. (2012). Extreme erosion on high-energy embayed beaches: Influence of megarips and storm grouping. Geomorphology 139 (140), 155-171

Lutjeharms, J. R. E. (2006). The Agulhas Current. Springer-Verlag, Berlin, Heidelberg. pp. 329.

Ma, G., Shi, F., & Kirby, J.T. (2012). Shock-capturing non-hydrostatic model for fully dispersive surface wave processes. Ocean Modelling 43(44), 22–35

MacMahan, J., Thornton, E., & Reniers, A. (2006). Rip current review. Coastal Engineering 53, 191 – 208.

Makowski, C., & Finkl, C. (2016). History of Modern Seafloor Mapping. In: Makowski, C., & Finkl, C. (eds.), Seafloor Mapping along Continental Shelves: Research and Techniques for Visualizing Benthic Environments, 13, pp. 1-18.

Manson, G., Davidson-Arnott, R., & Forbes, D. (2016). Modelled nearshore sediment transport in open-water conditions, central north shore of Prince Edward Island, Canada. Journal Earth Science 53 (1), 101-118.

Martin, A.K., & Flemming, B.W. (1986). The Holocene shelf sediment wedge off the south and east coast of South Africa. Canadian Society of Petroleum Geologists Memoir 2, 27-44.

Martin, A.K., & Flemming, B.W. (1987). Aeolianites of the South African coastal zone and continental shelf as sea-level indicators. South African Journal of Science 83, 507-508.

Martin, A.K., & Flemming, B.W. (1988). Physiography, structure and evolution of the Natal continental shelf. In: Schumann, E.H. (Bd.), Lecture notes on coastal and estuarine studies, 26, Springer Verlag, New York, 1146.

Mather, A.A., and Stretch, D.D. (2012). A Perspective on Sea Level Rise and Coastal Storm Surge from Southern and Eastern Africa: A Case Study near Durban, South Africa. Journal: Water, 4, 237-250.

Masselink, G., Gehrels, R. (eds.). (2014). Coastal Environments and Global Change. John Wiley & Sons Ltd., pp. 448.

Maud, R.R. (1968). Quaternary geomorphology and soil formation in coastal Natal. Annals of Geomorphology 7, 155-199.

McCarthy, M.J. (1967). Stratigraphical and sedimentological evidence from the Durban region of major sea-level movements since the late Tertiary. Transactions of the Geological Society of South Africa 70, 135-165

McKenzie, P. (1958). Rip-Current Systems. Journal of Geology 66 (2), 103-113.

McMillan I.K. (2003). Foraminiferally defined biostratigraphic episodes and sedimentation pattern of the Cretaceous drift succession (Early Barremian to Late Maastrichtian) in seven basins on the South African and southern Namibian continental margin. South African Journal of Science 99 (11/12), 537-576.

Munk, W.H., & Traylor, M.A. (1947). Refraction of ocean waves: A process linking underwater topography to beach erosion. Journal of Geology 55, 1–26.

Murray, A.B., & Thieler, E.R. (2004). A new hypothesis for the formation of large-scale inner-shelf sediment sorting and 'rippled scour depressions'. Continental Shelf Research 24, 295–315.

Niedoroda, A., Swift, D., Hopkins, T., & Ma, C. (1984). Shoreface morphodynamics on wave-dominated coasts. Marine Geology 39, 331-354.

Niedoroda, A.W., Swift, D.J.P., & Hopkins, T.S. (1985). The shoreface. In: Davis, R.A. (ed.), Coastal Sedimentary Environments. New York: Springer, pp. 533–624.

Nnafie, A., deSwart, H.E.M., Calvete, D., & Garnier, R. (2014a). Effects of sea level rise on the formation and drowning of shoreface-connected sand ridges, a model study. Continental Shelf Research 80, 32–48.

Nnafie, A., de Swart, H.E., Calvete, D., & Garnier, R. (2014b). Modeling the response of shoreface-connected sand ridges to sand extraction on an inner shelf. Ocean Dynamics 64 (5), 723–740.

Nwogu, O. (1993). Alternative form of Boussinesq equations for nearshore wave propagation. Journal of Waterway, Port, Coastal, and Ocean Engineering 119(6), 618–638.

Nwogu, O., & Demirbilek, Z. (2001). BOUSS-2D: A Boussinesq Wave Model for Coastal Regions and Harbors. Technical Report CHL-98-26, US Army Corps of Engineers Waterways Experiment Station, Vicksburg, MS 39180.

Palmer, B.J., Van der Elst, R, Mackay, F., Mather, A.A., Smith, A.M., Bundy, S.C., Thackeray, Z., Leuci, R. & Parak, O. (2011). Preliminary coastal vulnerability assessment for KwaZulu-Natal, South Africa. Journal of Coastal Research, Special Issue (ICS2011 Proceedings) 64, 1390-1395.

Park, S.C., Han, H.S., & Yoo, D.G. (2003). Transgressive sand ridges on the mid-shelf of the southern sea of Korea (Korea Strait): formation and development in high-energy environments. Marine Geology 193, 1–18.

Parker,G., Lanfredi, N.W., & Swift, D.J.P. (1982). Seafloor response to flow in a southern hemisphere sand-ridge field: Argentine inner shelf. Sedimentary Geology 22, 195–216.

Partridge, T. C., Botha, G. A. and Haddon, I. G. (2006). Cenozoic deposits of the interior. In: Johnson, M. R., Annhauser, C. R. and Thomas, R. J. (eds.), The Geology of South Afric*a*. Geological Society of South Africa, Johannesburg/Council for Geoscience, Pretoria, 585-605.

Pearce, A.F., Schumann, E.H. & Lundie, G.S.H. (1978). Features of the Shelf Circulation off the Natal Coast. South African Journal of Science 74, 328-331

Pearson, T. (1995). African Keyport – The story of the Port of Durban. Accucut Books, Rossburgh. 178-186

Perritt, S., Leuci, R. and Bosman, C. (2003). Maydon Wharf channel and Congella basin bathymetric and seismic survey. Council for Geoscience Report 2003-0074, 24.

Preston, J. (2009). Automated acoustic seabed classification of multibeam images of Stanton Banks. Applied Acoustics 70 (10), 1277-1287.

Preston-Whyte, R.A., & Tyson, P.D. (1988). Atmosphere and weather of southern Africa. Oxford University Press

Price, T., & Ruessink, B. (2008). Morphodynamic zone variability on a microtidal barred beach. Marine Geology 251, 98–109.

Ramsay, PJ. (1994). Marine geology of the Sodwana Bay shelf, Southeast Africa. Marine Geology 120. 225-247

Ramsay, P.J. & Cooper, J.A.G. (2002). Late Quaternary sea-level change in South Africa. Quaternary Research 57, 82-90.

Ramsay, P.J., Smith, A.M. and Mason, T.R. (1996). Geostrophic sand ridge, dune fields and associated bedforms from the northern KwaZulu-Natal shelf, southeast Africa. Sedimentology 43, 407-419.

Ramsay, P. J., Smith, A. M., Lee-Thorp, J. C., Vogel, J. C., Tydlsley, M and Kidwell, W. (1993). 130 000-year-old fossil elephant found near Durban, South Africa: preliminary report. Suid Afrikaanse Tydskrif vir Wetenskap 89, 165.

Ranasinghe, R., McLoughlin, R., Short, A.D., & Symonds, G. (2004). The Southern Oscillation Index, wave climate, and beach rotation. Marine Geology 204, 273-287

Ratliff, K.M., & Murray, A.B. (2014). Modes and emergent time scales of embayed beach dynamics. Geophysical Research Letters 41, 7270–7275

Reimnitz, E. T., L.J., Shepard, F.P., & Gutierrez-Estrada, M. (1976). Possible rip current origin for bottom ripple zones to 30-m depth. Geology 4 (7), 395-400.

Reniers, A. J. H. M., Roelvink, J. A., & Thornton, E. B. (2004). Morphodynamic modeling of an embayed beach under wave group forcing. Journal of Geophysical Research 109, 1-22.

Roberts, D. L., Botha, G. A., Maud, R. R. and Pether, J. (2006). Coastal Cenozoic deposits. In: Johnson, M. R., Annhauser, C. R. and Thomas, R. J. (eds.), The Geology of South Africa. Geological Society of South Africa, Johannesburg/Council for Geoscience, Pretoria, 605-628

Roelvink, D., Reniers, A., D., van Dongeren, A., van Thiel de Vries, J., McCall, R., & Lescinski, J. (2009). Modelling storm impacts on beaches, dunes and barrier islands. Coastal Engineering 56, 1133-1152

Roland, A., & Ardhuin, F. (2014). On the developments of spectral wave models: numerics and parameterizations for the coastal ocean. Ocean Dynamics 64, 833-846.

Rossouw, J. (1984). Review of existing wave data, wave climate and design waves for South Africa and South West African (Namibian) coastal waters. CSIR Report T/SEA 8401, Stellenbosch 66.

Roy, P., Cowell, P., Ferland, M., & Thom, B. (1994). Wave-dominated coasts. In. Carter, R., & Woodroffe, C. (eds.), Coastal Evolution: Late Quaternary Shoreline Morphodynamics Cambridge: Cambridge University Press, pp. 121-186.

Ruessink, B.G., & Kroon, A. (1994). The behaviour of a multiple bar system in the nearshore zone of Terschelling, the Netherlands: 1965–1993. Marine Geology 121, 187–197.

Ruessink, B.G., & Ranasinghe, R. (2014). Beaches. In: Masselink, G., & Gehrels, R. (eds.), Coastal Environments and Global Change West Sussex: John Wiley & Sons Ltd, pp. 150-176.

Rusu, E., & Soares, C.G. (2013). Coastal impact induced by a Pelamis wave farm operating in the Portuguese nearshore. Renewable Energy 58, 34-49.

Safak, I., List, J.H., Warner, J.C., & Schwab, W.C. (2017). Persistent shoreline shape induced from offshore geologic framework: effects of shoreface connected ridges. Journal of Geophysical Research 122, 1-18.

Seymour, R. (2005). Cross-shore Sediment Transport. In: Schwartz, M. (ed.), Encyclopaedia of Coastal Science. Washington: Springer Netherlands, pp. 352-353.

Shand, R.D., & Bailey, D.G. (1999). A review of net offshore bar migration with photographic illustrations from Wanganui, New Zealand. Journal of Coastal Research 15 (2), 365–378.

Shepard, F.P. (1963). Submarine Geology. Harper and Row, New York, p. 551

Shepard, F.P., Curray, J.R., Innan, D.L., Murray, E.A., Winterer, E.L., Dill, R.F. (1964). Submarine Geology by Diving Saucer: Bottom currents and precipitous submarine canyon walls continue to a depth of at least 300 meters. Science 145, 1042.

Shepard, F.P., Emery, K.O., & La Fond, E.C. (1941). Rip Currents: A Process of Geological Importance. The Journal of Geology 49, 337-369.

Short, A.D. (1985). Rip current type, spacing and persistence, Narrabeen Beach, Australia. Marine Geology 65, 47–71.

Short, A.D. (2010). Role of geological inheritance in Australian beach morphodynamics. Coastal Engineering 57, 52-97.

Short, A., & Trembanis, A.C. (2004) Decadal Scale Patterns in Beach Oscillation and Rotation Narrabeen Beach, Australia—Time Series, PCA and Wavelet Analysis. Journal of Coastal Research 20 (2), 523 – 53.

Short, A.D., Cowell, P.J., Cadee, M.; Hall, W., & van Dijk, B. (1995). Beach rotation and possible relation to southern oscilation. In: Aung, T.H. (ed.), Ocean Atmosphere Pacific Conference. National Tidal Facility, Adelaide, pp. 329-334

Smith, J.A. & Largier, J.L. (1995). Observations of nearshore circulation: Rip currents. Journal of Geophysical Research 100, 10967-10975.

Smith, A.M., Mather, A.A., Bundy, S.C., Cooper, J.A.G., Guastella, L.A., Ramsay, P.J. & Theron, A. (2010). Contrasting styles of swell-driven coastal erosion: examples from KwaZulu-Natal, South Africa. Geological Magazine 147 (6), 940-953.

Soulsby, R. (1997). Dynamic of Marine Sands. London: Thomas Telford.

South African Committee for Stratigraphy (SACS), (1980). Stratigraphy of South Africa. Part 1. Lithostratigraphy of the Republic of South Africa, South West Africa/Namibia, and the Republics of Bophuthatswana, Transkei and Venda (L. E. Kent, comp.). Handbook of the Geological Survey of South Africa 8, 690.

Stelling, G., & Zijlema, M. (2003). An accurate and efficient finite-difference algorithm for non-hydrostatic free-surface flow with application to wave propagation. International Journal for Numerical Methods in Fluids 43, 1-23.

Stive, M., & Wind, H. (1968). Cross-shore mean flow in the surf zone. Coastal Engineering 10, 325-340.

Stubblefield, W.L., McGrail, D.W., & Kersey, D.G. (1984). Recognition of transgressive and post-transgressive sand ridges on the New Jersey continental shelf. In: Tillman, R.W., Siemers, C.T. (eds.), Siliciclastic Shelf Sediments. SEPM Special Publication, 34, pp. 1–23.

Stutz, M., Smith, A., & Pilkey, O. (1998). Differing Mechanisms of Wave Energy Dissipation in the Wave Shoaling Zone, Surf Zone, and Swash Zone. Journal of Coastal Research 26, 214-218.

Swart, D.H. (1987). Erosion of manmade dune, Beachwood Mangrove Nature Reserve. CSIR Research Report T/SEA 8713, Pretoria, South Africa, 28.

Swift, D.J.P., & Field, M.E. (1981). Evolution of a classic sand ridge field: Maryland sector, North American inner shelf. Sedimentology 28, 461–482.

Swift, D.J.P., & Freeland, G.L. (1978). Current lineations and sand waves on the inner shelf, middle Atlantic bight of North America. Journal of Sedimentary Petrology 48, 1257–1266

Swift, D.J.P., Holliday, B., Avignone, N., & Shideler, G. (1972). Anatomy of a shoreface ridge system, False Cape, Virginia. Marine Geology 12, 59–84.

Svendsen, I.A. (1984). Mass flux and undertow in the surf zone. Coastal Engineering 8, 347-365.

Svendsen, I.A. (2006) Introduction to nearshore hydrodynamics. Advanced Series on Ocean Engineering. Singapore: World Scientific 1-9.

Traykovski, P., Hay, A.E., Irish, J.D., & Lynch, J.F. (1999). Geometry, migration, and evolution of wave orbital ripples at LEO-15. Journal of Geophysical Research 104 (C1), 1505–1524.

Thieler, E.R., Brill, A.L., Cleary, W.J., Hobbs, C.H., & Gammisch, R.A. (1995). Geology of Wrightsville Beach, North Carolina shoreface: implications for the concept of shoreface profile of equilibrium. Marine Geology 126, 271–287.

Thomas, T.J., & Dwarakish, G.S. (2015). Numerical Wave Modelling – A Review. Aquatic Procedia 4, 443-448.

Thomas, T.M., Williams, P.A. & Jenkins, R. (2011), Short-term beach rotation, wave climate and the North Atlantic Oscillation (NAO). Progress in Physical Geography 35(3), 333–352

Tolman, H.L. (2008). A mosaic approach to wind wave modelling. Ocean Modelling 25, 35-47.

Trowbridge, J.H. (1995). A mechanism for the formation and maintenance of the shore oblique sand ridges on storm-dominated shelves. Journal of Geophysical Research 100 (C8), 16,071–16,086.

U.S. Army Corps of Engineers (1984) Shore protection manual (4th Edition): Washington, D.C., U.S., Government Printing Office, 882.

Wang, P., Davis, R.D., & Kraus., (1998). Cross-shore distribution of sediment texture under breaking waves under low-energy coasts. Journal of Sedimentary Research 68 (3), 497–506.

Watkeys, M. K. (2006). Gondwana break-up: A South African perspective. In: Johnson, M. R., Annhauser, C. R. and Thomas, R. J. (eds.), The Geology of South Africa. Geological Society of South Africa, Johannesburg/Council for Geoscience, Pretoria, 531-539.

Wiberg, P.L., & Harris, C.K. (1994). Ripple geometry in wave-dominated environments. Journal of Geophysical Research 99, 775-789.

Wijnberg, K., & Kroon, A. (2002). Barred beaches. Geomorphology 48, 103-120.

Wright, L.D., & Short, A. (1984). Morphodynamic variability of surf zones and beaches: A synthesis. Marine Geology 1 (4), 93-118.

Wright, L.D., Boon, J., Kim, S., & List, L. (1991). Modes of cross-shore sediment transport on the shoreface of the Middle Atlantic Bight. Marine Geology 96, 19-51.

van Enckevort, I.M.J., Ruessink, B.G., Coco, G., Suzuki, K., Turner, I.L., Plant, N.G., & Holman, R.A. (2003). Observations of nearshore crescentic sandbars. Journal of Geophysical Research 109 (C06028), 1-17.

van de Meene, J.W.H., & van Rijn, L.C. (2000) . The shoreface-connected ridges along the central Dutch coast—part 1: field observations. Continental Shelf Research 20, 2295–2323.

van der Westhuysen, A. (2012). Spectral modeling of wave dissipation on negative current gradients. Coastal Engineering 68, 17-30.

van der Westhuysen, A., Padilla, R., Santos, P., Gibbs, A., Gaer, D., Nicolini, T., Tjaden, S., Devaliere, E., & Tolma, H. (2013). Development and Validation of the Nearshore Wave Prediction System. Proceedings in the 38th NWA Annual Meeting, Charleston 1-11

Visser, D.J.L. (1989). The geology of the Republics of South Africa, Transkei, Bophuthatswana, Venda and Ciskei and the Kingdoms of Lesotho and Swaziland. Explanation of the 1: 1 000 000 Geological Map (4th Edition) Geological Survey of South Africa pp. 491.

Vis-Star, N.C., de Swart, H.E., & Calvete, D. (2007). Effect of wave-topography interactions on the formation of sand ridges on the shelf. Journal of Geophysical Research 112, 1-17.

Xu, J.P., & Wright, L.D., 1998. Observations of wind-generated shoreface currents off Duck, North Carolina. Journal of Coastal Research 14(2), 610–619.

Xu, T., Haas, K., List, J.H., & Safak, I. (2016). Wave transformation and sediment transport over obliquely-oriented shoreface-connected ridges. Abstract presented at 2016 Ocean Sciences Meeting, American Geophysical Union, New Orleans, LA.

Zijlema, M., van Vledder, G., & Holthuijsen, L. (2012). Bottom friction and wind drag for wave models. Coastal Engineering 65, 19-26.

Personal Communication

Loureiro, C. 2017